

1-1-2012

Free vibration analyses of abs (acrylonitrile-butadiene-styrene) rectangular plates with completely free boundary conditions

Mehmet Akif Dundar
Wayne State University,

Follow this and additional works at: http://digitalcommons.wayne.edu/oa_theses

Recommended Citation

Dundar, Mehmet Akif, "Free vibration analyses of abs (acrylonitrile-butadiene-styrene) rectangular plates with completely free boundary conditions" (2012). *Wayne State University Theses*. Paper 175.

**FREE VIBRATION ANALYSES OF ABS (ACRYLONITRILE-BUTADIENE-
STYRENE) RECTANGULAR PLATES WITH COMPLETELY FREE
BOUNDARY CONDITIONS**

by

MEHMET AKIF DUNDAR

THESIS

Submitted to Graduate School

of Wayne State University,

Detroit, Michigan

in partial fulfillment of the requirements

for the degree of

MASTER OF SCIENCE

2012

MAJOR: MECHANICAL ENGINEERING

Approved by:

Advisor

Date

ACKNOWLEDGEMENTS

I would like to express my sincere thanks and gratitude to my supervisor, Dr. E.O. Ayorinde, who's understanding, expertise, and patience. I appreciate his vast skill and knowledge in many areas, such as vibrations, acoustics, and composite materials, and his assistance in writing this thesis.

I would like to thank my colleague, Mohammad Ahmad Al-Zoubi for his great support and cooperation throughout my preparation of this thesis.

Finally, very special thanks go out to my family for their perpetual encouragements and supports.

TABLE OF CONTENTS

Acknowledgements.....	ii
List of Tables.....	v
List of Figures.....	vi
CHAPTER 1 INTRODUCTION.....	1
CHAPTER 2 LITERATURE REVIEW AND OBJECTIVES.....	4
2.1 Theoretical Vibration Method.....	4
2.2 Finite Element Modal Frequency Method.....	8
2.3 Conclusions of Literature Review.....	9
2.4 Objectives.....	10
CHAPTER 3 THE ANALYTICAL MODEL OF VIBRATING PLATES	12
3.1 The Free Vibration of Rectangular Plates with Completely Free Boundaries.....	12
CHAPTER 4 EXPERIMENTAL MODAL ANALYSIS.....	17
4.1 Introduction.....	17
4.2 The Test Procedure of Vibration.....	18
CHAPTER 5 FINITE ELEMENT ANALYSIS.....	25

5.1 Introduction.....	25
5.2 Finite Element Modal Analysis.....	25
CHAPTER 6 RESULTS AND DISCUSSIONS.....	32
6.1 Theoretical Results.....	32
6.2 Experimental Results.....	32
6.3 Finite Element Results.....	33
6.4 Comparisons.....	35
CHAPTER 7 CONCLUSIONS AND RECOMMENDATIONS.....	37
7.1 Conclusions.....	37
7.2 Recommendations for Future Work.....	39
Appendix A: Eigenvalue Outputs of Sample 1 in Abaqus	70
Appendix B: Eigenvalue Outputs of Sample 2 in Abaqus.....	79
Appendix C: Eigenvalue Outputs of Sample 3 in Abaqus.....	88
References.....	97
Abstract.....	99
Autobiographical Statement.....	101

LIST OF TABLES

Table 1: Frequency Parameter λ^2 for F-F-F-F Plates ($\nu=0.3$).....	16
Table 2: The Properties of Vibration Finite Element Analysis Samples.....	31
Table 3: The Dimensions of Vibration Finite Element Analysis Samples.....	31
Table 4: Theoretical Natural Frequencies for ABS Rectangular Samples.....	65
Table 5: Theoretical Frequency Ratios for ABS Rectangular Samples.....	65
Table 6: Experimental Natural Frequencies for ABS Rectangular Samples.....	66
Table 7: Experimental Frequency Ratios for ABS Rectangular Samples.....	66
Table 8: Finite Element Natural Frequencies for ABS Rectangular Samples.....	67
Table 9: Finite Element Frequency Ratios for ABS Rectangular Samples.....	67
Table 10: Comparisons of Calculated Experimental, Finite Element and Theoretical Natural Frequencies.....	68
Table 11: Comparisons of Calculated Experimental, Finite Element and Theoretical Frequencies Ratios.....	69
Table 12: Modal Densities.....	69

LIST OF FIGURES

Figure 3.1: Geometry dimensions and coordinates of a rectangular plate with uniform thickness.....	12
Figure 4.1: Schematic of hardware used in performing a vibration test.....	21
Figure 4.2: Experimental Model of Sample 1.....	22
Figure 4.3: Geometry used in Pulse modal software and the Hammer hit points of Sample1.....	22
Figure 4.4: Experimental Model of Sample 2.....	23
Figure 4.5: Geometry used in Pulse modal software and the Hammer hit points of Sample2.....	23
Figure 4.6: Experimental Model of Sample 3.....	24
Figure 4.7: Geometry used in Pulse modal software and the Hammer hit points of Sample3.....	24
Figure 5.1: FEM Model of Sample1.....	28
Figure 5.2: FEM Model of Sample2.....	29
Figure 5.3: FEM Model of Sample3.....	30
Figure 6.1: The First Mode Shape of the Sample1 from PULSE.....	41
Figure 6.2: The Second Mode Shape of the Sample1 from PULSE.....	42
Figure 6.3: The Third Mode Shape of the Sample1 from PULSE.....	43
Figure 6.4: FRF of the Sample1.....	44
Figure 6.5: The First Mode Shape of the Sample2 from PULSE.....	45
Figure 6.6: The Second Mode Shape of the Sample2 from PULSE.....	46
Figure 6.7: The Third Mode Shape of the Sample2 from PULSE.....	47
Figure 6.8: FRF of the Sample2.....	48
Figure 6.9: The First Mode Shape of the Sample3 from PULSE.....	49
Figure 6.10: The Second Mode Shape of the Sample3 from PULSE.....	50

CHAPTER 1

INTRODUCTION

Plates are essential components of many engineering structures; therefore, the vibration analyses of plates are mandatory for safe design. The rectangular plates have been commonly used in various engineering fields, such as marine, nuclear, and aerospace. Many researchers have attempted to obtain accurate solutions for the vibration analyses of rectangular plates with completely free boundary conditions. However, the most analytical solutions have been considered as approximate. Especially, Leissa has gone through many solution approaches concerning this problem in his literature of plate vibration. The primary difficulty of this problem is to obtain accurate functions which fully satisfy the free boundary conditions and governing equation of motion at the same time. The vibrations solutions of plates have been taken in the form of a series of products of free-free eigenfunctions by most of the researchers. Nevertheless, we are familiar with these eigenfunctions which do not completely satisfy the free edge boundary conditions of rectangular plates. Therefore, the energy method, which is considered to be the best approximate, is used to describe Eigenvalues.

Great classical researchers, such as Cauchy, Poisson, Navier, Lagrange and, Kirchhoff as will be detailed later, have played an incredibly significant role to derive the accurate solutions for the vibrations of plates with completely free. They have proposed and developed various methods which are still used today. In conjunction with modern technological development, the finite element method, which is one of the most powerful

methods for the vibration analysis of plates, has become really useful for the dynamical analysis of structures, and will be widely employed in this work.

In this research, the dynamic characteristics of ABS (Acrylonitrile-Butadiene-Styrene) rectangular plates, such as frequencies and mode shapes, are obtained by the experimental and finite element modal analysis techniques. ABS materials have started being used in many industrial products exponentially because of its special properties, including high impact strength, ductility, good impact resistance, good chemical resistance, and abrasion resistance. Particularly, ABS exhibits really high impact strength; therefore, it is used in industry products which require high impact strength materials, such as construction safety helmets, and military helmets. The determination of the dynamic characteristics of ABS samples is going to provide us very good indications for their stiffness and easy to measure by other means detailed performance expectations in various service situations.

Industry has been looking for new innovative materials to develop a new military helmet which is lighter, more resistant to blast, ballistic and blunt impact. Among innovative materials, plastics are really attractive to researchers because of their unique properties. ABS, which is a thermoplastic material, seems to be very convenient to design new military helmets and increase the levels of ballistic protection because of its special properties as mentioned earlier. Particularly, its impact strength is much better than most other thermoplastics. Nevertheless, one concern is that it is difficult to manufacture this kind of material due to its rigidity and stiffness. In this research, the modal densities of ABS samples are obtained experimentally to have a valid idea concerning how complex

our samples are. The sample, which has the highest modal density, requires more effort and costs more money in design.

In this study, three different ABS rectangular plates, which have dimensions 114.3mm x 76.2 mm x 6 mm, 106.68 mm x 71.12 mm x 6 mm, and 76.2 mm x 50.8 mm x 6 mm, respectively.

The first three fundamental frequencies of each sample are calculated analytically to compare them with the fundamental frequencies which are acquired by the experiment and finite element methods.

CHAPTER 2

LITERATURE REVIEW AND OBJECTIVES

The aim of this section is to review the theoretical and finite element backgrounds of this research in respect of the vibration of rectangular plates. Section 2.1 evaluates articles regarding theoretical vibration approaches of rectangular plates. Section 2.2 deals with the finite element modal frequency analysis of rectangular plates. What conclusions we obtained from the Section 2.1 and Section 2.2 are illustrated in Section 2.3. Finally, the Section 2.4 provides the objectives of this research.

2.1 Theoretical Vibration Method

Rectangular plates have been widely used in various engineering fields, including aerospace, mechanical, nuclear, marine, and structural engineering. There are many references available for the numerical and theoretical vibration analysis of rectangular plates. The study of plate began with the German physicist, Chladni (1787). Nodal patterns for a flat square plate were observed by Chladni. In his experiments on the vibrating plate, he noticed that vertical displacements were equal to zero along nodal lines.

A differential equation for transverse deformation of plates was obtained by a French mathematician- Sophie Germain- in the early 1800s. Nevertheless, she made a crucial mistake with disregarding the strain energy from the warping of the plate midplane. The right form of the governing equation, without its derivation, was discovered in Lagrange's notes in 1813, after he passed away. Hence, Lagrange has been accepted to be the first person who has used the right differential equation for the

vibration analysis of thin plates. The accurate differential equation for rectangular plates with flexural resistance was obtained by Navier (1785-1836). The precise bending solutions for simply supported rectangular plates were easily calculated by Navier. Navier's work was developed for vibration analysis of circular plates by Poisson in 1829. The developed plate theory was considered as the combination of bending and stretching actions which has been credited to Kirchhoff (1850).

A present theory for the determination of the natural frequencies of vibrating structures was derived by Lord Rayleigh in 1877. Based on Kirchhoff and Rayleigh's theory, Voigt (1893) and Carrington (1925) indicated remarkable achievements with obtaining the exact vibration frequency solutions for a simply- supported rectangular plate and a fully-clamped circular plate. The problem of the freely vibrating plate was solved by Ritz in 1909. He illustrated how to reduce the upper bound frequencies by taking more than a single admissible function into consideration and performing a minimization with respect to the unknown coefficients of these admissible functions. The method is known as the Ritz method.

Based on the Kirchhoff plate theory for thick plates, where the effect of shear deformation is important and cannot be negligible, a first order shear deformation plate theory was proposed by Hencky (1947) and Reissner (1945). A variational approach for deriving the governing plate equation for free vibration of first-order shear deformable plates and incorporated the effect of rotary inertia was explained by Mindlin in 1951. However, in Mindlin's theory, using a shear correction factor is necessary to compensate for the error due to the assumption of a constant shear strain (and thus constant shear stress) through the plate thickness that breaks the zero shear condition at the free

surfaces. The correction factors not only rely on the boundary conditions and loading but also on material and geometric parameters. However, Wittrick (1973) pointed out that obtaining the shear correction factors for general orthotropic plates may be impossible.

Reddy (1984, 1997) proposed a more improved and refined theory without shear correction factors. His third-order shear deformation theory confirms that the zero shear stress at the free surfaces of the plate is satisfied at the outset.

In 1970, Srinivas developed a three dimensional linear, small deformation theory of elasticity solution by the direct method for the free vibration of simply-supported thick rectangular plates.

By using a lower order finite layer technique, Cheung and Chakrabarti (1972) examined the free vibration of isotropic plates with different types of boundary conditions, for three different aspect ratios. The resultant frequencies for the smallest thickness/span ratio are close to those existing for thin plates, while frequencies for higher thickness/span ratios tend to be of lower values.

In the paper by Gorman (1978), the superposition method was used in free vibration analysis of completely free rectangular plates. In this new approach to the problem, he obtained a new solution which satisfies the boundary conditions and the differential equation identically with any desired degree of accuracy. In plate vibration problem, there are three characteristic families of modes, such as doubly antisymmetric, doubly symmetric and symmetric-antisymmetric. The exact description was made between the three families of modes by Gorman. Using this method is considered to be easy, convergence is extraordinarily fast, and it is easy to obtain eigenvalues and modal

shapes of any degree of exactitude, because the method is described in dimensionless form at length by Gorman.

In 1996, Ding calculated natural frequencies of rectangular plates by using a set of static beam functions in Rayleigh-Ritz method. The static beam functions, which are developed by Ding, are used to be the basis functions in the Rayleigh-Ritz method to work on the vibrational attributes of isotropic, thin rectangular plates. In applications, using a small number of basis functions is needed, and a small amount of computation is mandatory. He gave some numerical results for rectangular plates with different aspect ratios and boundary conditions. Therefore, he obtained good accuracy and fast convergence. This approach is found to be easy and straightforward.

In the paper by Gorman (2004), analytical-type solutions for free in-plane vibration of rectangular plates are derived by using the method of superposition. The boundary conditions and differential governing equations are indicated in dimensionless form. He considered the problem of free in-plane vibration of the completely free rectangular plate, as well, and obtained rapid convergence.

In 2003, Sheikh analyzed the free vibration of both the thin and thick plates. The solution depends upon the Reissner-Mindlin Theory by adopting a new type of triangular element with three nodes at corners, three others at mid of the three sides and one internal node at the center of the element.

In 2007, Wu, Liu, and .Chen calculated the exact solutions for free-vibration analysis of rectangular plates by using Bessel functions. They proposed the novel Bessel function to derive the exact solutions of the free vibration analysis of rectangular thin

plates with three edge conditions: fully simply supported, fully clamped, and two opposite edges simply supported and the other two edges clamped. Because Bessel functions satisfy the biharmonic differential equation of solid thin plate, the basic idea of the method is to superpose different Bessel functions to satisfy the edge conditions such that the governing differential equation and the boundary conditions of the thin plate are exactly satisfied. It is indicated that the method provides direct, simple, and highly accurate solutions for this family of problems.

In 2009, Xing, and Liu proposed new exact solutions for free vibrations of rectangular thin plates by symplectic dual method. In the paper, the separation of variables is applied to resolve the Hamiltonian dual form of the eigenvalues problem for transverse free vibrations of thin plates, and formulation of the natural mode in closed form is performed. The closed form natural mode satisfies the governing equation of the eigenvalue problem of thin plate precisely and is applicable for any types of boundary conditions. With all combinations of simply supported and clamped boundary conditions applied to the natural mode, the mode shapes are obtained uniquely and two eigenvalues equations are derived with respect to spatial coordinates, with the aid of which normal modes and frequencies are solved exactly.

2.2 Finite Element Modal Frequency Analysis

The finite element method started being used around the mid of 1950s to determine natural frequencies and mode shapes for structures. The method, which permits to handle the numerical solution of complex plate and shell problems in an

efficient way, was introduced by Turner, et al. in 1951. Argyris (1960) and Zienkiewicz (1977) made many contributions to this field.

In recent years, particularly, the Ritz method has been accepted to be an effective alternative to other numerical approaches for the free vibration analysis of plates of arbitrary shape and boundary conditions. One of the most significant advantages of the Ritz method is to automatically satisfy the geometric boundary conditions. The development of the Ritz method allows handling the vibration analysis of complicated plate structures.

2.3 Conclusions of Literature Review

For rectangular plates, there are 21 various boundary conditions which include all possible combinations of classical boundary conditions, such as fixed, clamped, simply supported and free. Exact vibration solutions are available for plates with at least two opposite edges simply supported. Therefore, the remaining 15 cases have caught the attention of researchers. [18]

From Section 2.1, it is readily seen that obtaining accurate solutions to determine natural frequencies and mode shapes of plates with completely free boundary conditions is much more difficult than plates with other boundary conditions. The difficulty is to determine the governing differential equations which satisfy all boundary conditions because of the free edges and free corners and also additional symmetry. One of the most significant methods is the Ritz method to determine natural frequencies and mode shapes for plates with completely free boundary conditions. In the Ritz approach, the boundary

conditions of displacements are precisely satisfied; however, the natural boundary conditions and the governing differential equations are approximately satisfied.

The theoretical difficulty of describing natural frequencies and mode shapes for rectangular plates inspires us to use the finite element method which is explained in the Section 2.2. The finite element approach allows us to calculate natural frequencies and determine mode shapes in an effective way for any structure with arbitrary boundary conditions. The finite element method is based on the Ritz method. As mentioned earlier, the Ritz method is an approximate method; therefore, conducting an experimental modal analysis is required in order to figure out the natural frequencies and mode shapes to compare them with the finite element results.

2.4 Objectives

From the literature review, the vibration method used to determine the fundamental frequencies of the ABS rectangular samples. The finite element method and the experimental modal analysis are done to describe the natural frequencies and mode shapes. The objectives of this study may be written as follow:

The primary objective of this research is to conduct the experimental modal analysis on the ABS rectangular plates to obtain their modal parameters, such as frequencies and mode shapes.

The second objective is to acquire modal parameters from the finite element modal analysis.

The third objective is to analytically calculate the first three natural frequencies for each sample

The fourth objective of this research is to obtain a constant ratio between the first, second, and third fundamental frequencies regardless of the dimensions of the samples.

The fifth objective is to compare the experimental, analytical and finite element results.

The sixth and final objective is to figure out the modal densities and damping ratios of samples.

As stated earlier, it is really difficult to analytically determine natural frequencies for rectangular plates with completely free boundary conditions because of free edges. Therefore, conducting the vibration experiment is vital to obtain certain resonance frequencies of rectangular plates. The finite element analysis is also significant to obtain natural frequencies and mode shapes. When the experimental and finite element results, such as mode shapes, and frequencies, are compared, it will make us sure regarding the results. The significance of determining the modal densities and damping ratios of the samples is to make a decision on how complex the samples and how soft or hard the samples are, respectively. If the modal density is higher, the structure is more complex. More complex materials require more effort in design manufacturing processes. In other words, they cost more money.

CHAPTER 3

THE ANALYTICAL MODEL OF VIBRATING PLATES

3.1 The Free Vibration of Rectangular Plates with Completely Free

The geometric configuration of an isotropic rectangular plate is shown in Fig 3.1.

The plate has a length a , width b and a uniform thickness h .

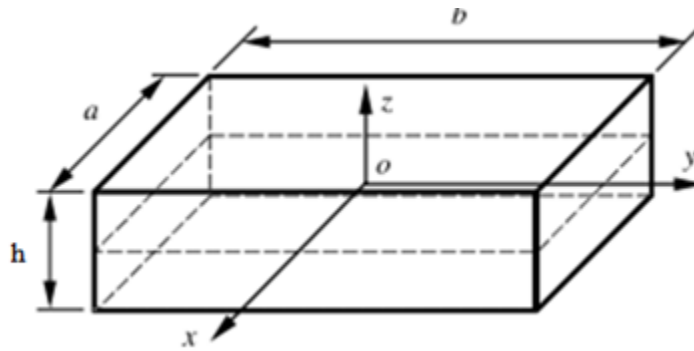


Fig 3.1 Geometry, dimensions and coordinates of a rectangular plate with uniform thickness

The x - y plane is taken to be the middle plane of the plate and deflections in the z direction are assumed to be small, when they are compared with the thickness h . In addition, we assume that the normal to the middle plane of the plate remains normal to the deflected middle surface during vibrations. Then, the strains can be written as:

$$\varepsilon_x = -z \frac{\partial^2 w}{\partial x^2} \quad \varepsilon_y = -z \frac{\partial^2 w}{\partial y^2} \quad \gamma_{xy} = -2z \frac{\partial^2 w}{\partial x \partial y} \quad (3.1)$$

The deflection of the plate in the z direction in these expressions is represented by w . The normal strains and the shear strain in the thin layer are denoted by ε_x , ε_y , and γ_{xy} , respectively.

The stress and strain relationships for the plate may be written as;

$$\begin{aligned}\sigma_x &= \frac{E}{1-\nu^2} (\varepsilon_x + \nu\varepsilon_y) = -\frac{Ez}{1-\nu^2} \left(\frac{\partial^2 w}{\partial x^2} + \nu \frac{\partial^2 w}{\partial y^2} \right) \\ \sigma_y &= \frac{E}{1-\nu^2} (\varepsilon_y + \nu\varepsilon_x) = -\frac{Ez}{1-\nu^2} \left(\frac{\partial^2 w}{\partial y^2} + \nu \frac{\partial^2 w}{\partial x^2} \right) \\ \tau_{xy} &= G\gamma_{xy} = -\frac{Ez}{(1+\nu)} \frac{\partial^2 w}{\partial x \partial y}\end{aligned}\quad (3.2)$$

In these equations, ν represents the Poisson's ratio.

During deformation, the potential energy of the element is written as:

$$dU = \left(\frac{\varepsilon_x \sigma_x}{2} + \frac{\varepsilon_y \sigma_y}{2} + \frac{\gamma_{xy} \tau_{xy}}{2} \right) dx dy dz \quad (3.3)$$

When the equations (3.1) and (3.2) are substituted into the equation (3.3), the new potential energy equation is obtained as written below.

$$dU = \frac{Ez^2}{2(1-\nu^2)} \left\{ \left(\frac{\partial^2 w}{\partial x^2} \right)^2 + \left(\frac{\partial^2 w}{\partial y^2} \right)^2 + 2\nu \frac{\partial^2 w}{\partial x^2} \frac{\partial^2 w}{\partial y^2} + 2(1-\nu) \left(\frac{\partial^2 w}{\partial x \partial y} \right)^2 \right\} dx dy dz \quad (3.4)$$

The integration of the equation (3.4) gives us the bending potential energy as:

$$U = \iiint dU = \frac{D}{2} \iint \left\{ \left(\frac{\partial^2 w}{\partial x^2} \right)^2 + \left(\frac{\partial^2 w}{\partial y^2} \right)^2 + 2\nu \frac{\partial^2 w}{\partial x^2} \frac{\partial^2 w}{\partial y^2} + 2(1-\nu) \left(\frac{\partial^2 w}{\partial x \partial y} \right)^2 \right\} dx dy \quad (3.5)$$

Where, D is known as the flexural rigidity of the plate.

$$D = \frac{Eh^3}{12(1-\nu^2)} \quad (3.6)$$

E is Young's modulus, ν is Poisson's ratio, and h is the plate thickness.

$$T = \frac{\rho h}{2} \iint w^2 dx dy \quad (3.7)$$

The equation (3.7) represents the kinetic energy for the transversely vibrating plate.

It is necessary to mention that overcoming the free vibration problems of plates with completely free boundary conditions is much more difficult than plates with other boundary conditions, such as fixed and simply supported. The Ritz's first approach, which is really practical for the calculation of natural frequencies of plates with completely free boundary conditions, is applied to the plate by making some assumptions.

$$w = Z \cos(\omega t - \alpha) \quad (3.8)$$

The mode of vibration is approximated by Z , which is a function of x and y . The maximum kinetic and potential energies for the plate can readily be derived by substituting the equation (3.8) into the equations (3.5) and (3.7) as followed:

$$U_{\max} = \frac{D}{2} \iint \left\{ \left(\frac{\partial^2 Z}{\partial x^2} \right)^2 + \left(\frac{\partial^2 Z}{\partial y^2} \right)^2 + 2\nu \frac{\partial^2 Z}{\partial x^2} \frac{\partial^2 Z}{\partial y^2} + 2(1-\nu) \left(\frac{\partial^2 Z}{\partial x \partial y} \right)^2 \right\} dx dy \quad (3.9)$$

$$T_{\max} = \frac{\rho h}{2} \omega^2 \iint Z^2 dx dy \quad (3.10)$$

The solution for ω^2 is obtained by equating the equations (3.9) and (3.10) as indicated below.

$$\omega^2 = \frac{2}{\rho h} \frac{U_{\max}}{\iint Z^2 dx dy} \quad (3.11)$$

When the function Z is taken in the form of a series, we can write as:

$$Z = a_1 \phi_1(x, y) + a_2 \phi_2(x, y) + a_3 \phi_3(x, y) + \dots \quad (3.12)$$

The determination of coefficients a_1, a_2, a_3 is required. Each term of the equation (3.12) fulfils the boundary conditions of the plate. The system equation, which is shown below, is derived by minimizing the outcomes of equation (3.11).

$$\frac{\partial}{\partial a_j} \iint \left\{ \left(\frac{\partial^2 Z}{\partial x^2} \right)^2 + \left(\frac{\partial^2 Z}{\partial y^2} \right)^2 + 2\nu \frac{\partial^2 Z}{\partial x^2} \frac{\partial^2 Z}{\partial y^2} + 2(1-\nu) \left(\frac{\partial^2 Z}{\partial x \partial y} \right)^2 - \frac{\omega^2 \rho h}{D} Z^2 \right\} dx dy = 0 \quad (3.13)$$

The frequency equation is obtained by equating to zero the determinant of the coefficients in the above equations. This method was applied by Ritz to a square plate with free edges. The equation (3.12) was taken into consideration by describing it in the form

$$Z = \sum_m \sum_n a_{mn} X_m(x) Y_n(y) \quad (3.14)$$

The different modes of vibration for the frequencies can be expressed as:

$$\omega = \frac{\lambda^2}{a^2} \sqrt{\frac{D}{\rho h}} \quad (3.15)$$

In this formula, λ^2 represents a constant value depending on the mode. Values of constant λ^2 for completely free rectangular plates with various aspect ratios (a/b) are tabulated in Table 1.

Table1. Frequency Parameter λ^2 for F-F-F-F plates ($\nu=0.3$)

Mode Sequence	a/b				
	0.4	2/3	1	1.5	2.5
1	3.4629	8.9459	13.489	20.128	21.643
2	5.2881	9.6015	19.789	21.603	33.050
3	9.6220	20.735	24.432	46.654	60.137
4	11.437	22.353	35.024	50.293	71.484
5	18.793	25.867	35.024	58.201	117.45
6	19.100	29.973	61.256	67.494	119.38

CHAPTER 4

EXPERIMENTAL MODAL ANALYSIS

4.1 Introduction

The primary aim of the experimental modal analysis is to determine the modal parameters (frequencies, modal scaling, modal factors and damping factors) of a linear, time invariant system by way of an experimental approach. Although the modal parameters can be determined by finite element analysis, the experimental modal analysis is mandatory for the correction/verification of the results of the finite element analysis. Mainly, experimental modal analysis is used to describe a dynamics problem, vibration, which is not clear from analytical models. It is significant to be aware that most vibration problems are a function of both the forcing functions and the system characteristics explained by the modal parameters. Experimental modal analysis methods are based on the theoretical relationship between measured quantities and the classic vibration theory that is generally illustrated as matrix differential equations. All modern methods rely on the matrix differential equations; however, a final mathematical form is obtained in terms of measured data. The measured data can be some form of processed data, including impulse response function and frequency response function. The measured data can also be output and raw input file. Hence, basically, modal analysis is a method to describe a structure in terms of its dynamic properties, such as frequency, damping and mode shapes.

4.2 The Test Procedure of Vibration

All uncontrolled undesirable phenomenon gives rise to noise, causes mechanical stress and is a possible cause of structural failure. As part of a general environmental test program or as a part of engineering design, vibration testing performs the vital role of finding out how well a component can endure the vibration environments which it is likely to encounter in a real life situation.

The Pulse 15.1-MTC software vibration analysis which is produced by the Bruel & Kjaer Company is used to determine the fundamental frequencies and the mode shapes in the frequency range of 0 Hz to 6000 Hz. The software is calibrated by the company. The used force transducer and impact hammer type 8203 that is also manufactured by the Bruel & Kjaer Company, is a unique structural testing kit designed for use with lightweight and delicate structures. The force transducer measures the force applied to the structure. This type of the impact hammer has many advantages, such as good linearity, excellent long term stability, individually calibrated and easily mounted, easily attached to the stringer and hammer kits, and aluminum shaft to reduce the occurrence of double impact. The piezoelectric accelerometer is preferred to acquire data for the determination of natural frequencies because it offers tremendous versatility for vibration measurements and it is widely accepted as the best available transducer for the absolute measurement of vibration. This sensor can withstand adverse environmental conditions. The piezoelectric accelerometer exhibits better all-round characteristics than any other type of vibration transducer. It has very wide frequency and dynamic ranges with good linearity throughout the ranges. It is relatively robust and reliable so that its characteristics remain stable over a long period of time. Additionally, the piezoelectric accelerometer is self-

generating, so that it doesn't need a power supply. There are no moving parts to wear out, and finally, its acceleration proportional output can be integrated to give velocity and displacement proportional signals. The Figure 4.1 shows the schematic of hardware used in performing a vibration test. It is significant to emphasize that using sufficient measurement points is important to describe all of the modes of interest. If adequate response points are not selected carefully and measured, particular mode may not be represented sufficiently. How measurement points for each experimental sample were selected diligently illustrated in the Figure4.2, Figure4.4 and Figure4.6. Geometries used in the Pulse software and the hammer hit points of each sample were indicated in the Figure 4.3, Figure 4.5 and Figure 4.7. 49 measurement points were used in the Sample1, which has dimensions 114.3 mm x 76.2mm x 6 mm. 28 measurement points were used in the Sample2, which has dimensions 106.68 mm x 71.12mm x 6 mm. Finally, 35 measurement points were used in the Sample2, which has dimensions 76.2 mm x 50.8 mm x 6 mm. The finite element modal analysis, which is going to be introduced in the Chapter 5, is going to figure out, if sufficient measurement points were used or not.

The vibration test procedure for measurement as follows.

- 1) Make a decision on which channel is going to be used in the experiment and introduced to the hardware.
- 2) Check the sensitivity of the accelerometer, according to the given information in the calibration sheet.
- 3) Prepare ABS rectangular samples which have dimension 114.3mm x 76.2mm x 6 mm, 106.68mm x 71.12 mm x 6, 76.2 mm x 50.8 mm x 6 mm as shown in

the Figure 4.2, Figure 4.6 and Figure 4.6, respectively. Divide them into 36 , 18 and 24 parts, respectively.

- 4) Create the geometry in the software by selecting rectangular shape and by inserting the length and width of the sample.
- 5) Assign the transducer to the points in the grid of the geometry as shown in Figure 4.3, Figure 4.5 and Figure 4.7, respectively.
- 6) Determine the frequency range from 0 Hz to 6000 Hz, hit 5 times on each point and average them to obtain accurate results.
- 7) To assign an average value of force to be used for the hammer trigger.
- 8) Set up the hammer weighting to filter the signal which is generated by the hammer from any noise.
- 9) Set up the response weighting to make sure that the signal decays exponentially in the specific time interval.
- 10) Measurements start exciting the structure by the hammer 5 times on each point, the accelerometer detects the response of the sample and sends the electrical voltage signal to the front-end processor which evaluates the data and sends it to the pulse software to calculate the natural frequencies by using FFT.
- 11) Do the post-analysis to acquire the natural frequencies, and the mode shapes.

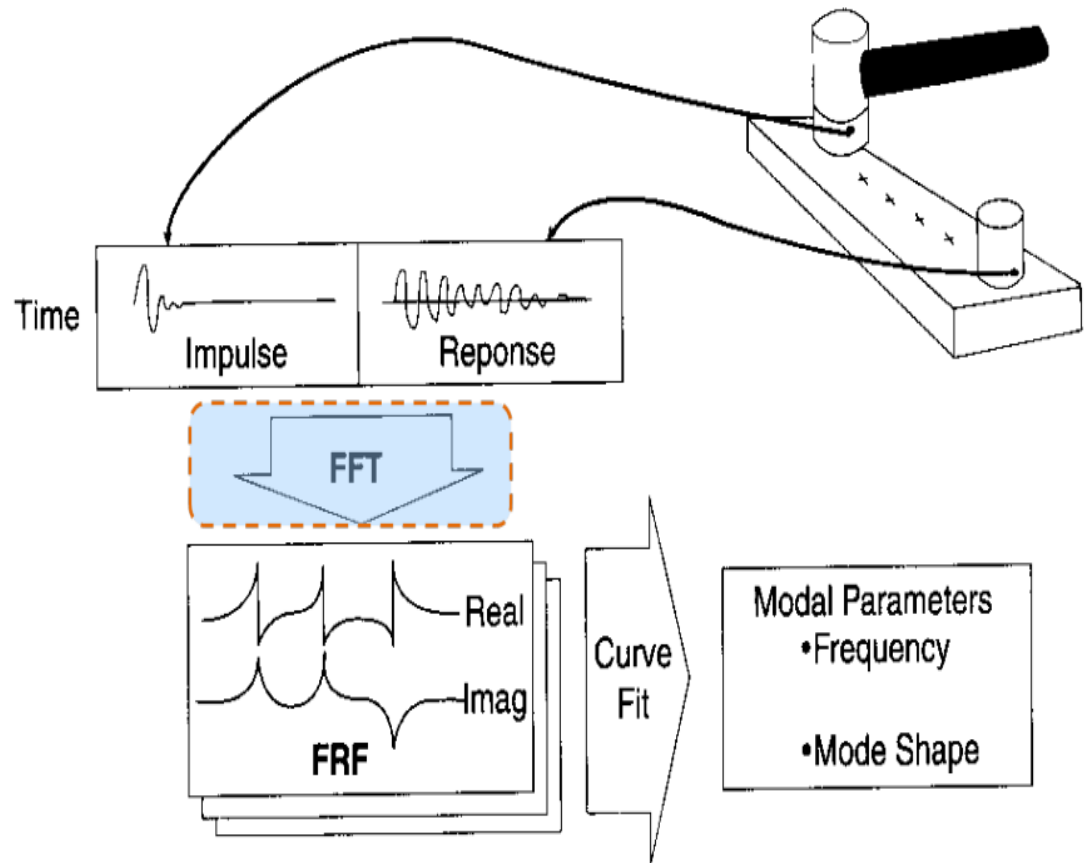


Figure 4.1 Schematic of hardware used in performing a vibration test

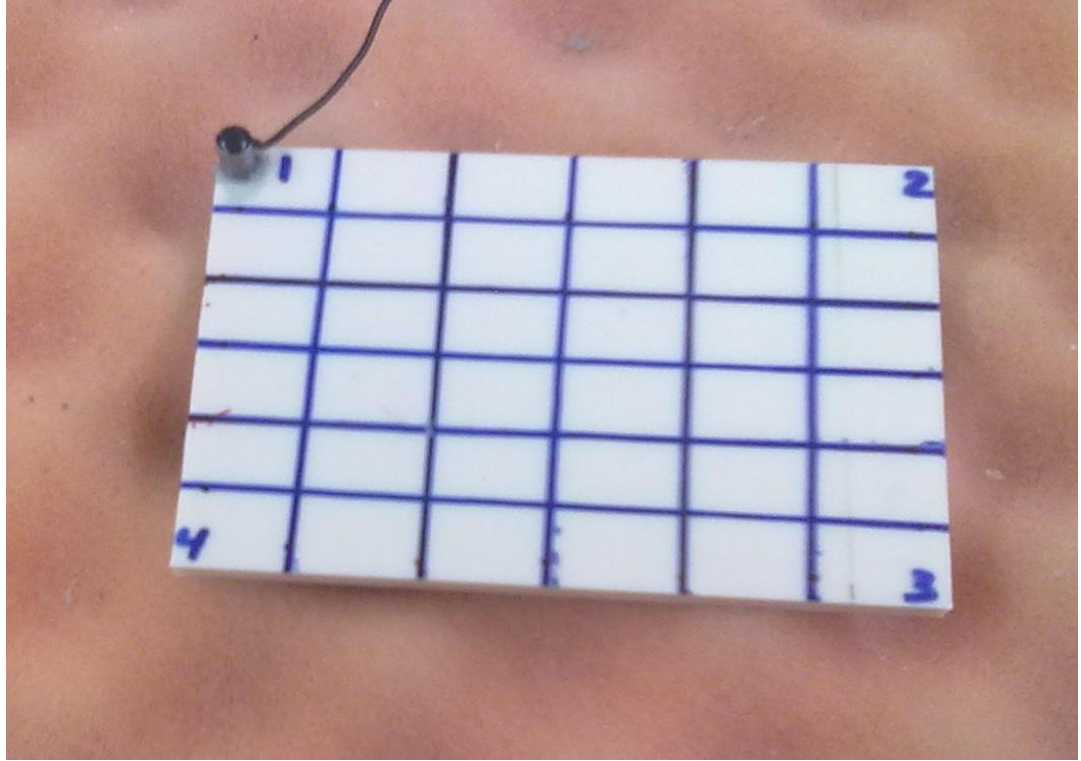


Figure 4.2 Experimental Model of Sample 1

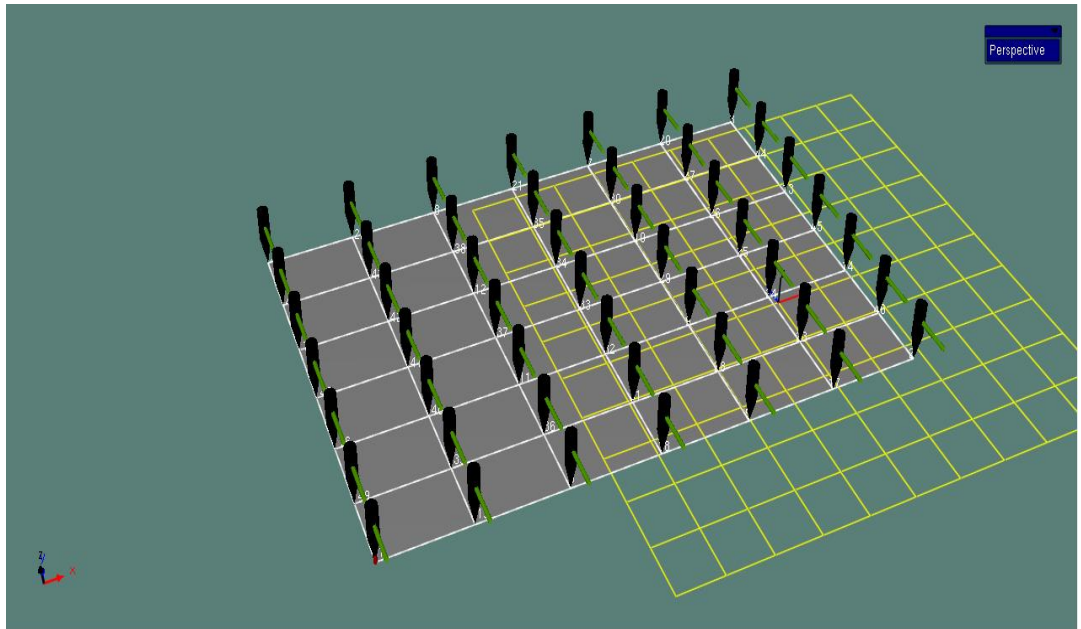


Figure 4.3 Geometry used in Pulse modal software and the Hammer hit points of Sample1

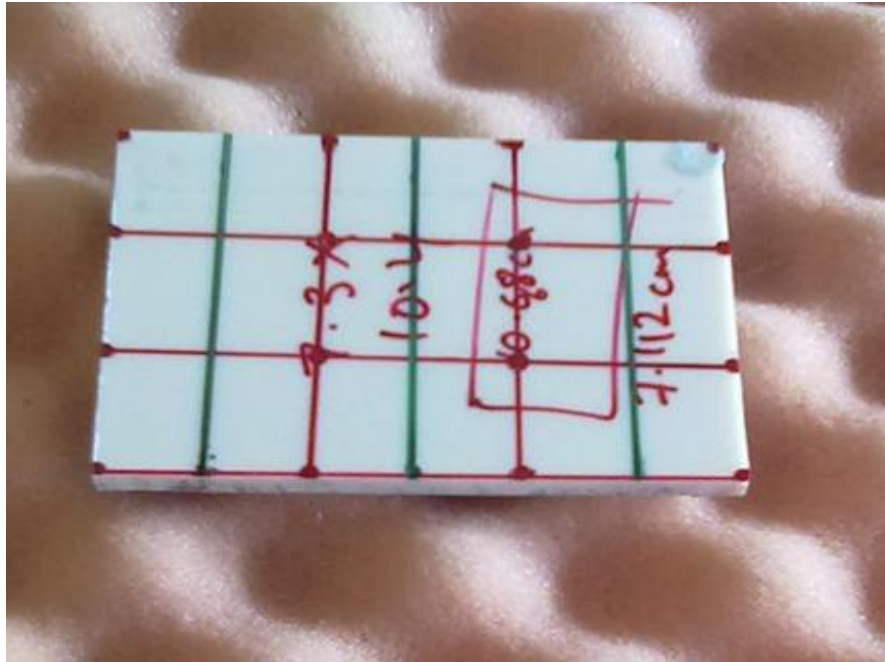


Figure 4.4 Experimental Model of Sample 2

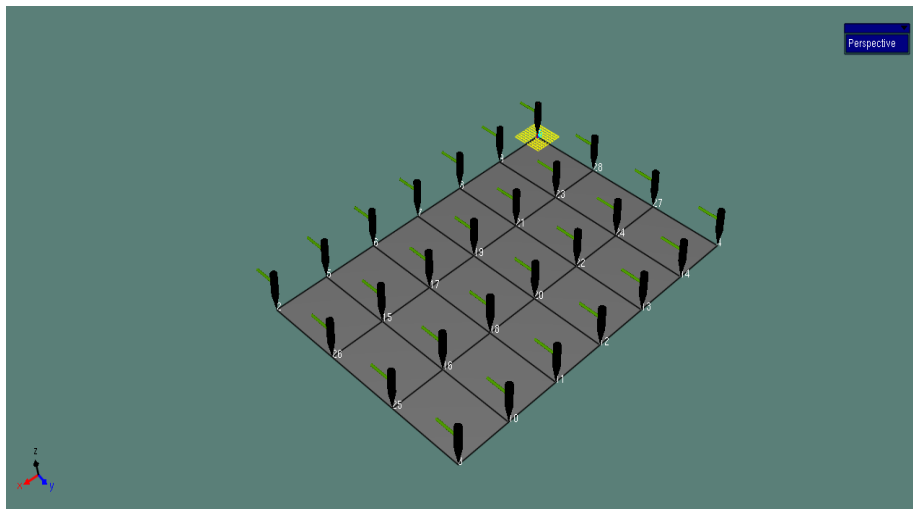


Figure 4.5 Geometry used in Pulse modal software and the Hammer hit points of Sample 2

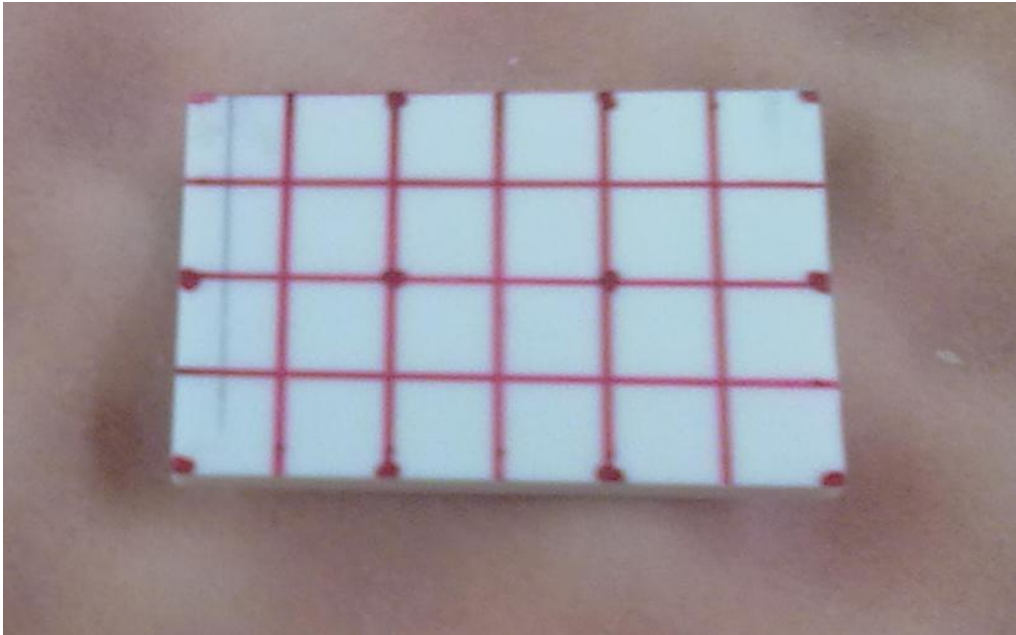


Figure 4.6 Experimental Model of Sample 3

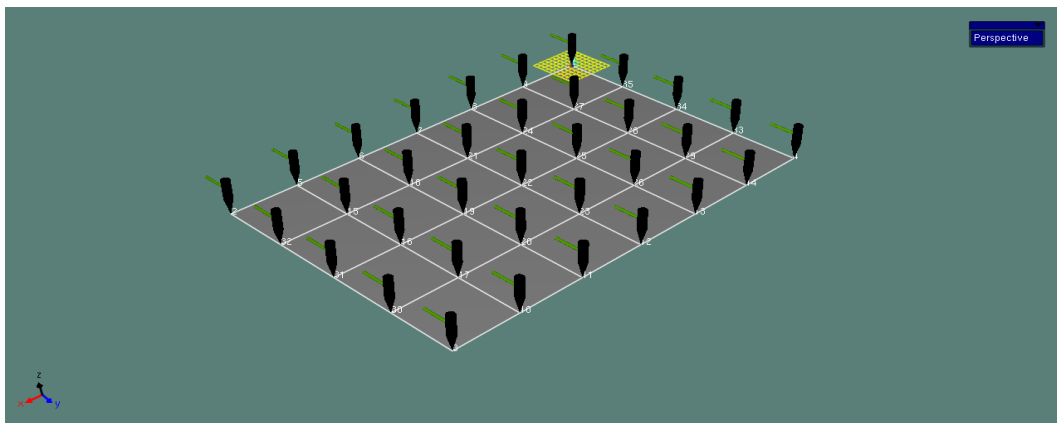


Figure 4.7 Geometry used in Pulse modal software and the Hammer hit points of Sample3

CHAPTER 5

FINITE ELEMENT ANALYSIS

5.1 Introduction

The finite element method is an extremely effective technique which uses interpolation and variational methods to determine natural frequencies and mode shapes for complex mechanical structures with unusual geometric shapes, such as frames, trusses and machine parts. In this method, the actual structure is divided into elements or parts which are called finite elements. Each element has nodes, which connect to the next element. A solution or approximation of an equation of motion for any structure is easy, because each element is really simple, such as a plate or beam. The combination of nodes and elements is called a finite element mesh. The governing equation of vibration is described and resolved for each individual element. Then the solutions of the individual element equations are approximated by a linear combination of low-order polynomials. These solutions are combined to obtain global and stiffness matrices, which illustrate the vibration of the entire structure. Natural frequencies and mode shapes are approximately derived by global and stiffness matrices. It is significant to state that the finite element method is based on the Ritz method which is an approximation method to calculate natural frequencies and mode shapes. Therefore, the finite element method provides approximate solutions for natural frequencies and mode shapes.

5.2 Finite Element Modal Analysis

All the samples are meshed by using the Hypermesh v10 as a preprocessor and Abaqus/Standard 3D is used as a solver to calculate the first three natural frequencies and

the mode shapes of the samples. The Lancsoz Eigensolver Method is selected in Abaqus/Standard 3D to describe the first three fundamental frequencies and mode shapes because this method is a powerful tool for extraction of the extreme eigenvalues and the corresponding eigenvectors of a sparse symmetric generalized eigenproblem. The samples are considered as solid rather than shell. It should be mentioned that using an appropriate element type is really significant in ABAQUS software to obtain accurate results. The C3D20R quadric element type, which is the second order of the C3D8R quadric element type, is the preferred one used in all the simulations. This element type allows us to increase the integration points on each element and to obtain more accurate results. There is no boundary condition which we need to determine because of the completely free boundary conditions specification. Displacements are normalized. Hypermesh post-processor is used to see the natural frequencies, displacements of results and mode shapes. The finite element calculation was carried out for ABS rectangular plates with the material properties and dimensions as indicated in Table2 and Table3, respectively.

The grid geometry of the Sample 1 was designed as ten layers of C3D20R brick elements with aspect ratio of 3.342. 21660 elements and 96199 nodes were used in the calculation of the Sample1, which is shown in the Figure 5.1.

The grid geometry of the Sample 2 was designed as ten layers of C3D20R brick elements with aspect ratio of 3.355. 19080 elements and 84913 nodes are used in the calculation of the Sample 2, which is shown in Figure 5.2.

The grid geometry of the Sample 3 was designed as ten layers of C3D20R brick elements with aspect ratio of 2.352. 19440 elements and 86493 nodes are used in the calculation of the Sample 3.

The input file for all samples is written below.

```

**HM_comp_by_property "ABS" 3

*SOLID SECTION, ELSET=ABS, MATERIAL=ABS

*MATERIAL, NAME=ABS

*DENSITY

1.0240E-09,0.0

*ELASTIC, TYPE = ISOTROPIC

2275.0 ,0.38 ,0.0

**HMNAME LOADSTEP 1 normal modes

*STEP, INC = 1000, PERTURBATION

*FREQUENCY, EIGENSOLVER = LANCZOS, NORMALIZATION =

DISPLACEMENT

12,,,,,

*NODE FILE

U,

*EL FILE, POSITION = AVERAGED AT NODES

S,

*END STEP

```

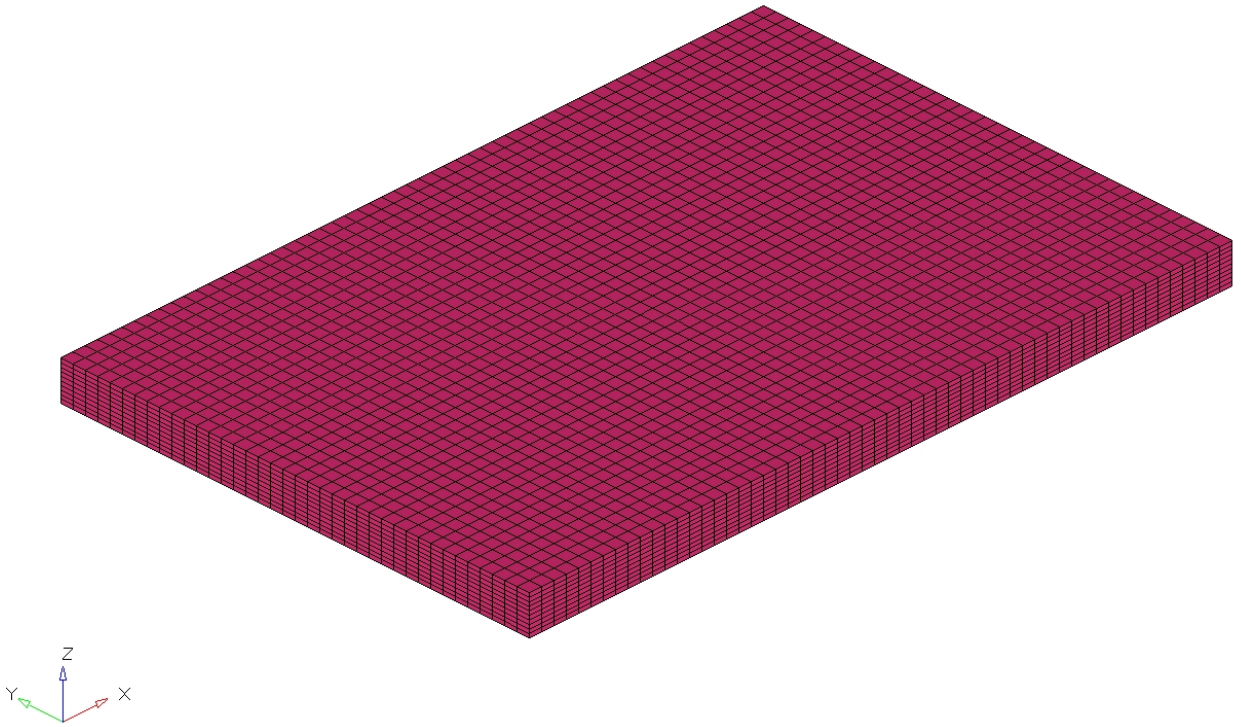


Figure 5.1 FEM Model of Sample1

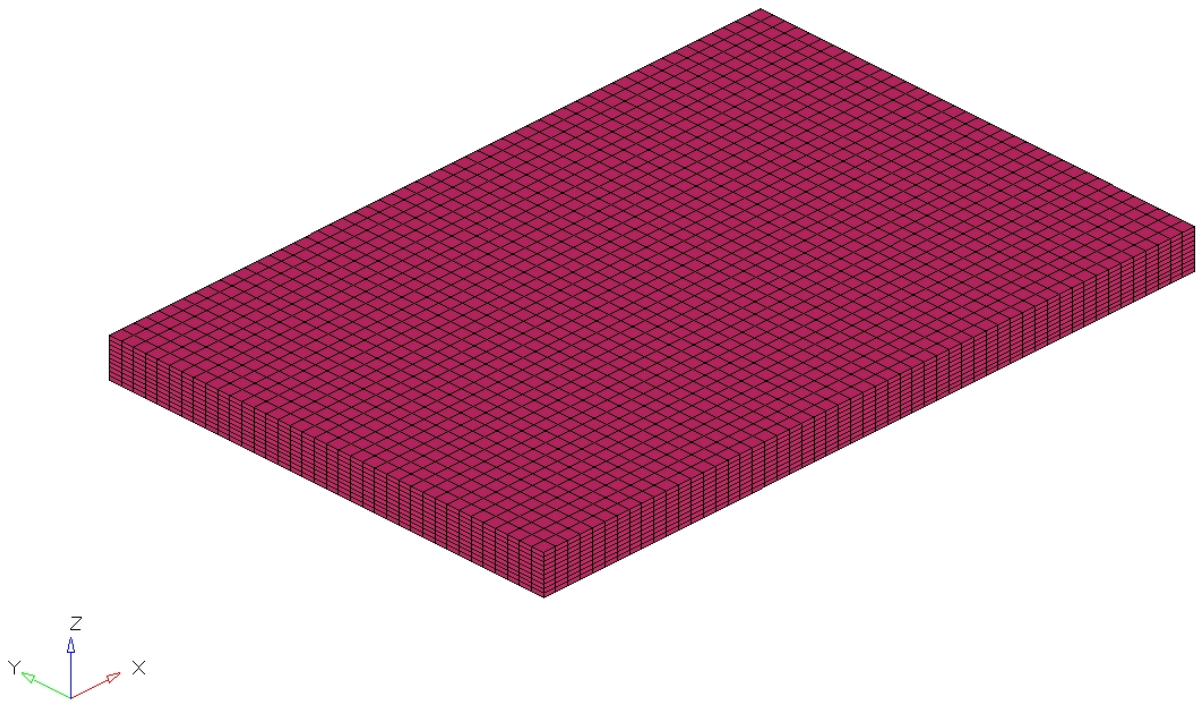


Figure 5.2 FEM Model of Sample2

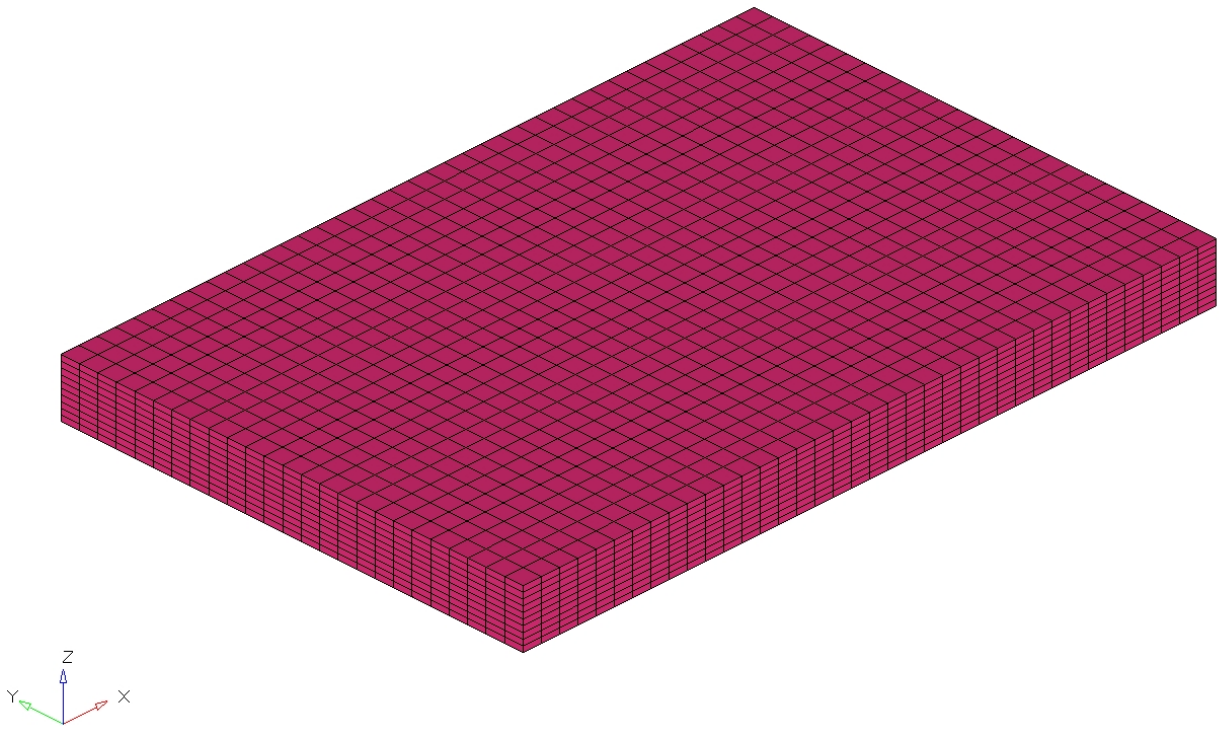


Figure 5.3 FEM Model of Sample3

Table2. The Properties of Vibration Finite Element Analysis Samples

	Young's Modulus (Mpa)	Poisson's Ratio	Density(ton/mm ³)
Rectangular ABS Model	2275	0.38	1024E-12

Table3. The Dimensions of Vibration Finite Element Analysis Samples

Rectangular ABS Samples	Length(mm)	Width(mm)	Thickness(mm)
Sample1	114.3	76.2	6
Sample2	106.68	71.12	6
Sample3	76.2	50.8	6

CHAPTER 6

RESULTS AND DISCUSSIONS

6.1 Theoretical Results

Natural frequencies for each sample were calculated analytically by using the equation (3.15). In all our cases, the aspect ratio (a/b) is always equal to 1.5; therefore, λ^2_1 , λ^2_2 and λ^2_3 were taken from the Table1 to be 20.168, 21.603 and 46.654, respectively. The obtained results were tabulated in the Table4. From the Table4, it can be concluded that while dimensions decrease with keeping the aspect ratio constant, natural frequencies increase. The f_1/f_2 and f_1/f_3 for each sample were obtained to figure out if there is any correlation between natural frequencies or not. The ratios were indicated in the Table5. According to the Table5, f_1/f_2 is always equal to 0.932 and f_1/f_3 is always equal to 0.431. Perhaps, we can say that there is no need to calculate the second and the third fundamental frequency for any rectangular plates with the aspect ratio 1.5

6.2 Experimental Results

By the Pulse software, the first three fundamental frequencies and mode shapes were obtained for each ABS sample. It is supposed to be mentioned that the mode shapes in the Pulse software are not the exact mode shapes. They are called deformation mode shapes, which are different than the exact mode shapes. In all experimental mode shape images, the number of points, which we hit, can be seen readily. The first mode shape of each ABS rectangular plate was shown in Figure 6.1, Figure 6.5 and Figure 6.9. This mode shape is known as the first twisting mode shape. In this mode shape, each sample has two nodal lines on which deflections are zero.

The frequency response function, which explains how the response of the plate due to the applied force, is shown in the Figure 6.4 for the Sample1. The Figure 6.2, Figure 6.6 and Figure 6.10 indicate the second mode shape for each sample. This mode shape is a bending mode shape. Two nodal lines can be seen on each sample. The frequency response function for the Sample2 is indicated in Figure 6.8. The third mode shape for each sample was illustrated in Figure 6.3, Figure 6.7 and Figure 6.11. In this mode shape, three nodal lines were seen on each sample. This mode shape is called the second twisting mode shape in our case. The frequency response function for the Sample3 was shown in Figure 6.12. The all obtained natural frequencies for each sample were tabulated in Table 6. From the Table 6, the all natural frequencies increase, while the dimensions of ABS rectangular plates decrease. The experimental frequency ratios of f_1/f_2 and f_1/f_3 were indicated in Table7 for each sample. From the Table 7, it may be deduced that all ratios for each sample are close to one another. The damping ratios of the ABS samples for the first three modes were experimentally calculated by the Pulse and these results were compared in Figure 6.32. The Table 12 shows the modal densities of the samples which were acquired from the Pulse. A large frequency range was used to obtain the modal densities.

6.3 Finite Element Results

As mentioned earlier in the Chapter 5, the Abaqus/Standard3D was used to obtain the first three fundamental frequencies and see the first three mode shapes for each sample. The first three mode shapes and fundamental frequencies for the Sample 1, Sample 2 and Sample 3 were shown in the Figure 6.13, Figure 6.19 and Figure 6.25, respectively. It can be readily seen from the Figure 6.14, Figure 6.20 and Figure 6.26

that the first mode shape has two nodal lines along where the deflection is equal to zero. Each ABS rectangular sample was equally divided into four parts by the nodal lines. While the two parts go down, the other two parts go up. This mode shape is called the first twisting mode of rectangular plates with completely free. The second mode shape of each sample was indicated in the Figure 6.15, Figure 6.21 and Figure 6.27. In this mode shape, two nodal lines, which are in transverse direction, were seen clearly from the Figure 6.16, Figure 6.22 and Figure 6.28. In the second mode shapes of the ABS rectangular plates, we have two nodal lines in the transverse direction which are located in near the edges of the samples. The outer parts of the samples move in the same direction, while the inner part moves in the opposite direction to the outer parts. This second mode is called the first bending mode in our case. The Figure 6.17, Figure 6.23 and Figure 6.29 indicate the third mode shapes for the Sample 1, Sample 2 and Sample 3, respectively. It is obvious to see from the Figure 6.18, Figure 6.23 and Figure 6.30 that there are 3 nodal lines. One of them crosses the longitudinal axis of the samples and divides them into two equal parts. The other two nodal lines are in the transverse direction near the edges of the samples. Therefore, we have 6 different regions that deflect in a twisting shape. This third mode shape is the second fundamental twisting mode in our case. The behaviors of samples in this mode are that three parts move in the same direction, while the other three parts move in the opposite direction at the same time and vice versa. The results, which we obtained, coincide with the mode shapes of the rectangular plates with completely free which is shown in [15, 20]. The finite element natural frequency results for each sample was

tabulated in the Table 8. Also, the finite element frequency ratios were tabulated in Table 9.

6.4 Comparisons

The obtained experimental, theoretical and finite element natural frequencies for all samples were tabulated in the Table 10. The Figure 6.31 indicates the compatibility between the obtained natural frequencies of the ABS rectangular plates. When we look at the Table 11 and Figure 6.31, it is going to be really obvious to deduce that all natural frequencies increase, while the dimensions of the samples decrease. The Figure 6.32 shows the FRF comparison of the samples. The experimental, theoretical and finite element frequency ratios were tabulated for each sample in the Table 10. It can be seen from the Table 10 that there is a constant ratio between the first fundamental frequency, second fundamental frequency and third fundamental frequency. This is true for free vibrations of rectangular plates with completely free boundary conditions and the aspect ratio (a/b) is equal to 1.5. The experimental results coincide with the finite element results much more than the theoretical results. As stated earlier, there are twenty-one various boundary conditions exist in rectangular plates, and the vibrations analysis of rectangular plates with completely free is the worst behaved of all 21 boundary conditions of rectangular plates. In other words, obtaining accurate theoretical solutions for completely free rectangular plates is the most difficult case. Therefore, conducting an experimental modal analysis and doing a finite element modal analysis become mandatory to obtain accurate natural frequencies for any rectangular plates with completely free

boundary conditions. The Sample 3, which has the smallest dimensions, has the lowest modal density. The Sample 2 has the highest damping ratio.

CHAPTER 7

CONCLUSIONS AND RECOMMENDATIONS

7.1 Conclusions

From the experimental, finite element and theoretical results for this research, the following conclusions may be written as:

1. From the Table 10, there is no doubt that while the dimensions of the ABS rectangular plates decrease the natural frequencies of the plates increase. The formula, which is written below, clearly indicates why the natural frequencies increase with the decreasing dimensions of the samples. In our case, all the parameters in this formula for the samples are constant, except a^2 . While a^2 decreases, ω increases automatically.

$$\omega = \frac{\lambda^2}{a^2} \sqrt{\frac{D}{\rho h}}$$

2. The Figure 6.31 indicates that the experimental, finite element and theoretical results compare very favorably one another. The error ratios between the experimental natural frequencies and finite element natural frequencies are very small. It shows that sufficient measurement points were used in all samples to calculate the natural frequencies experimentally and our finite element analysis approach was very effective. In other words, the experiment has been conducted properly and it has been verified by the finite element results.

3. The experimental results generally coincide with the finite element results much more than theoretical results. The reason is that there are twenty-one different boundary conditions existing in rectangular plates and the free vibrations analysis of rectangular plates with completely free boundary conditions are the worst behaved among the twenty-one cases. As a result, especially, the experimental and finite element modal analyses are mandatory to obtain accurate solutions for rectangular plates with completely free boundaries.
4. The maximum error ratio between the experimental and finite element results was found to be 13.6 % in the third fundamental frequency of the Sample3 which has the smallest dimensions within the samples. It is more difficult to handle the Sample 3 experimentally than other two samples because when we hit the one specific measurement point, the entire structure vibrates due to the dimensions of the Sample 3. Therefore, it is difficult for the Pulse software to obtain an accurate solution for the specific measurement point.
5. The obtained experimental deflection mode shapes and finite element mode shapes definitely coincide with each other. The first mode shape is known as the first twisting mode shape and it has two nodal lines where the deflections are equal to zero. In this mode shape, the maximum deflections occur at the edges of the samples. The second mode shape is called the bending mode shape. There are two nodal lines located in transverse direction. The maximum deflections occur at the middle of the width of samples. The third mode shape is known as the second twisting mode shape. Three nodal lines have been seen in this mode shape and the maximum deflections occur at the edges of the samples in all cases.

6. When the dimensions of the samples change with keeping the aspect ratio same ($a/b=1.5$), there are slightly different constant ratios found between fundamental frequencies regardless of their dimensions. These constant ratios, which were tabulated in Table 11, make our calculations easier. In other words, if the first fundamental frequency is calculated, these ratios give us a really good indication for the second and third fundamental frequencies.
7. When we look at the table 12, it will be readily deduced that when the dimensions of the samples increase, the modal densities increase. In other words, while the dimensions increase, the samples become more complex, and require a more effort and money in design process.
8. In mode 1, the sample 2 has the highest damping ratio which leads to absorb more energy than other samples.

7.2 Recommendations for Future Work

From the conclusions, the following recommendations may be proposed for future work

1. The Poisson's ratio effect may be evaluated to figure out how the natural frequencies and mode shapes of the samples change.
2. By changing the thickness of samples, the natural frequencies and mode shapes may be examined to see the thickness effect on them.

3. The laser accelerometer can be used to obtain the response of the small samples. This type of accelerometer is going to provide us more accurate results because it is not physically attached to the samples.
4. This type of material may be fully studied for impact analysis because of its high compressive strength. One of the most vital applications can be the use of this material in the fabrication of soldiers' helmets. Therefore, an extensive study of impact analysis will be a valuable research area.

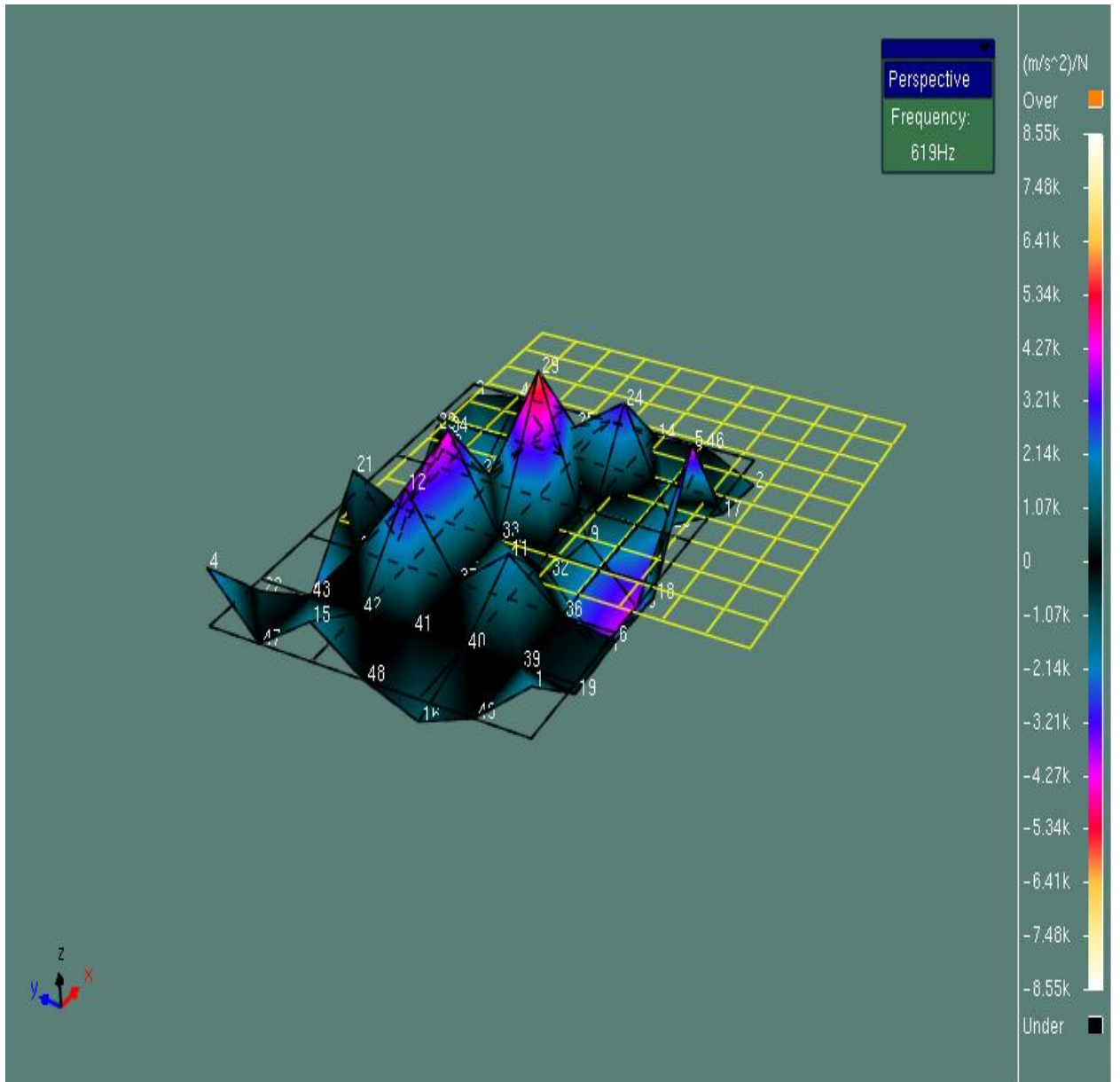


Figure 6.1. The First Mode Shape of the Sample1 from PULSE

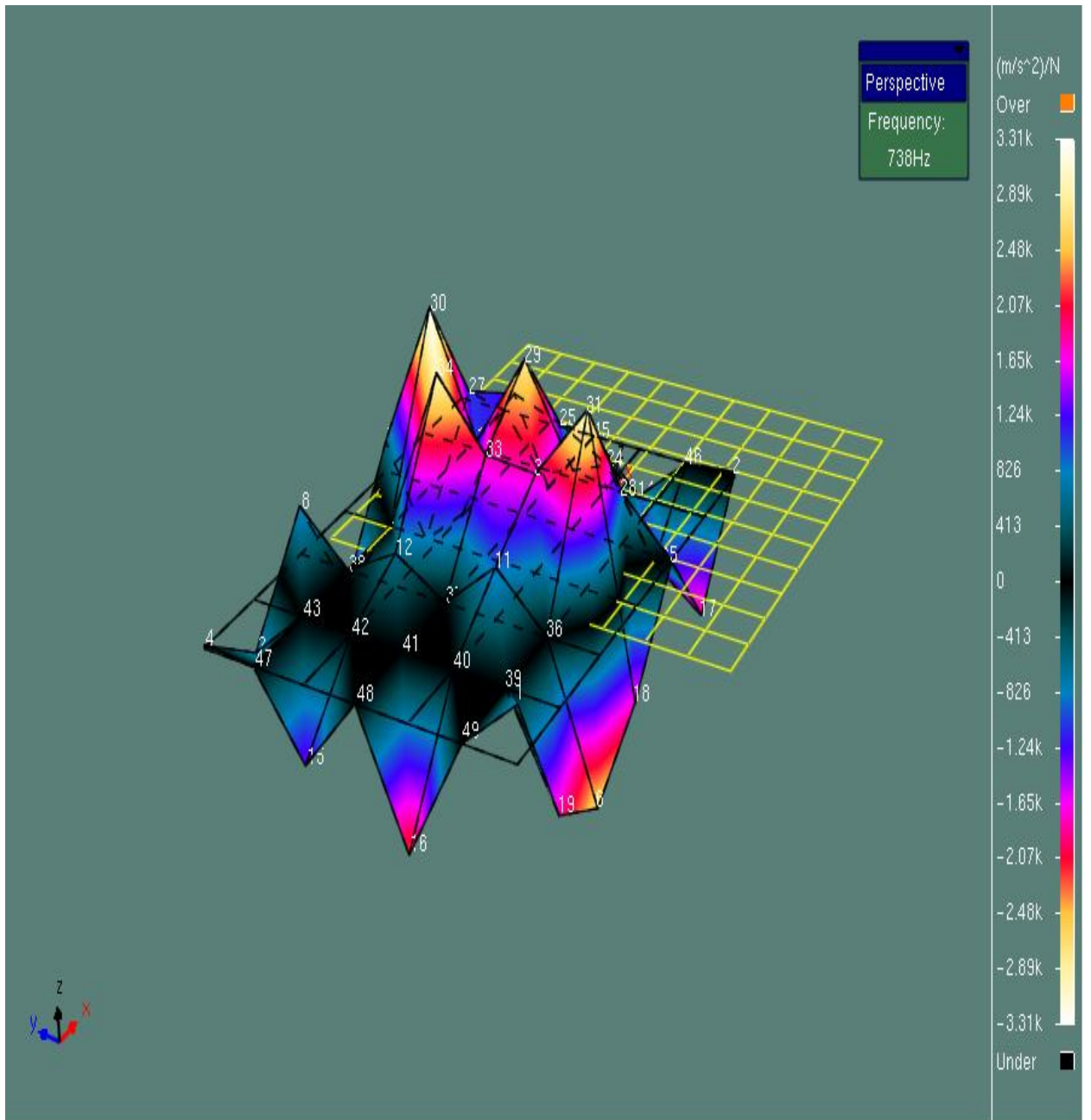


Figure 6.2. The Second Mode Shape of the Sample1 from PULSE

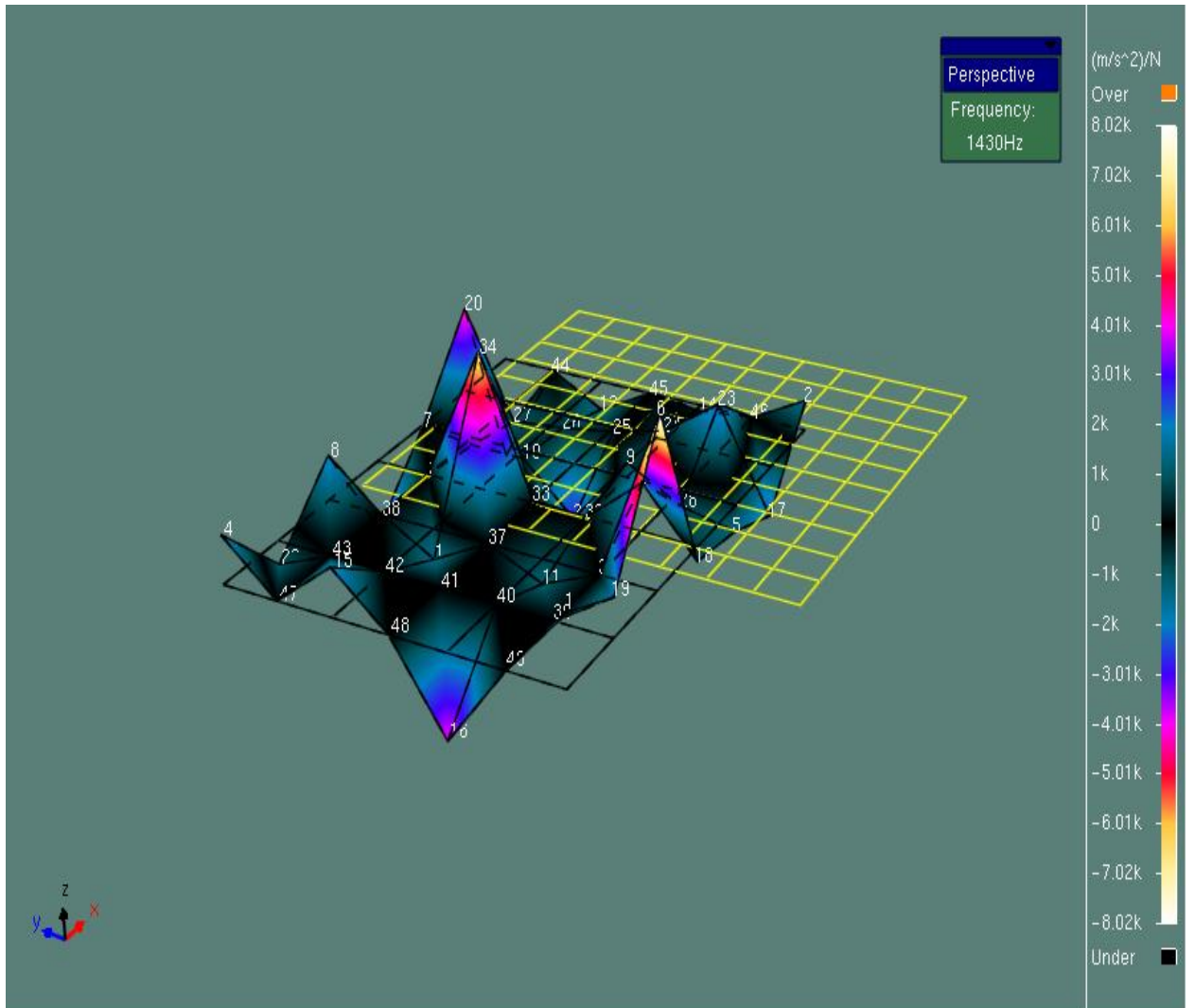


Figure 6.3. The Third Mode Shape of the Sample1 from PULSE

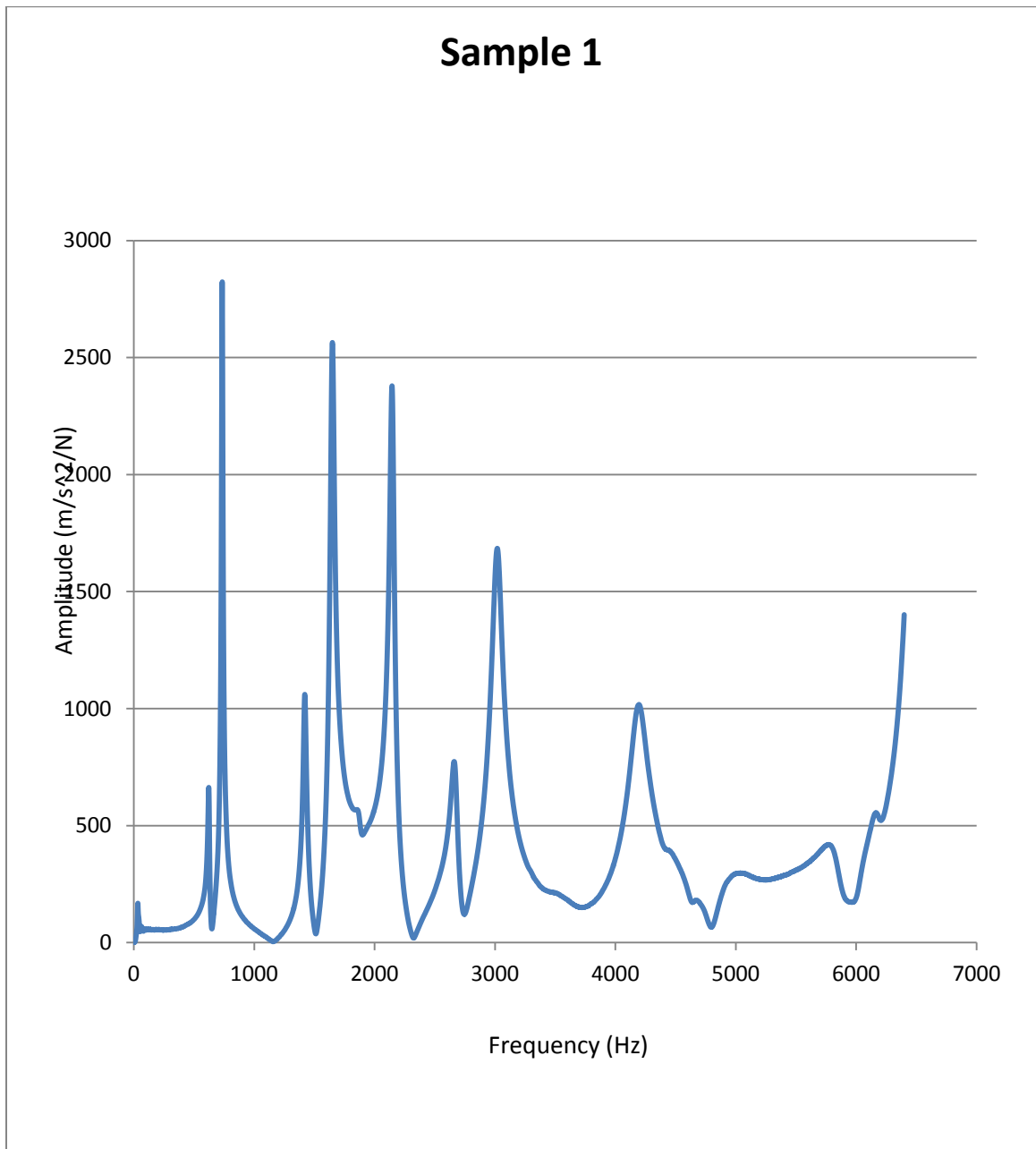


Figure 6.4 FRF of the Sample1

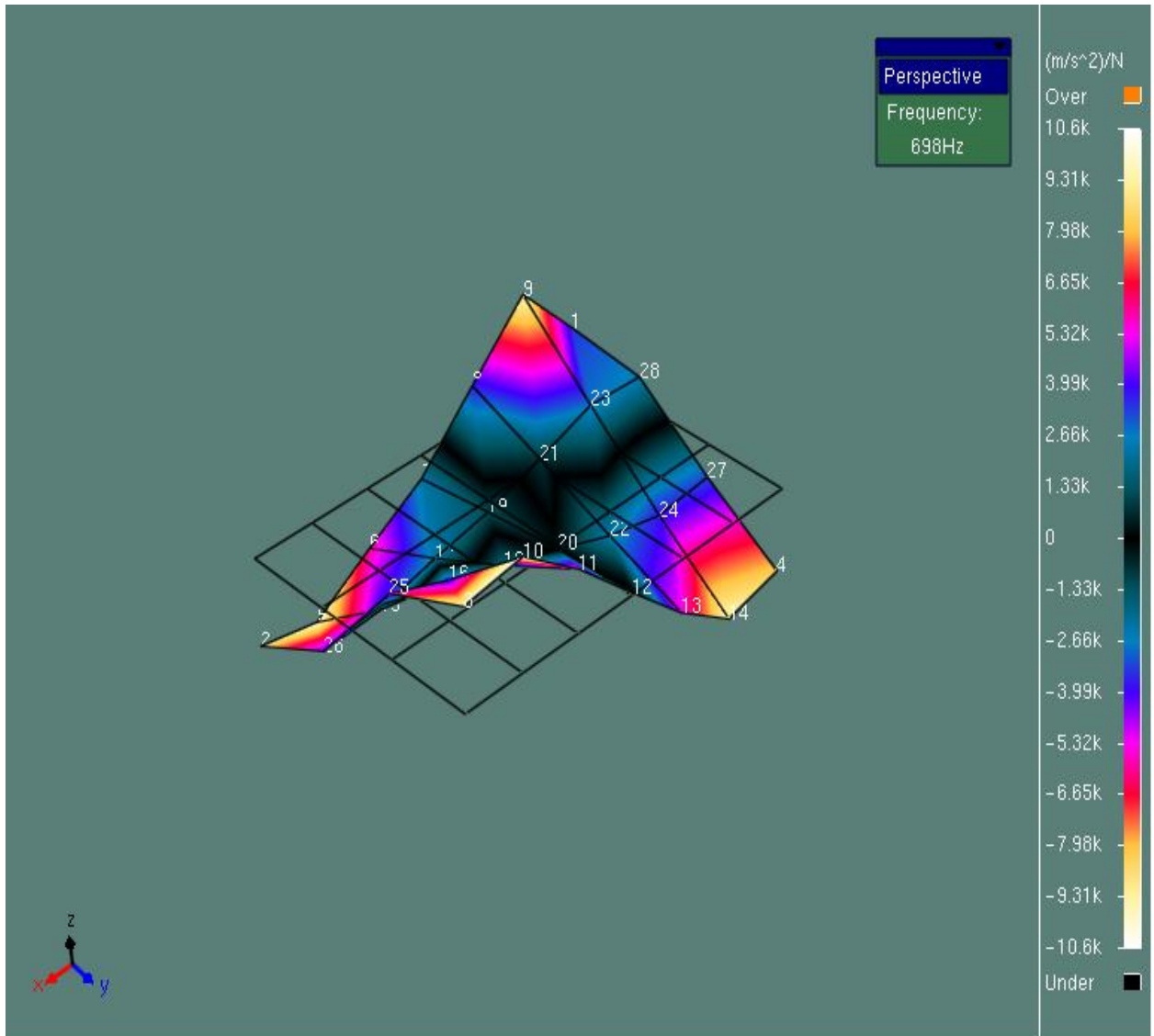


Figure 6.5. The First Mode Shape of the Sample2 from PULSE

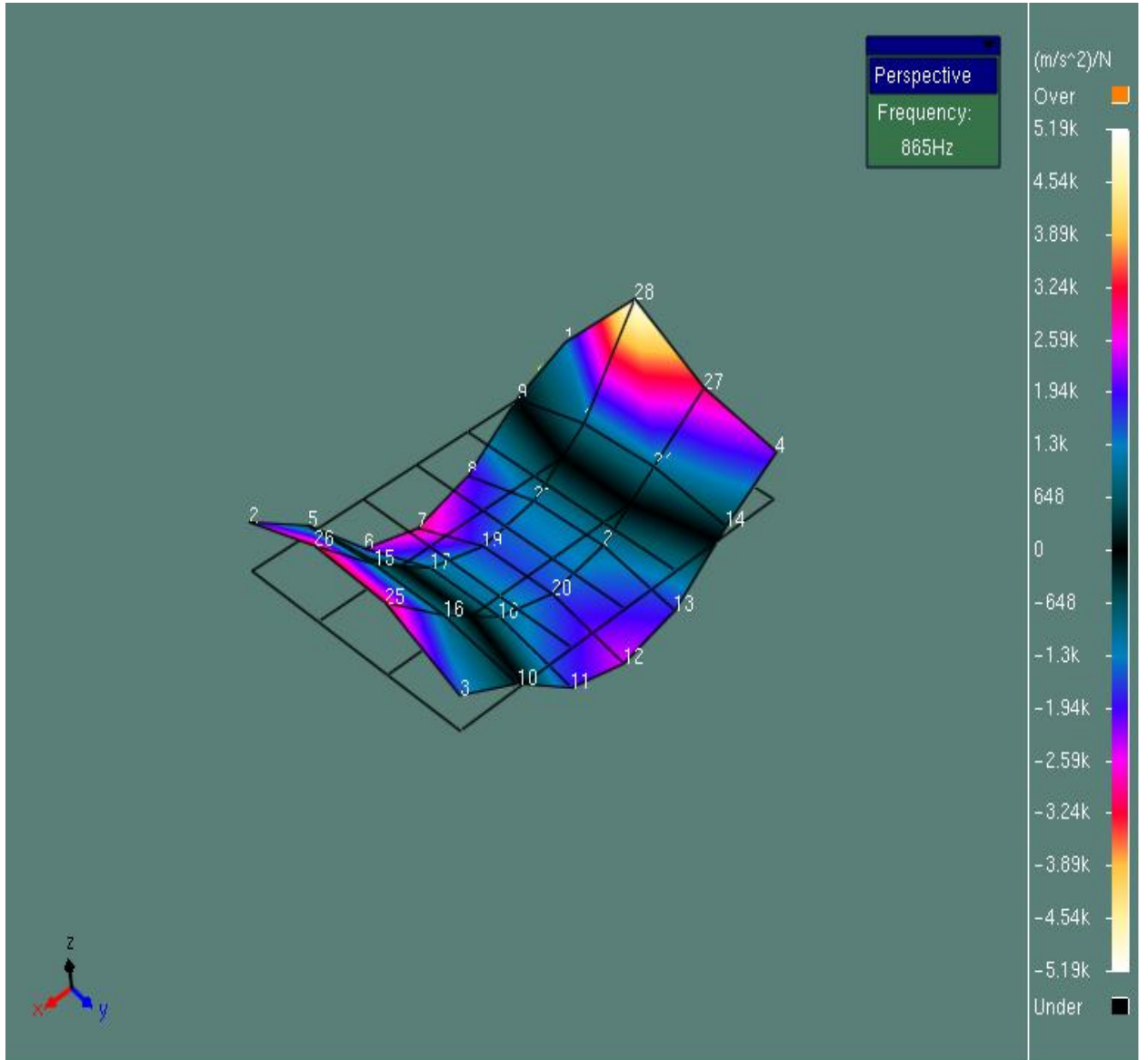


Figure 6.6. The Second Mode Shape of the Sample2 from PULSE

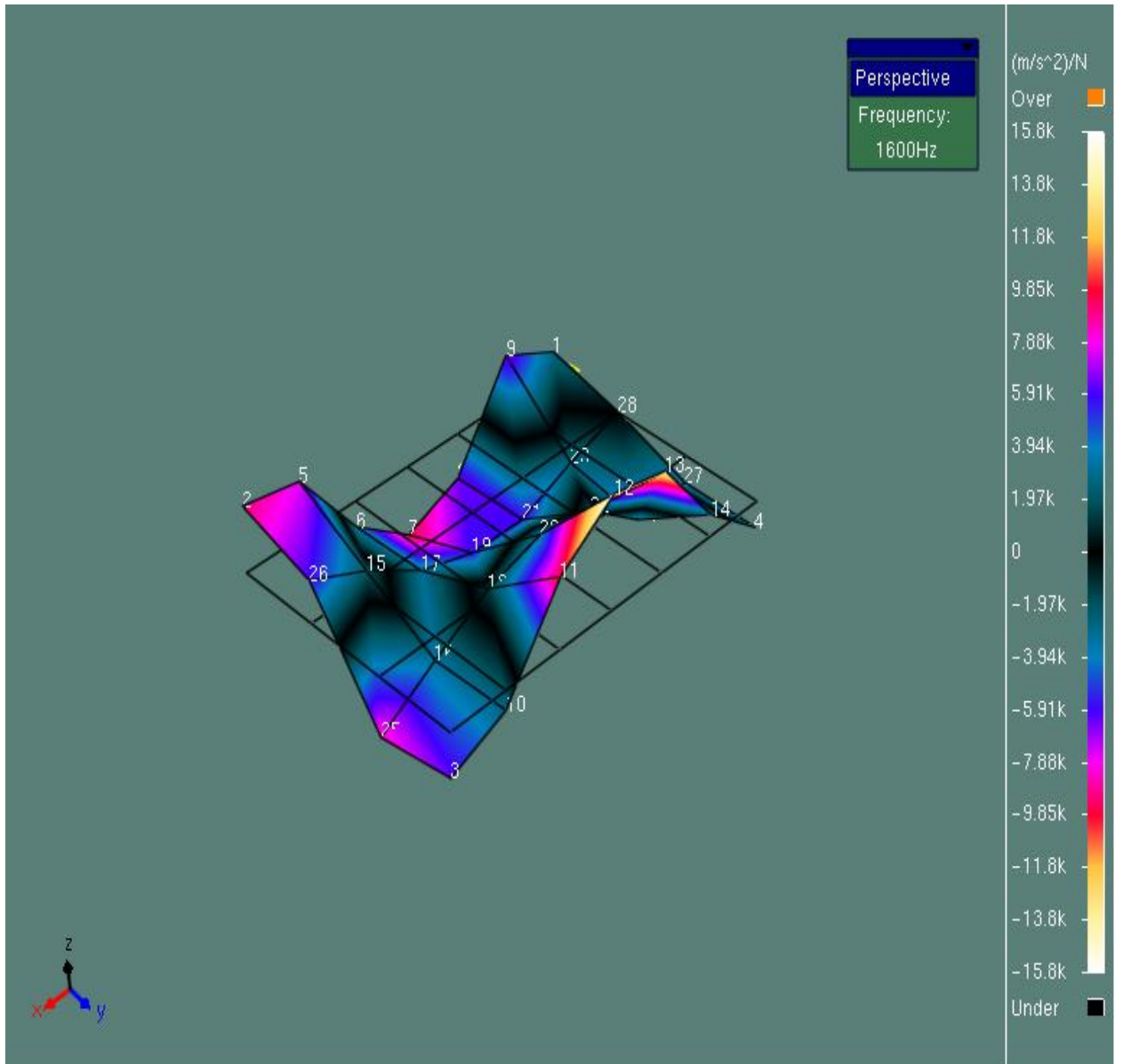


Figure 6.7. The Third Mode Shape of the Sample2 from PULSE

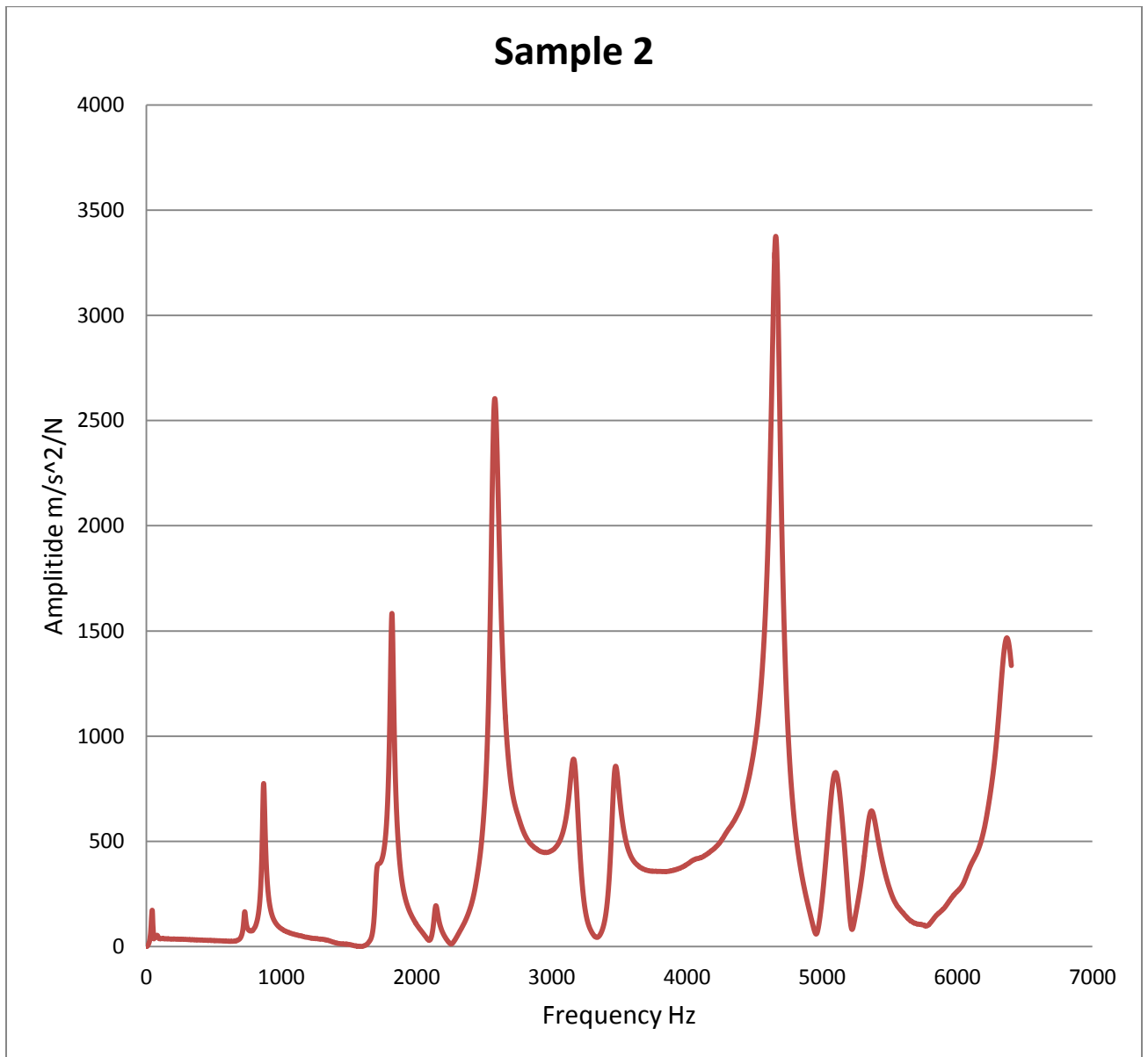


Figure 6.8 FRF of the Sample2

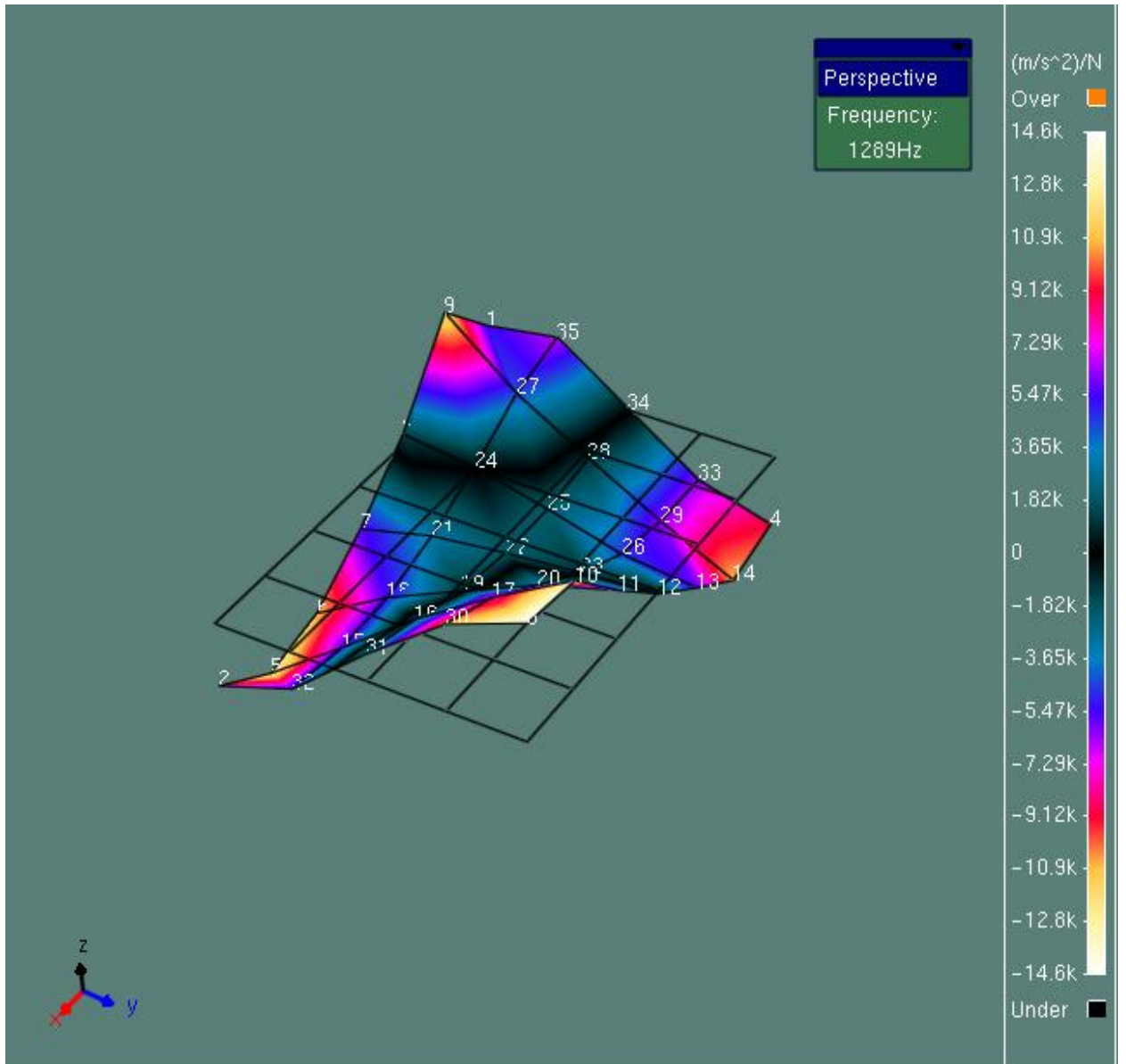


Figure 6.9. The First Mode Shape of the Sample3 from PULSE

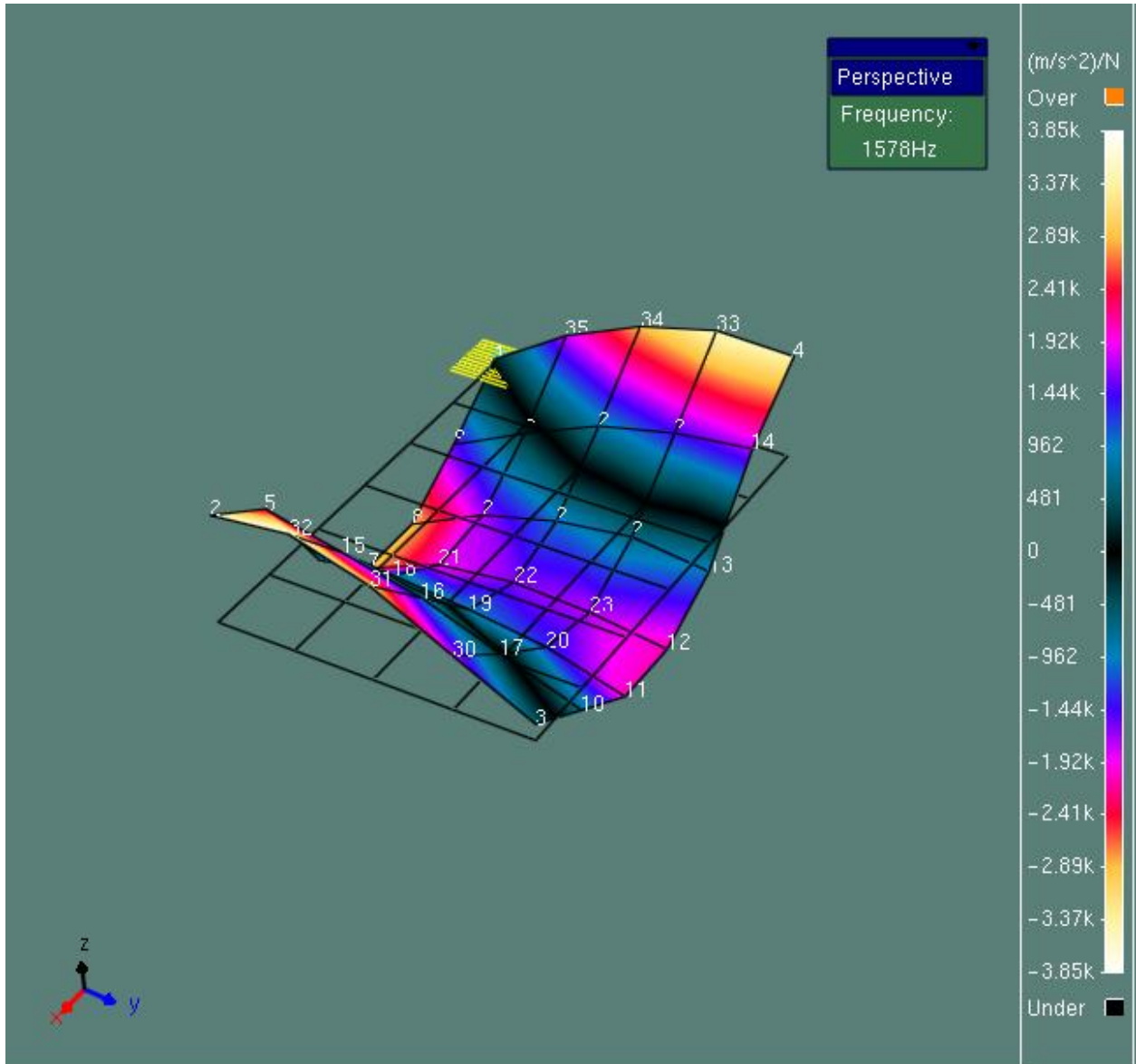


Figure 6.10. The Second Mode Shape of the Sample3 from PULSE

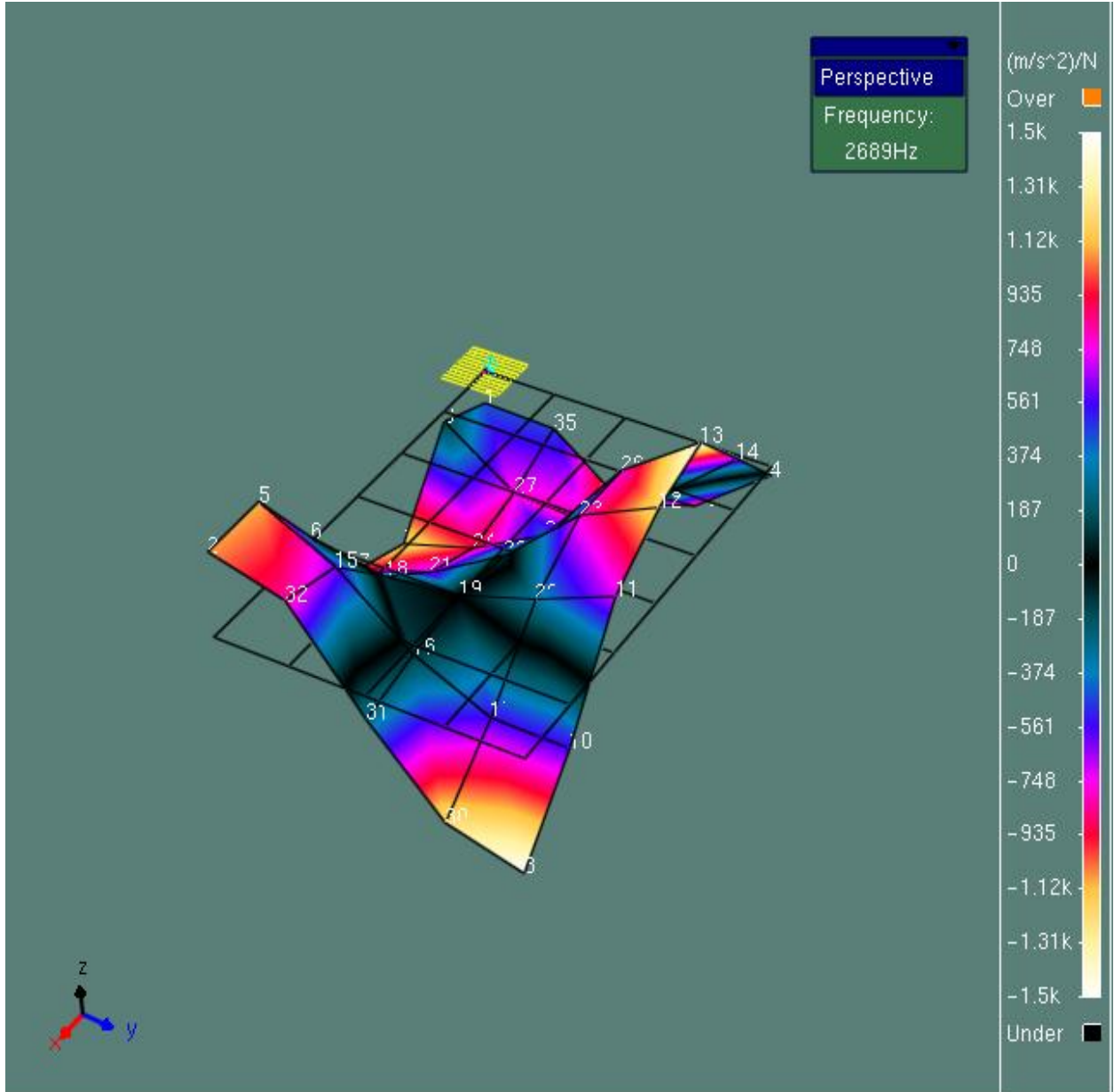


Figure 6.11. The Third Mode Shape of the Sample3 from PULSE

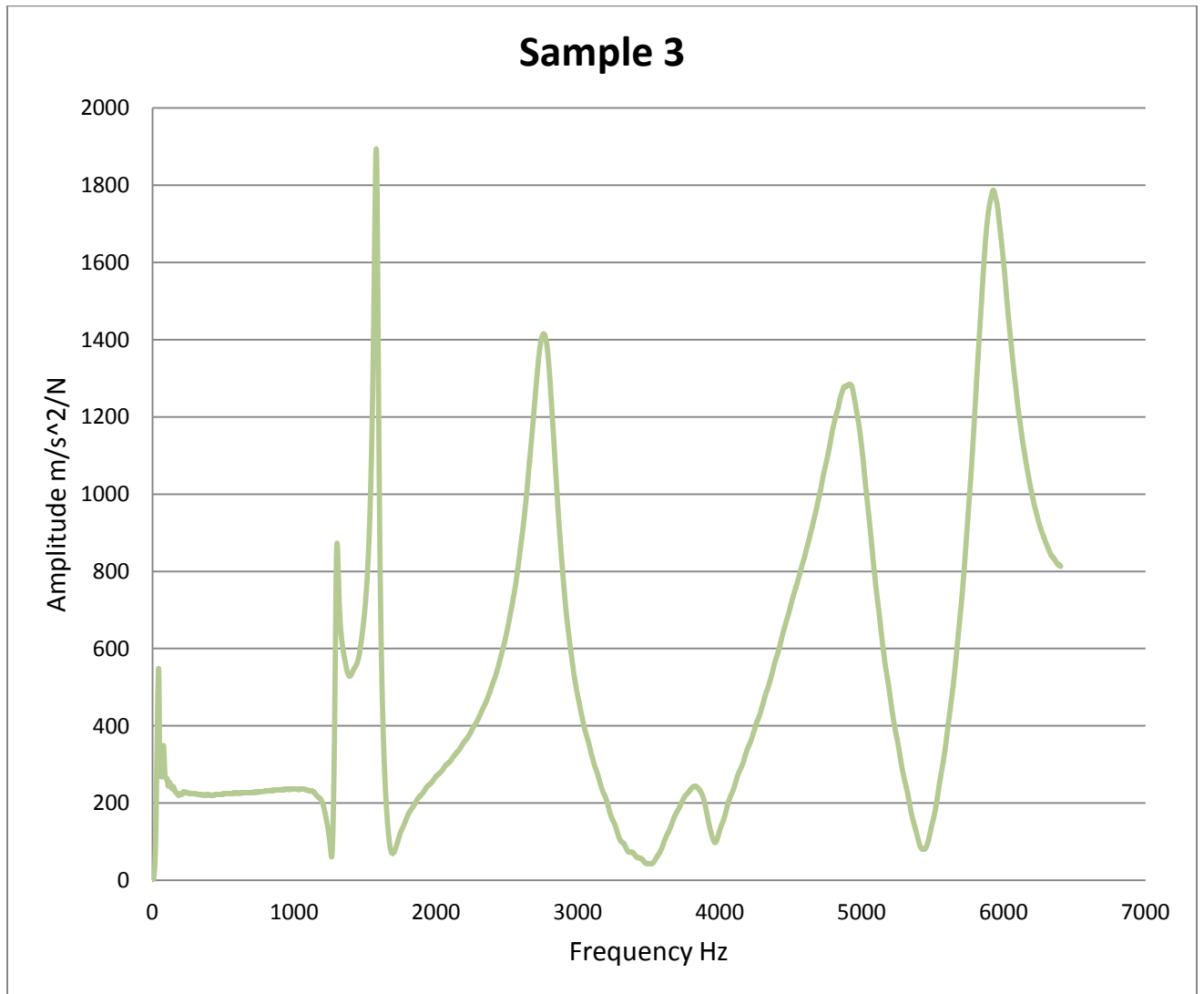


Figure 6.12 FRF of the Sample3

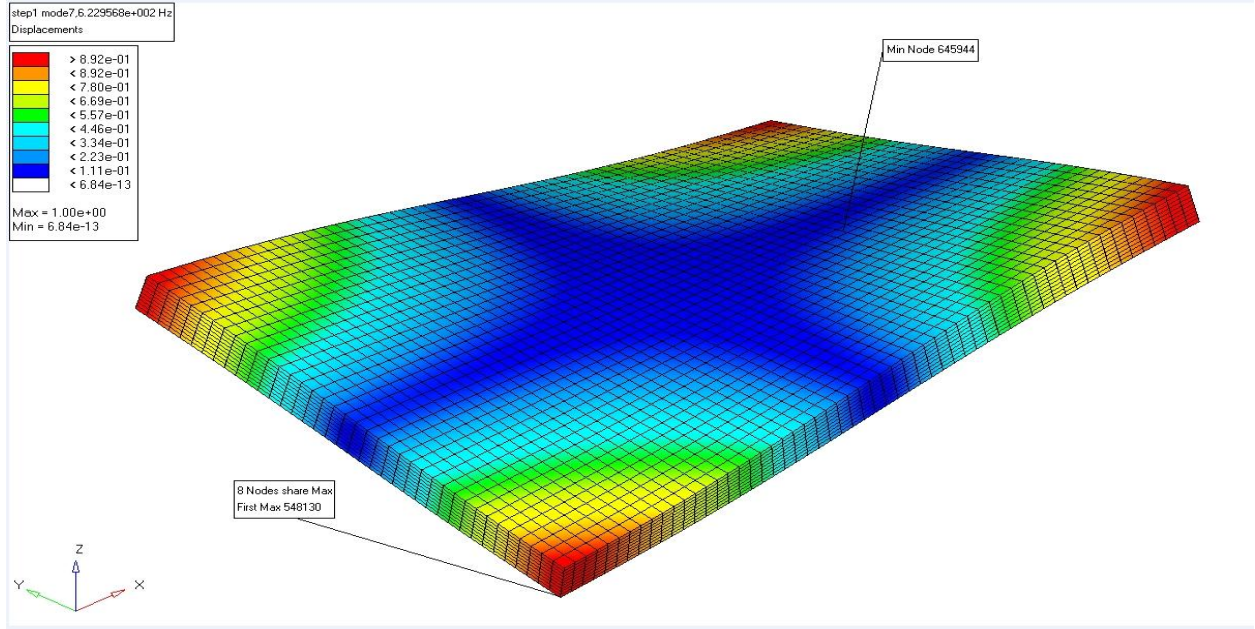


Figure 6.13.The First Mode Shape of the Sample1 from FEM

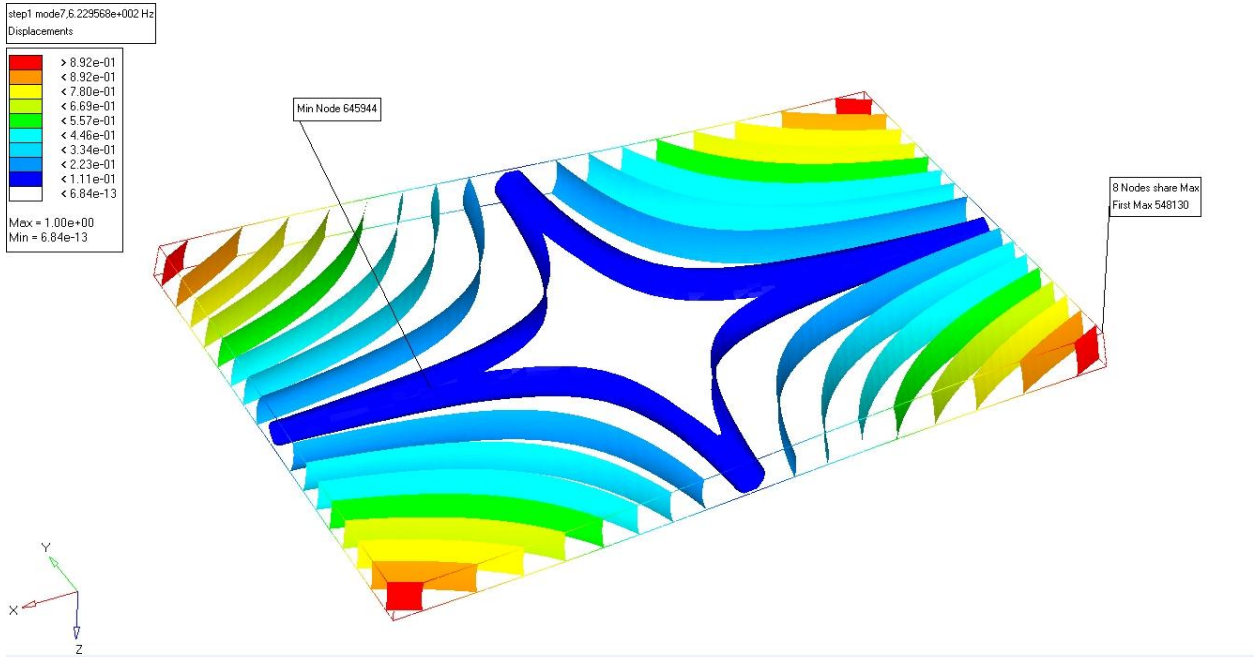


Figure 6.14.The Isosurface of the First Mode Shape for the Sample1 from FEM

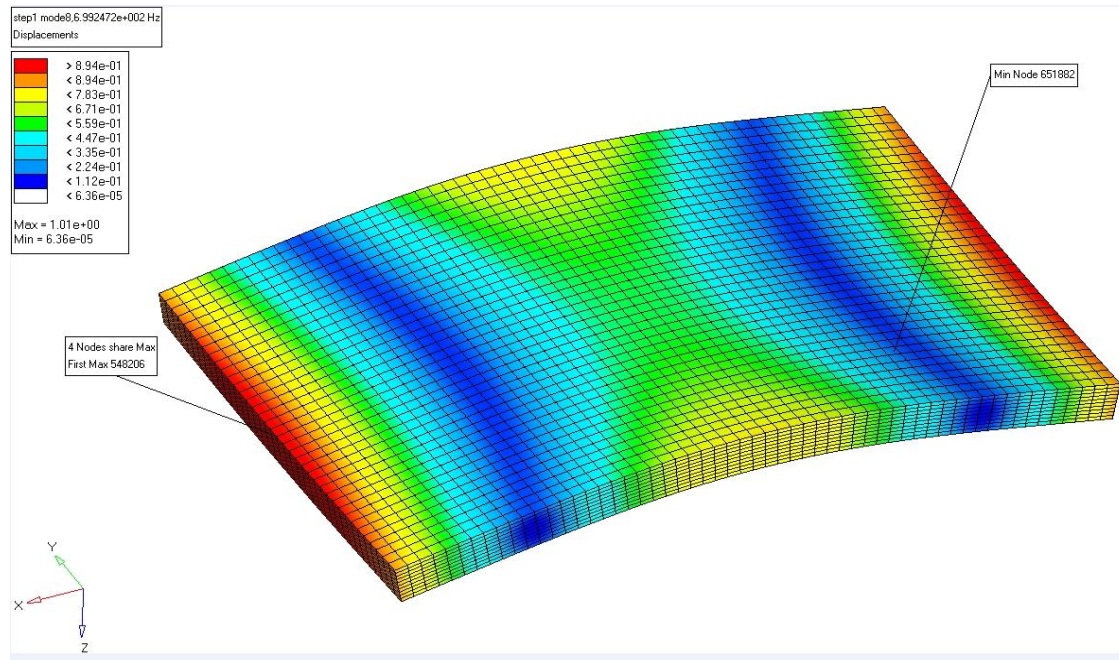


Figure 6.15. The Second Mode Shape of the Sample1 from FEM

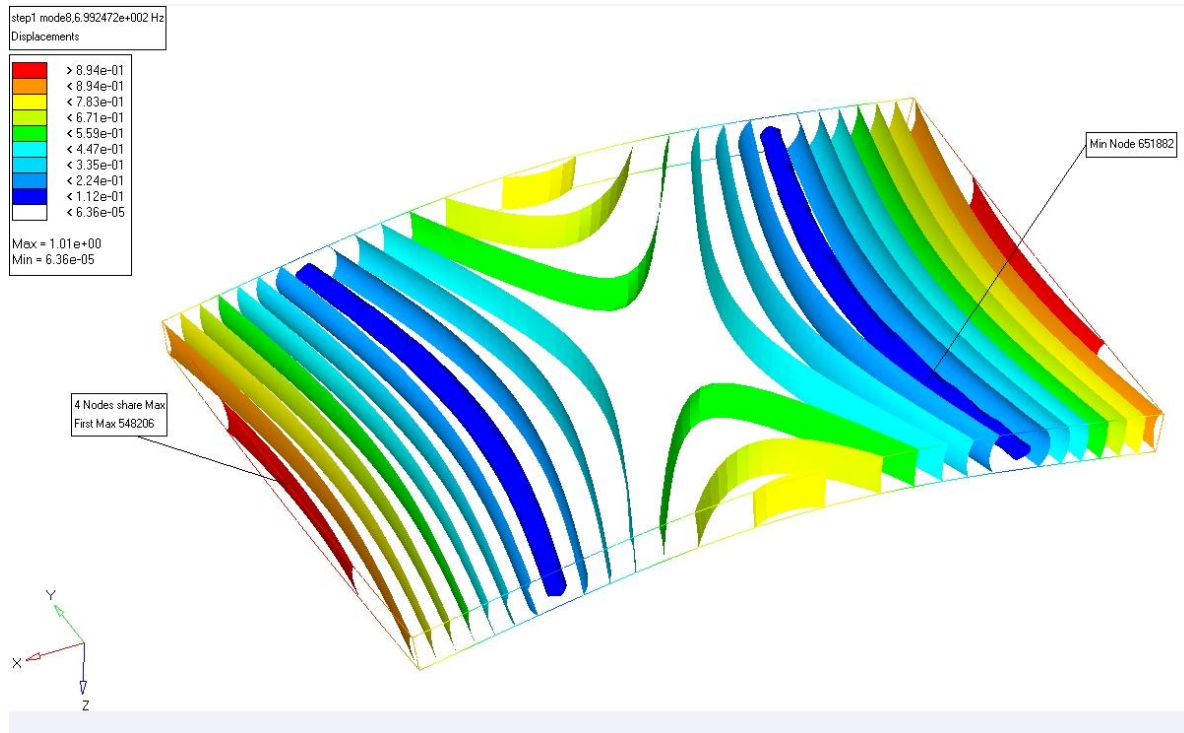


Figure 6.16. The Isosurface of the Second Mode Shape for the Sample1 from FEM

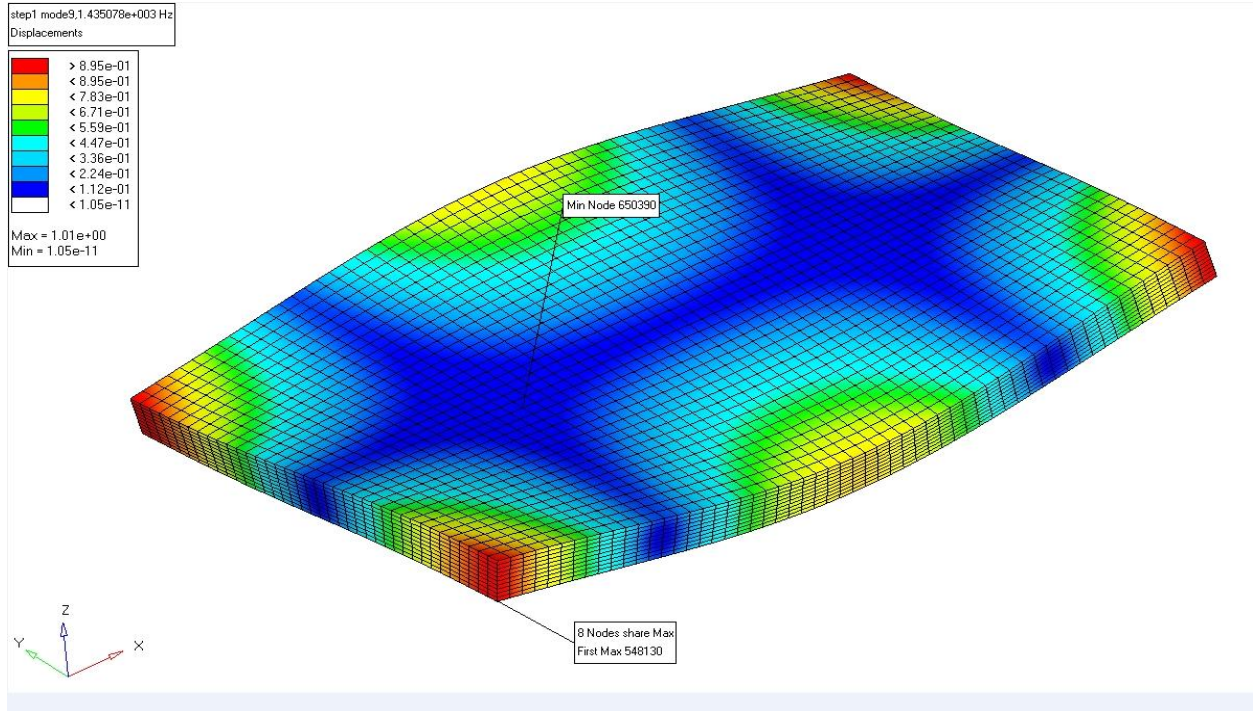


Figure 6.17. The Third Mode Shape of the Sample 1 from FEM

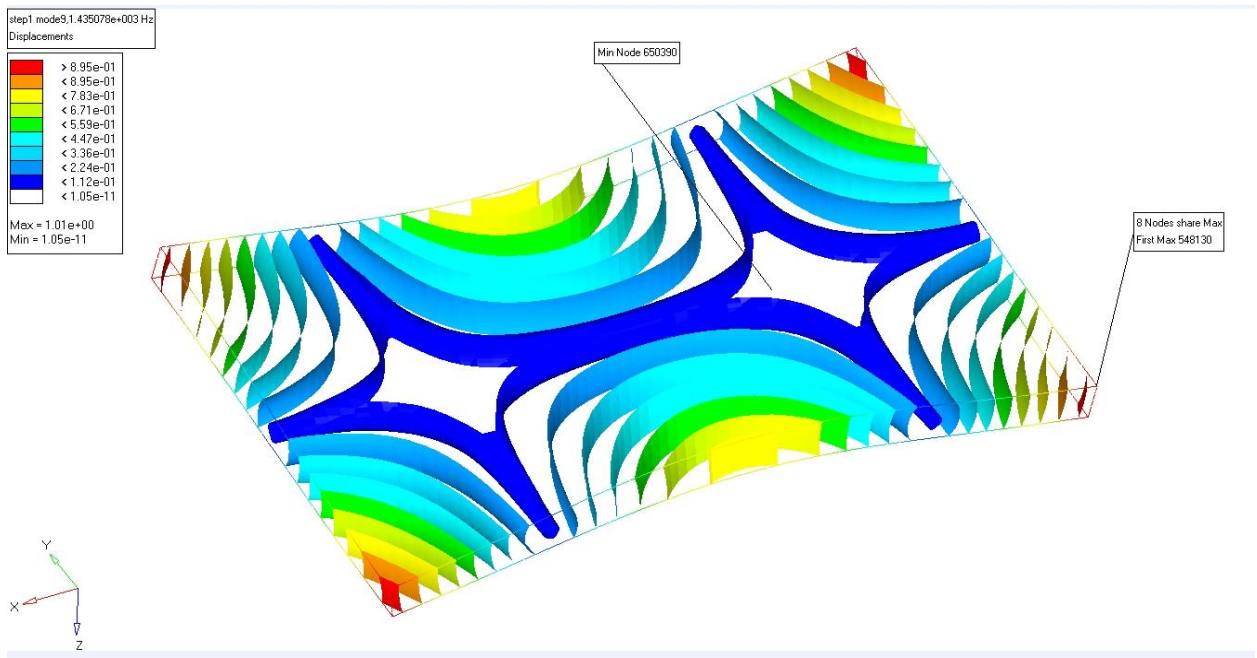


Figure 6.18. The Isosurface of the Third Mode Shape for the Sample 1 from FEM

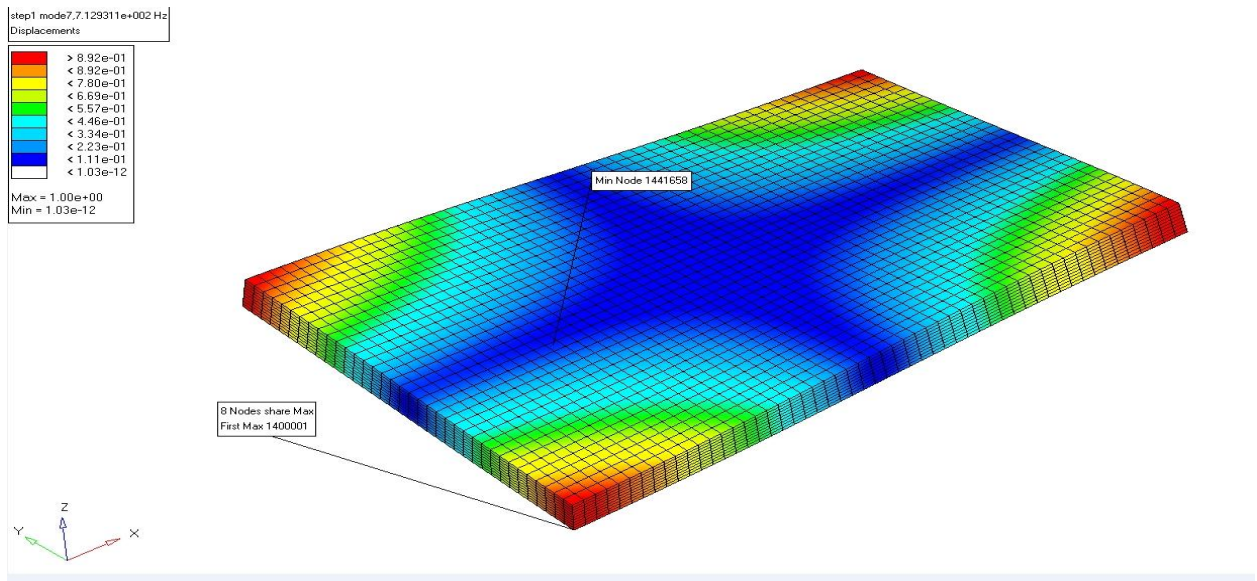


Figure 6.19.The First Mode Shape of the Sample2 from FEM

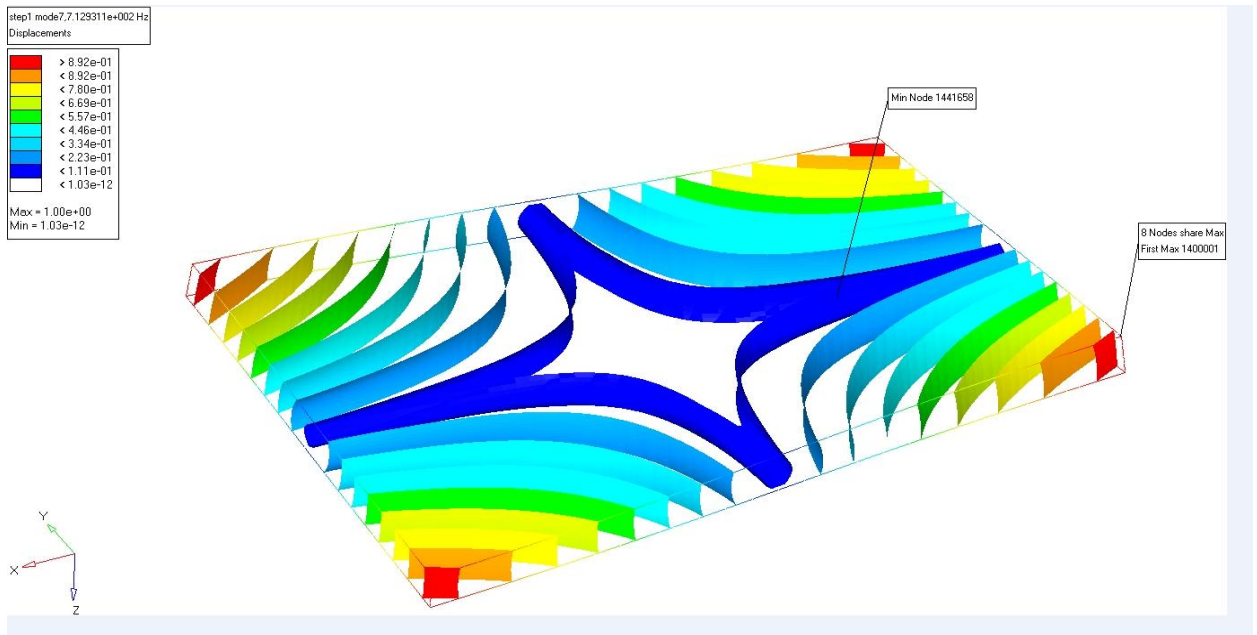


Figure 6.20.The Isosurface of the First Mode Shape for the Sample2 from FEM

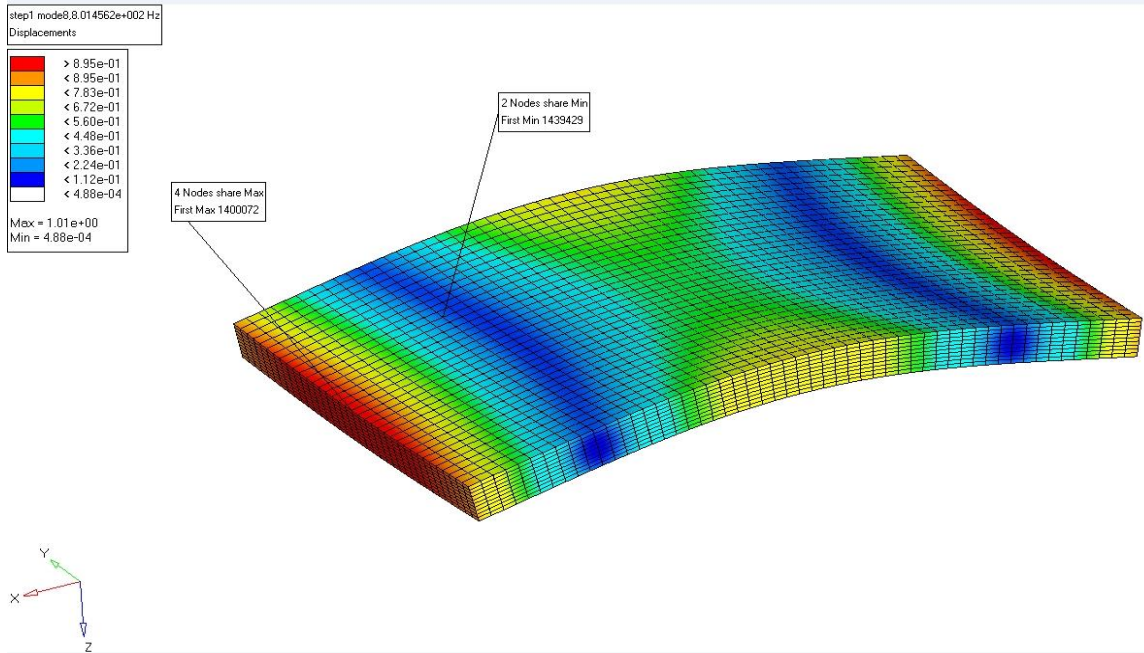


Figure 6.21. The Second Mode Shape of the Sample2 from FEM

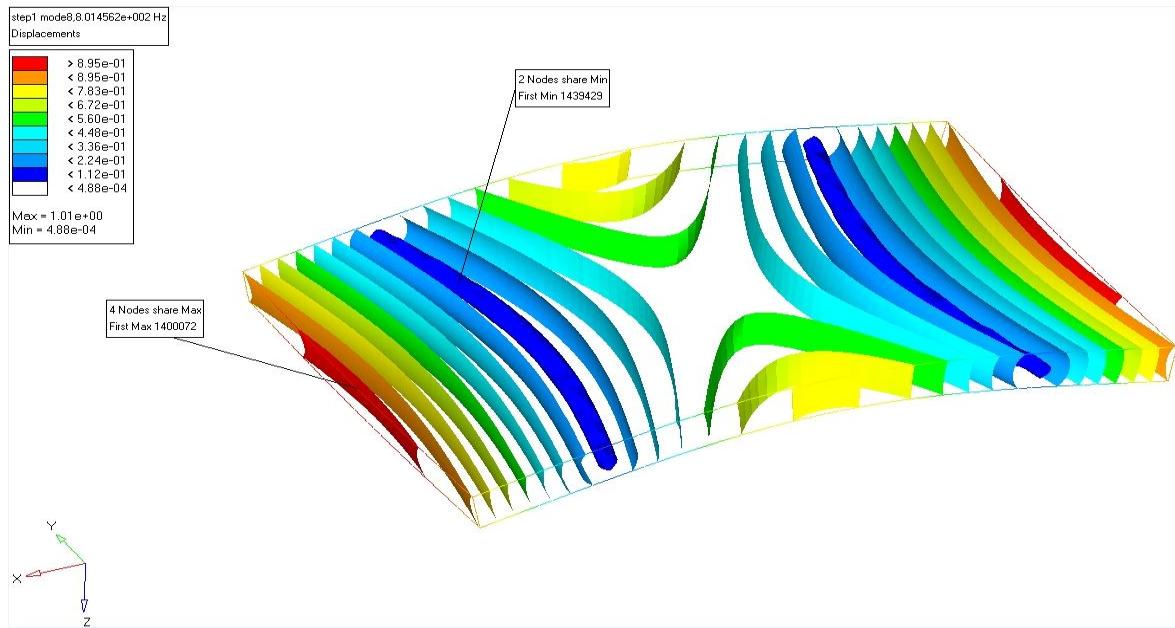


Figure 6.22. The Isosurface of the Second Mode Shape for the Sample2 from FEM

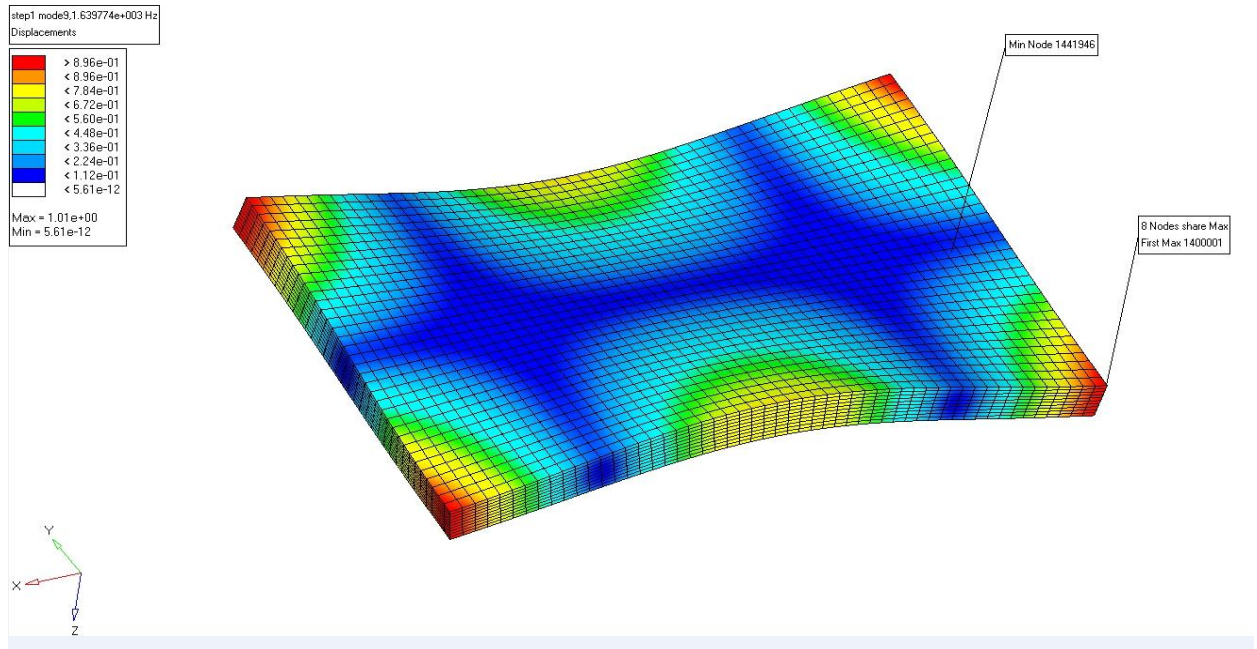


Figure 6.23. The Third Mode Shape of the Sample2 from FEM

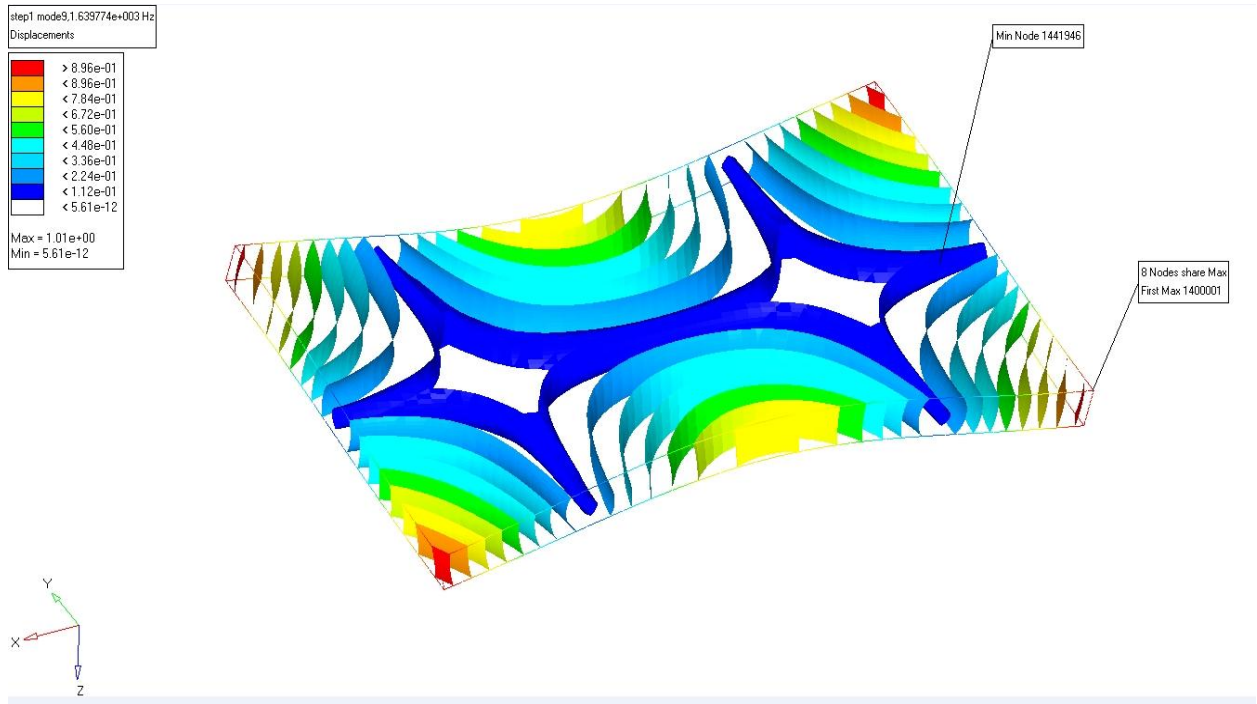


Figure 6.24. The Isosurface of the Third Mode Shape for the Sample2 from FEM

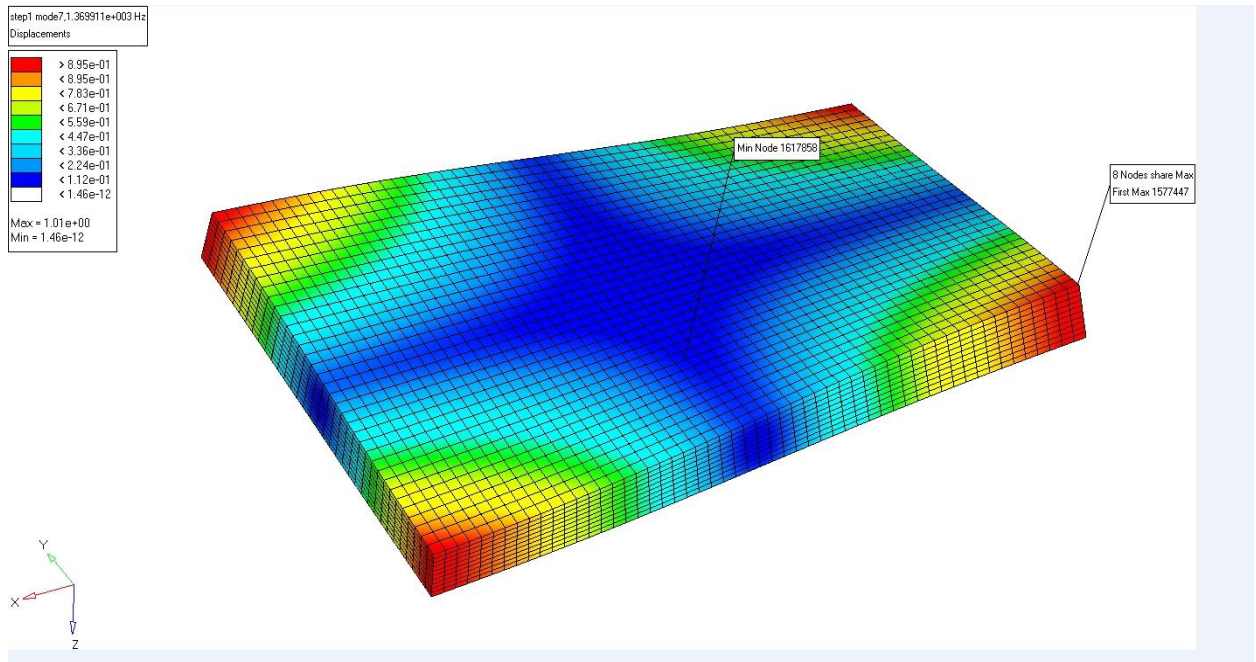


Figure 6.25. The First Mode Shape of the Sample3 from FEM

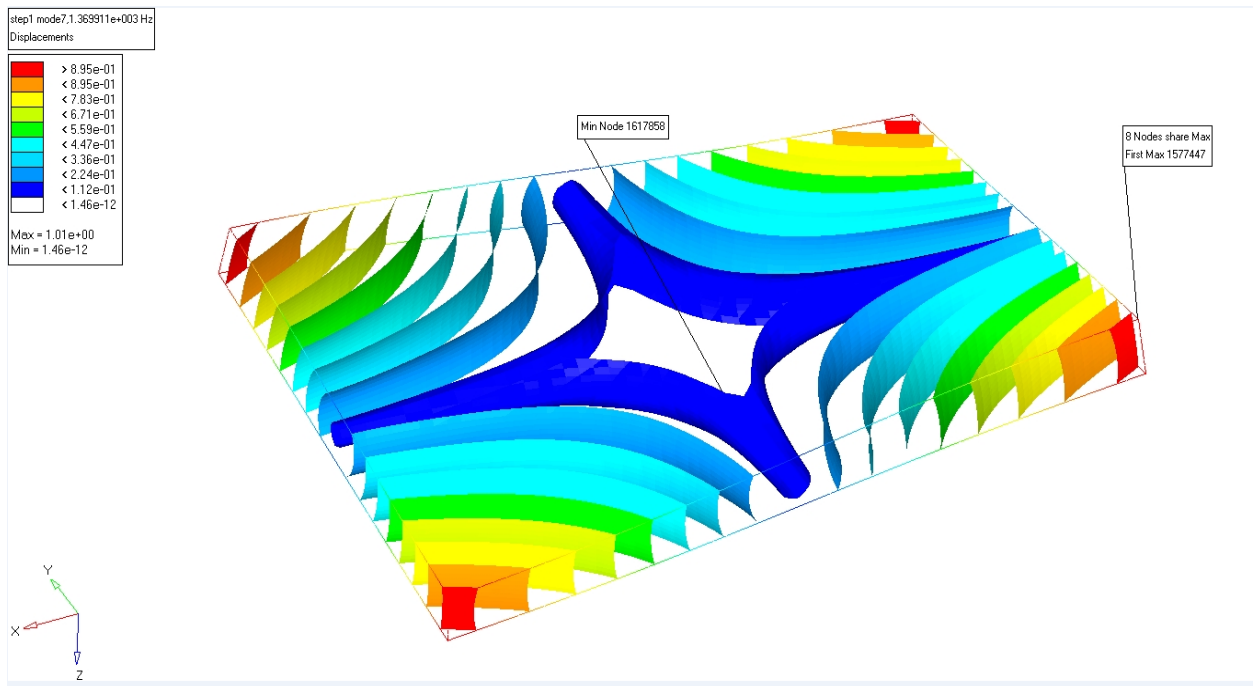


Figure 6.26. The Isosurface of the First Mode Shape for the Sample3 from FEM

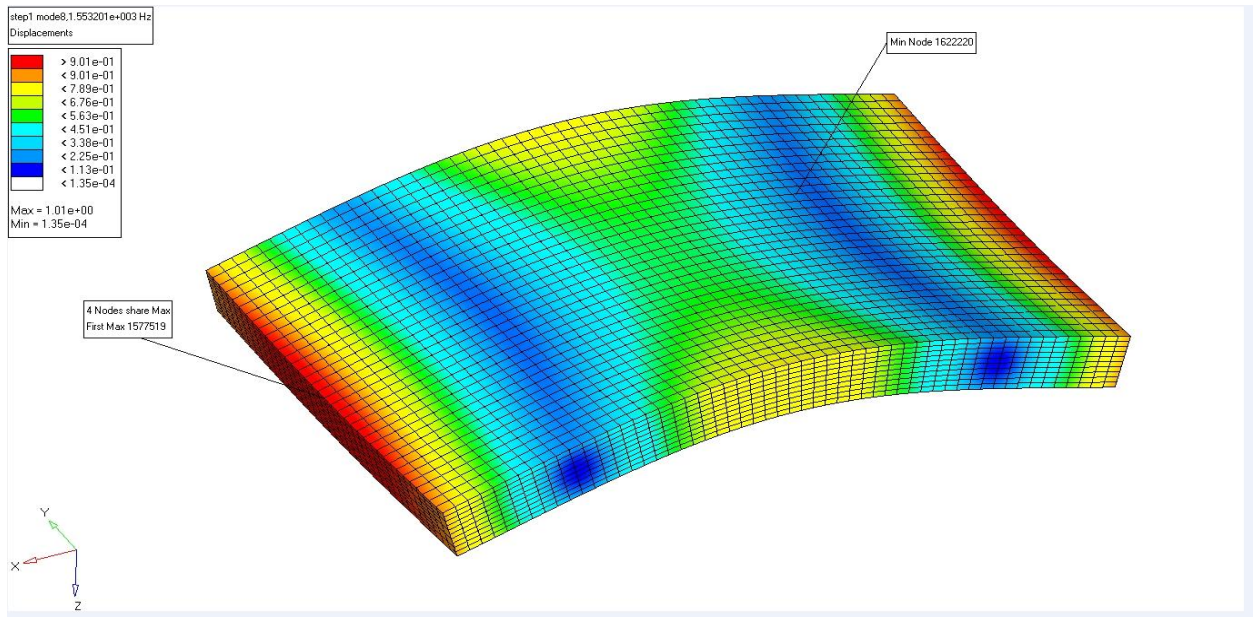


Figure 6.27. The Second Mode Shape of the Sample3 from FEM

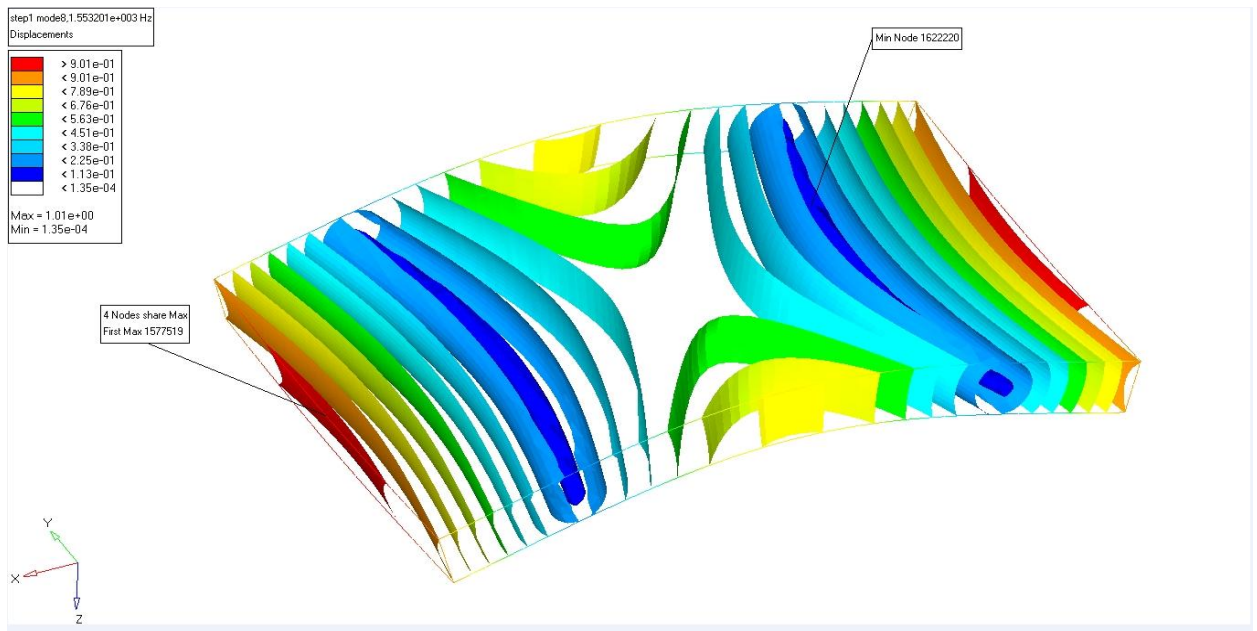


Figure 6.28. The Isosurface of the Second Mode Shape for the Sample3 from FEM

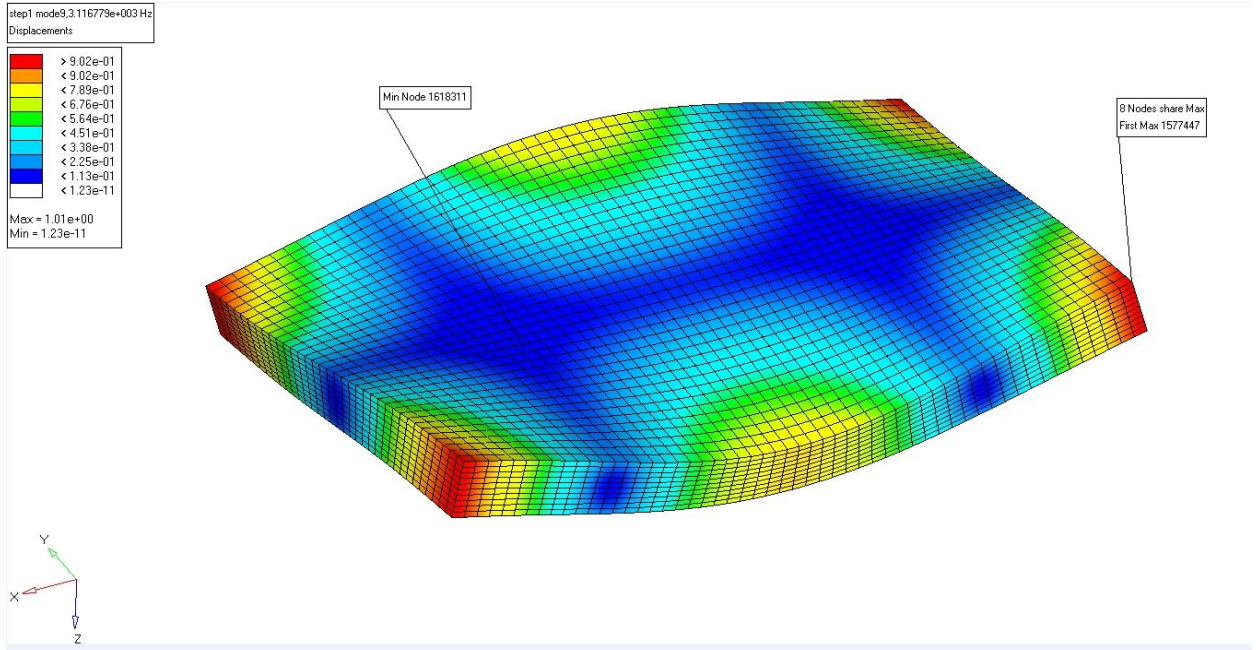


Figure 6.29.The Third Mode Shape of the Sample3 from FEM

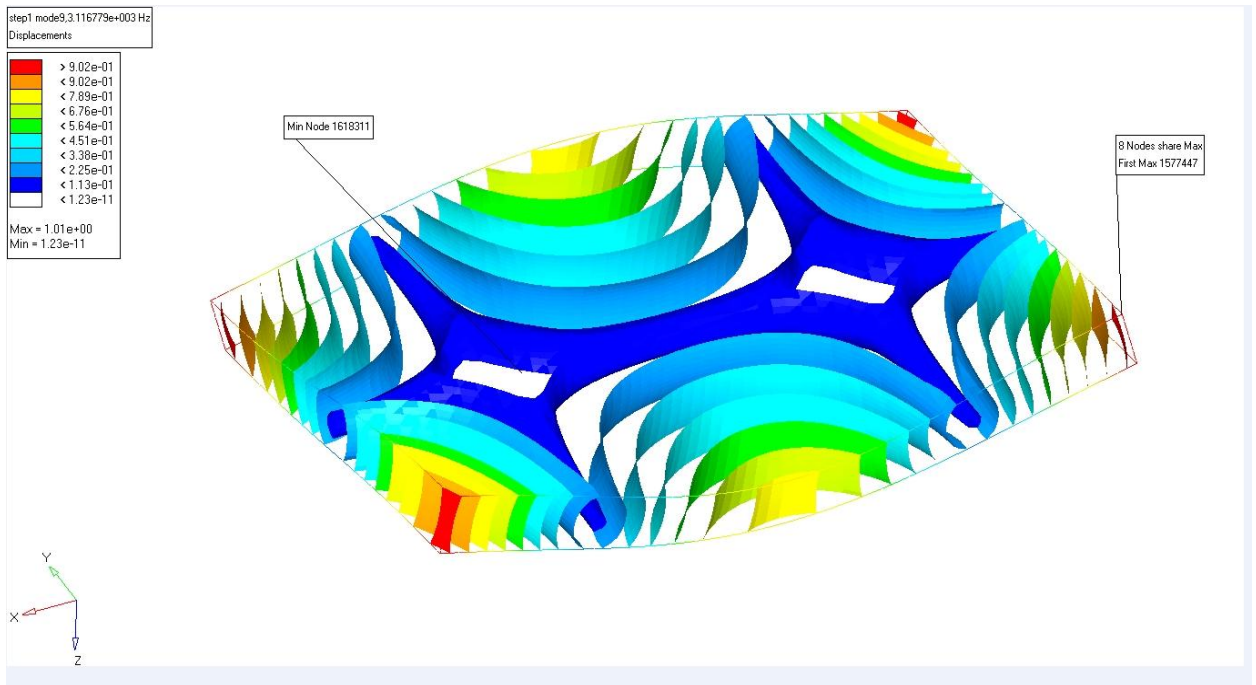


Figure 6.30.The Isosurface of the Third Mode Shape for the Sample3 from FEM

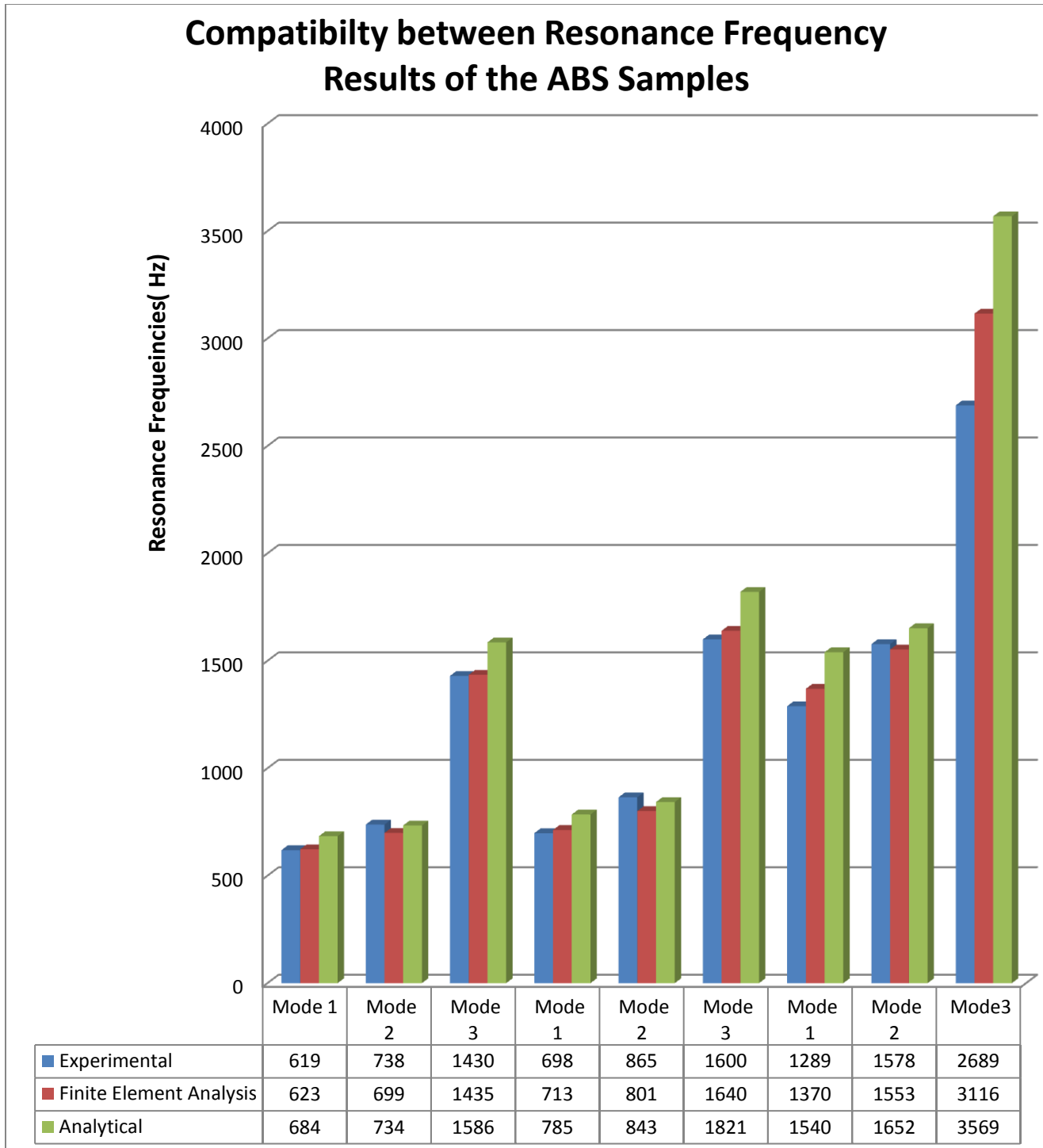


Figure 6.31. Compatibility between obtained natural frequencies of the rectangular ABS

Samples

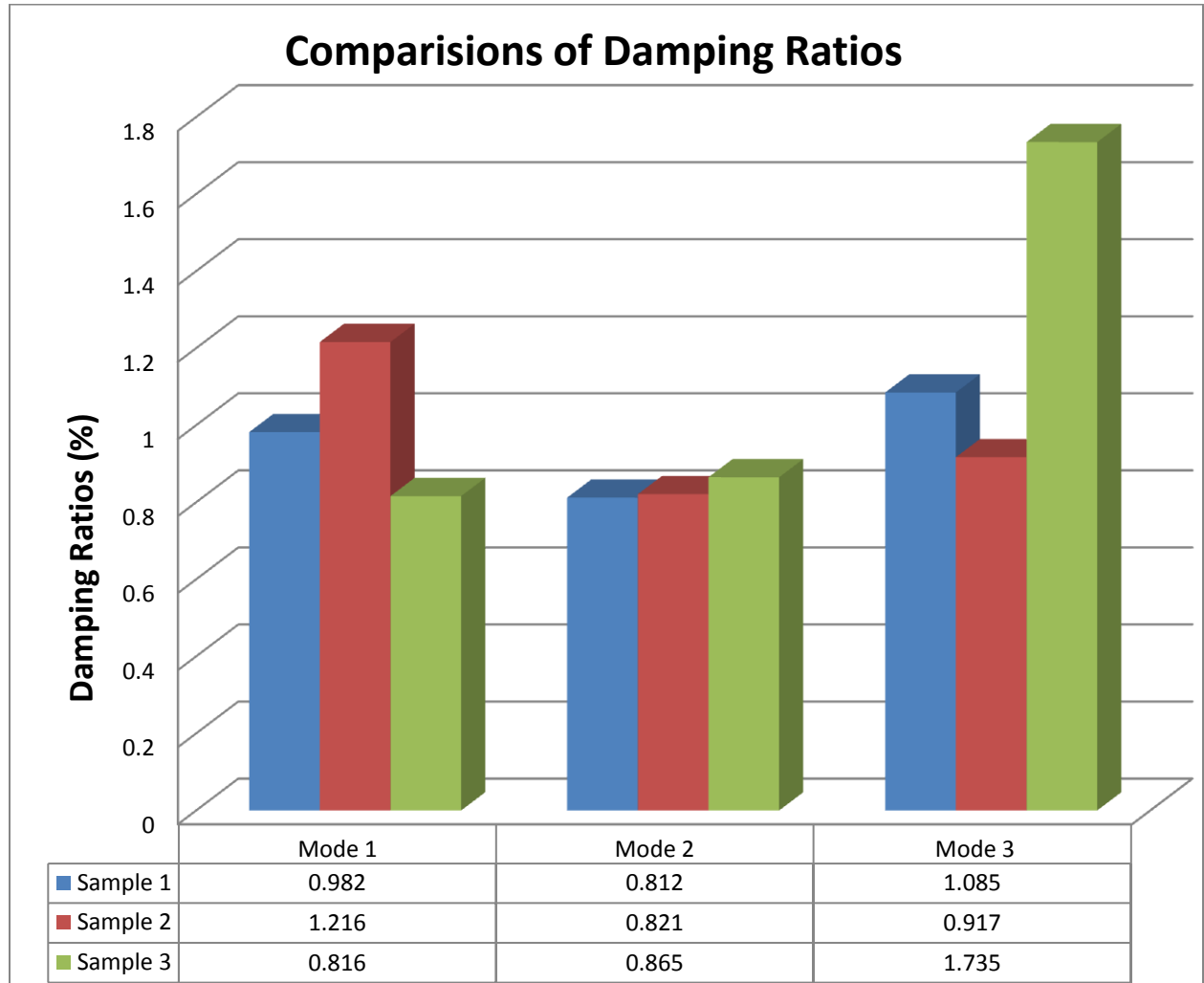


Figure 6.32. Comparisons of Damping Ratios

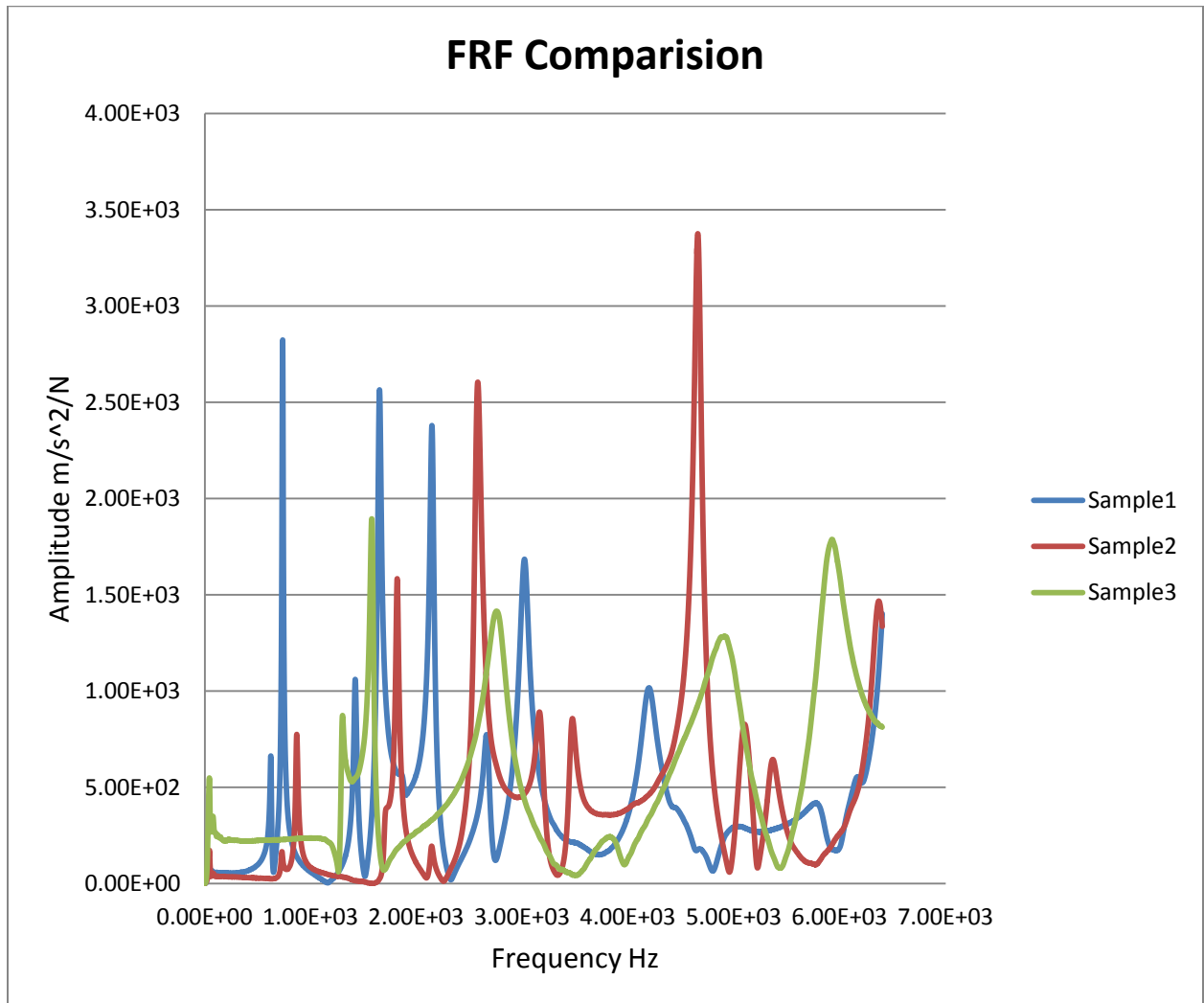


Figure 6.33 FRF Comparisons of the Rectangular ABS Samples

Table4.Theoretical Natural Frequencies for ABS Rectangular Samples

Sample No	Natural Frequencies(Hz)		
	f_1	f_2	f_3
1	684.46	734	1586
2	785.74	843	1821
3	1540	1652	3569

Table5.Theoretical Frequency Ratios for ABS Rectangular Samples

Frequency Ratio	Sample No		
	1	2	3
f_1/f_2	0.932	0.932	0.932
f_1/f_3	0.431	0.431	0.431

Table 6. Experimental Natural Frequencies for ABS Rectangular Samples

Sample No	Natural Frequencies (Hz)		
	f_1	f_2	f_3
1	619	738	1430
2	698	865	1600
3	1289	1578	2689

Table 7. Experimental Frequency Ratios for ABS Rectangular Samples

Frequency Ratio	Sample No		
	1	2	3
f_1/f_2	0.838	0.806	0.816
f_1/f_3	0.432	0.436	0.479

Table 8. Finite Element Natural Frequencies for ABS Rectangular Samples

Sample No	Natural Frequencies (Hz)		
	f_1	f_2	f_3
1	622.96	699.25	1435.1
2	712.93	801.46	1639.8
3	1369.9	1553.2	3166.8

Table 9. Finite Element Frequency Ratios for ABS Rectangular Samples

Frequency Ratio	Sample No		
	1	2	3
f_1/f_2	0.89	0.889	0.881
f_1/f_3	0.434	0.434	0.432

Table10. Comparisons of Calculated Experimental, Finite Element and Theoretical
Natural Frequencies (Hz)

Samples	Sample1			Sample2			Sample3		
	ω_{n1}	ω_{n2}	ω_{n3}	ω_{n1}	ω_{n2}	ω_{n3}	ω_{n1}	ω_{n2}	ω_{n3}
Experiment	619	738	1430	698	865	1600	1289	1578	2689
Finite Element	623	699	1435	713	801	1640	1370	1553	3116
Calculation	684	734	1586	785	843	1821	1540	1652	3569

Table 11. Comparisons of Calculated Experimental, Finite Element and Theoretical
Frequency Ratios

Sample No	Experimental		Finite Element		Theoretical	
	f_1/f_2	f_1/f_3	f_1/f_2	f_1/f_3	f_1/f_2	f_1/f_3
1	0.838	0.432	0.89	0.434	0.932	0.431
2	0.806	0.436	0.889	0.434	0.932	0.431
3	0.816	0.479	0.881	0.432	0.932	0.431

Table 12. Modal Densities

	Sample 1	Sample 2	Sample 3
Modal Densities	12	11	9

APPENDIX A

EIGENVALUE OUTPUTS OF SAMPLE 1 in ABAQUS

Abaqus 6.9-2

Date 13-Feb-2012 Time 18:37:21

For use at Wayne State University under license from Dassault Systemes or its subsidiary.

The Abaqus Software is a product of:

Dassault Systemes Simulia Corp.
Rising Sun Mills
166 Valley Street
Providence, RI 02909-2499, USA

Available for internal use at Wayne State University.
The Abaqus Online Support System is accessible through the "My Support" section of the SIMULIA Home Page at <http://www.simulia.com>.

Support policies for academic licenses are described on the SIMULIA web site at http://www.simulia.com/academics/academic_support.html.

On machine lan2.grid.wayne.edu
you are authorized to run
Abaqus/Standard until 04-Oct-2012

Your site id is: 08WAYNEUA

For assistance or any other information you may obtain contact information for your local office from the world wide web at:

<http://www.simulia.com/about/locations.html>

```

* * * * *
*
*          *****
*          * N O T I C E *
*          *****
*
*
*          Abaqus 6.9-2
*
*          BUILD ID: 2009_07_10-10.30.58 92676
*
*
* Please make sure you are using release 6.9 manuals
* plus the notes accompanying this release.
*
*
*
*
* This program may not be used for commercial purposes
* without payment of a commercial fee.
*
* * * * *

```

```

PROCESSING PART, INSTANCE, AND ASSEMBLY INFORMATION
*****

```

```

END PROCESSING PART, INSTANCE, AND ASSEMBLY INFORMATION
*****

```

```

OPTIONS BEING PROCESSED
*****

```

```

*NODE
*ELEMENT,TYPE=C3D20R,ELSET=ABS
*MATERIAL, NAME=ABS
*DENSITY
*ELASTIC, TYPE = ISOTROPIC
*SOLID SECTION, ELSET=ABS, MATERIAL=ABS
*SOLID SECTION, ELSET=ABS, MATERIAL=ABS

```

```

*STEP, INC =          1000, PERTURBATION
*FREQUENCY, EIGENSOLVER = LANCZOS, NORMALIZATION = DISPLACEMENT
*STEP, INC =          1000, PERTURBATION
*STEP, INC =          1000, PERTURBATION
*FREQUENCY, EIGENSOLVER = LANCZOS, NORMALIZATION = DISPLACEMENT
*FREQUENCY, EIGENSOLVER = LANCZOS, NORMALIZATION = DISPLACEMENT
*EL FILE, POSITION = AVERAGED AT NODES
*END STEP
*STEP, INC =          1000, PERTURBATION
*FREQUENCY, EIGENSOLVER = LANCZOS, NORMALIZATION = DISPLACEMENT
*FREQUENCY, EIGENSOLVER = LANCZOS, NORMALIZATION = DISPLACEMENT
*NODE FILE
*END STEP

```

P R O B L E M S I Z E

NUMBER OF ELEMENTS IS	21660
NUMBER OF NODES IS	96199
NUMBER OF NODES DEFINED BY THE USER	96199
TOTAL NUMBER OF VARIABLES IN THE MODEL	288597
(DEGREES OF FREEDOM PLUS ANY LAGRANGE MULTIPLIER VARIABLES)	

END OF USER INPUT PROCESSING

JOB TIME SUMMARY

USER TIME (SEC)	=	5.9800
SYSTEM TIME (SEC)	=	0.79000
TOTAL CPU TIME (SEC)	=	6.7700
WALLCLOCK TIME (SEC)	=	81

Abaqus 6.9-2

Date 13-Feb-2012 Time

18:37:31

For use at Wayne State University under license from Dassault Systemes or its subsidiary.

STEP 1 INCREMENT 1

TIME COMPLETED IN THIS STEP 0.00

S T E P 1 C A L C U L A T I O N O F E I G E N V A L U E S
 F O R N A T U R A L F R E Q U E N C I E S

THE LANCZOS EIGENSOLVER IS USED FOR THIS ANALYSIS

Abaqus WILL COMPUTE UNCOUPLED

STRUCTURAL AND ACOUSTIC MODES

NUMBER OF EIGENVALUES	12
HIGHEST FREQUENCY OF INTEREST	1.00000E+18
MAXIMUM NUMBER OF STEPS WITHIN RUN	35
BLOCK SIZE FOR LANCZOS PROCEDURE	7

THE EIGENVECTORS ARE SCALED SO THAT

THE LARGEST DISPLACEMENT ENTRY IN EACH VECTOR
 IS UNITY

THIS IS A LINEAR PERTURBATION STEP.

ALL LOADS ARE DEFINED AS CHANGE IN LOAD TO THE REFERENCE STATE

TOTAL MASS OF MODEL

5.3512151E-05

LOCATION OF THE CENTER OF MASS OF THE MODEL

57.15000	38.10000	3.000000
----------	----------	----------

MOMENTS OF INERTIA ABOUT THE ORIGIN

I (XX)	I (YY)	I (ZZ)
0.1042138	0.2336785	0.3366080

PRODUCTS OF INERTIA ABOUT THE ORIGIN

I (XY)	I (XZ)	I (YZ)
-0.1165182	-9.1746583E-03	-6.1164389E-03

MOMENTS OF INERTIA ABOUT THE CENTER OF MASS

I (XX)	I (YY)	I (ZZ)
--------	--------	--------

2.6053461E-02 5.8419617E-02 8.4152005E-02

PRODUCTS OF INERTIA ABOUT THE CENTER OF MASS

I (XY)	I (XZ)	I (YZ)
3.3389957E-14	1.6375790E-15	3.4338851E-15

M E M O R Y E S T I M A T E

PROCESS	FLOATING PT OPERATIONS PER ITERATION	MINIMUM MEMORY REQUIRED (MBYTES)	MEMORY TO MINIMIZE I/O (MBYTES)
1	1.26E+12	534	5796

NOTE:

(1) SINCE ABAQUS DOES NOT PRE-ALLOCATE MEMORY AND ONLY ALLOCATES MEMORY AS NEEDED DURING THE ANALYSIS,

THE MEMORY REQUIREMENT PRINTED HERE CAN ONLY BE VIEWED AS A GENERAL GUIDELINE BASED ON THE BEST

KNOWLEDGE AVAILABLE AT THE BEGINNING OF A STEP BEFORE THE SOLUTION PROCESS HAS BEGUN.

(2) THE ESTIMATE IS NORMALLY UPDATED AT THE BEGINNING OF EVERY STEP. IT IS THE MAXIMUM VALUE OF THE

ESTIMATE FROM THE CURRENT STEP TO THE LAST STEP OF THE ANALYSIS, WITH UNSYMMETRIC SOLUTION TAKEN

INTO ACCOUNT IF APPLICABLE.

(3) SINCE THE ESTIMATE IS BASED ON THE ACTIVE DEGREES OF FREEDOM IN THE FIRST ITERATION OF THE

CURRENT STEP, THE MEMORY ESTIMATE MIGHT BE SIGNIFICANTLY DIFFERENT THAN ACTUAL USAGE FOR

PROBLEMS WITH SUBSTANTIAL CHANGES IN ACTIVE DEGREES OF FREEDOM BETWEEN STEPS (OR EVEN WITHIN

THE SAME STEP). EXAMPLES ARE: PROBLEMS WITH SIGNIFICANT CONTACT CHANGES, PROBLEMS WITH MODEL

CHANGE, PROBLEMS WITH BOTH STATIC STEP AND STEADY STATE DYNAMIC PROCEDURES WHERE ACOUSTIC

ELEMENTS WILL ONLY BE ACTIVATED IN THE STEADY STATE DYNAMIC STEPS.

(4) FOR MULTI-PROCESS EXECUTION, THE ESTIMATED VALUE OF FLOATING POINT OPERATIONS FOR EACH PROCESS

IS BASED ON AN INITIAL SCHEDULING OF OPERATIONS AND MIGHT NOT REFLECT THE ACTUAL FLOATING

POINT OPERATIONS COMPLETED ON EACH PROCESS. OPERATIONS ARE DYNAMICALLY BALANCED DURING EXECUTION,

SO THE ACTUAL BALANCE OF OPERATIONS BETWEEN PROCESSES IS EXPECTED TO BE BETTER THAN THE ESTIMATE

PRINTED HERE.

(5) THE UPPER LIMIT OF MEMORY THAT CAN BE ALLOCATED BY ABAQUS WILL IN GENERAL DEPEND ON THE VALUE OF

THE "MEMORY" PARAMETER AND THE AMOUNT OF PHYSICAL MEMORY AVAILABLE ON THE MACHINE. PLEASE SEE

THE "ABAQUS ANALYSIS USER'S MANUAL" FOR MORE DETAILS. THE ACTUAL USAGE OF MEMORY AND OF DISK

SPACE FOR SCRATCH DATA WILL DEPEND ON THIS UPPER LIMIT AS WELL AS THE MEMORY REQUIRED TO MINIMIZE

I/O. IF THE MEMORY UPPER LIMIT IS GREATER THAN THE MEMORY REQUIRED TO MINIMIZE I/O, THEN THE ACTUAL

MEMORY USAGE WILL BE CLOSE TO THE ESTIMATED "MEMORY TO MINIMIZE I/O" VALUE, AND THE SCRATCH DISK

USAGE WILL BE CLOSE-TO-ZERO; OTHERWISE, THE ACTUAL MEMORY USED WILL BE CLOSE TO THE PREVIOUSLY

MENTIONED MEMORY LIMIT, AND THE SCRATCH DISK USAGE WILL BE ROUGHLY PROPORTIONAL TO THE DIFFERENCE

BETWEEN THE ESTIMATED "MEMORY TO MINIMIZE I/O" AND THE MEMORY UPPER LIMIT. HOWEVER ACCURATE

ESTIMATE OF THE SCRATCH DISK SPACE IS NOT POSSIBLE.

(6) USING "*RESTART, WRITE" CAN GENERATE A LARGE AMOUNT OF DATA WRITTEN IN THE WORK DIRECTORY.

E I G E N V A L U E O U T P U T

MODE NO	EIGENVALUE	FREQUENCY	GENERALIZED MASS
COMPOSITE MODAL DAMPING			
		(RAD/TIME)	(CYCLES/TIME)
1	-2.92391E-03	0.0000	0.0000
0.0000			1.04170E-05
2	-2.46711E-03	0.0000	0.0000
0.0000			8.46785E-06
3	-2.37438E-03	0.0000	0.0000
0.0000			8.01121E-06

4	3.46925E-04	1.86259E-02	2.96441E-03	1.79050E-05
0.0000				
5	4.70849E-04	2.16991E-02	3.45351E-03	5.17385E-05
0.0000				
6	7.12980E-04	2.67017E-02	4.24970E-03	1.79972E-05
0.0000				
7	1.53206E+07	3914.2	622.96	7.38637E-06
0.0000				
8	1.93028E+07	4393.5	699.25	1.19712E-05
0.0000				
9	8.13038E+07	9016.9	1435.1	6.11121E-06
0.0000				
10	1.06869E+08	10338.	1645.3	1.02242E-05
0.0000				
11	1.29583E+08	11383.	1811.7	7.04885E-06
0.0000				
12	1.87787E+08	13704.	2181.0	4.10722E-06
0.0000				

P A R T I C I P A T I O N F A C T O R S

MODE NO	X-COMPONENT	Y-COMPONENT	Z-COMPONENT	X-ROTATION	Y-
ROTATION	Z-ROTATION				
1	8.25229E-04	1.92505E-02	1.6596	50.334	-
142.08	1.5149				
2	5.49741E-03	1.30362E-02	1.6108	93.131	-
49.629	0.52629				
3	-1.50554E-02	-8.63332E-03	0.59585	-21.643	
15.790	-1.1165				
4	1.81183E-02	1.2129	-9.55789E-03	-3.8851	
0.38187	19.784				
5	1.0168	3.04774E-03	-3.73321E-04	-0.15440	
3.1627	-37.856				
6	-2.51291E-02	1.2286	-1.18396E-02	-4.4327	
1.1881	119.13				
7	-6.11039E-13	3.61370E-12	-1.89961E-11	1.10304E-09	
1.01544E-09	1.44772E-10				
8	-1.91731E-12	-9.31543E-13	2.79016E-12	-1.01969E-10	
7.55887E-10	-5.79674E-11				

9	3.95123E-13	-7.39269E-13	2.27749E-12	5.88778E-11	
8.75154E-11	-3.63949E-11				
10	1.86225E-13	3.72278E-13	5.00771E-12	2.07242E-10	-
2.89179E-11	2.46989E-11				
11	-6.09468E-14	-3.88932E-13	2.62438E-12	8.23943E-11	-
1.81429E-10	-4.24445E-11				
12	-1.87324E-13	7.58501E-14	-5.78566E-12	-1.30134E-10	
1.18382E-10	2.25026E-11				

E F F E C T I V E M A S S

MODE NO	X-COMPONENT	Y-COMPONENT	Z-COMPONENT	X-ROTATION	Y-
ROTATION	Z-ROTATION				
1	7.09402E-12	3.86035E-09	2.86916E-05	2.63916E-02	
0.21028	2.39065E-05				
2	2.55911E-10	1.43906E-09	2.19721E-05	7.34447E-02	
2.08565E-02	2.34540E-06				
3	1.81587E-09	5.97109E-10	2.84427E-06	3.75247E-03	
1.99746E-03	9.98728E-06				
4	5.87774E-09	2.63408E-05	1.63568E-09	2.70254E-04	
2.61093E-06	7.00824E-03				
5	5.34928E-05	4.80585E-10	7.21074E-12	1.23342E-06	
5.17533E-04	7.41441E-02				
6	1.13647E-08	2.71650E-05	2.52277E-09	3.53621E-04	
2.54047E-05	0.25542				
7	2.75784E-30	9.64573E-29	2.66537E-27	8.98702E-24	
7.61617E-24	1.54810E-25				
8	4.40070E-29	1.03882E-29	9.31955E-29	1.24471E-25	
6.83989E-24	4.02256E-26				
9	9.54097E-31	3.33989E-30	3.16987E-29	2.11851E-26	
4.68055E-26	8.09486E-27				
10	3.54572E-31	1.41698E-30	2.56394E-28	4.39121E-25	
8.54992E-27	6.23715E-27				
11	2.61830E-32	1.06627E-30	4.85481E-29	4.78534E-26	
2.32022E-25	1.26988E-26				
12	1.44123E-31	2.36298E-32	1.37485E-28	6.95551E-26	
5.75594E-26	2.07975E-27				
TOTAL	5.35122E-05	5.35122E-05	5.35122E-05	0.10421	
0.23368	0.33661				

THE ANALYSIS HAS BEEN COMPLETED

ANALYSIS COMPLETE

JOB TIME SUMMARY

USER TIME (SEC)	=	1359.6
SYSTEM TIME (SEC)	=	37.960
TOTAL CPU TIME (SEC)	=	1397.5
WALLCLOCK TIME (SEC)	=	140

APPENDIX B

EIGENVALUE OUTPUTS OF SAMPLE 2 in ABAQUS

Abaqus 6.9-2

Date 13-Feb-2012 Time 19:03:46

For use at Wayne State University under license from Dassault Systemes or its subsidiary.

The Abaqus Software is a product of:

Dassault Systemes Simulia Corp.
Rising Sun Mills
166 Valley Street
Providence, RI 02909-2499, USA

Available for internal use at Wayne State University.
The Abaqus Online Support System is accessible through the "My Support" section of the SIMULIA Home Page at <http://www.simulia.com>.

Support policies for academic licenses are described on the SIMULIA web site at http://www.simulia.com/academics/academic_support.html.

On machine lan2.grid.wayne.edu
you are authorized to run
Abaqus/Standard until 04-Oct-2012

Your site id is: 08WAYNEUA

For assistance or any other information you may obtain contact information for your local office from the world wide web at:

<http://www.simulia.com/about/locations.html>

```

* * * * *
*
*          *****
*          * N O T I C E *
*          *****
*
*
*          Abaqus 6.9-2
*
*          BUILD ID: 2009_07_10-10.30.58 92676
*
*
* Please make sure you are using release 6.9 manuals
* plus the notes accompanying this release.
*
*
*
*
* This program may not be used for commercial purposes
* without payment of a commercial fee.
*
* * * * *

```

```

PROCESSING PART, INSTANCE, AND ASSEMBLY INFORMATION
*****

```

```

END PROCESSING PART, INSTANCE, AND ASSEMBLY INFORMATION
*****

```

```

OPTIONS BEING PROCESSED
*****

```

```

*NODE
*ELEMENT,TYPE=C3D20R,ELSET=ABS
*MATERIAL, NAME=ABS
*DENSITY
*ELASTIC, TYPE = ISOTROPIC
*SOLID SECTION, ELSET=ABS, MATERIAL=ABS
*SOLID SECTION, ELSET=ABS, MATERIAL=ABS

```



```

*STEP, INC =          1000, PERTURBATION
*FREQUENCY, EIGENSOLVER = LANCZOS, NORMALIZATION = DISPLACEMENT
*STEP, INC =          1000, PERTURBATION
*STEP, INC =          1000, PERTURBATION
*FREQUENCY, EIGENSOLVER = LANCZOS, NORMALIZATION = DISPLACEMENT
*FREQUENCY, EIGENSOLVER = LANCZOS, NORMALIZATION = DISPLACEMENT
*EL FILE, POSITION = AVERAGED AT NODES
*END STEP
*STEP, INC =          1000, PERTURBATION
*FREQUENCY, EIGENSOLVER = LANCZOS, NORMALIZATION = DISPLACEMENT
*FREQUENCY, EIGENSOLVER = LANCZOS, NORMALIZATION = DISPLACEMENT
*NODE FILE
*END STEP

```

P R O B L E M S I Z E

```

NUMBER OF ELEMENTS IS          19080
NUMBER OF NODES IS            84913
NUMBER OF NODES DEFINED BY THE USER      84913
TOTAL NUMBER OF VARIABLES IN THE MODEL    254739
(DEGREES OF FREEDOM PLUS ANY LAGRANGE MULTIPLIER VARIABLES)

```

END OF USER INPUT PROCESSING

JOB TIME SUMMARY

```

USER TIME (SEC)      =    5.2800
SYSTEM TIME (SEC)   =    0.74000
TOTAL CPU TIME (SEC) =    6.0200
WALLCLOCK TIME (SEC) =           71

```

Abaqus 6.9-2
19:03:56

Date 13-Feb-2012 Time

For use at Wayne State University under license from Dassault Systemes or its subsidiary.

STEP 1 INCREMENT 1

TIME COMPLETED IN THIS STEP 0.00

STEP 1 CALCULATION OF EIGENVALUES
FOR NATURAL FREQUENCIES

THE LANCZOS EIGENSOLVER IS USED FOR THIS ANALYSIS

Abaqus WILL COMPUTE UNCOUPLED
STRUCTURAL AND ACOUSTIC MODES

NUMBER OF EIGENVALUES	12
HIGHEST FREQUENCY OF INTEREST	1.00000E+18
MAXIMUM NUMBER OF STEPS WITHIN RUN	35
BLOCK SIZE FOR LANCZOS PROCEDURE	7

THE EIGENVECTORS ARE SCALED SO THAT
THE LARGEST DISPLACEMENT ENTRY IN EACH VECTOR
IS UNITY

THIS IS A LINEAR PERTURBATION STEP.
ALL LOADS ARE DEFINED AS CHANGE IN LOAD TO THE REFERENCE STATE

TOTAL MASS OF MODEL

4.6615029E-05

LOCATION OF THE CENTER OF MASS OF THE MODEL

53.34000	35.56000	3.000000
----------	----------	----------

MOMENTS OF INERTIA ABOUT THE ORIGIN

I (XX)	I (YY)	I (ZZ)
7.9153165E-02	0.1773954	0.2554298

PRODUCTS OF INERTIA ABOUT THE ORIGIN

I (XY)	I (XZ)	I (YZ)
-8.8418008E-02	-7.4593370E-03	-4.9728913E-03

MOMENTS OF INERTIA ABOUT THE CENTER OF MASS

I (XX)	I (YY)	I (ZZ)
1.9788291E-02	4.4348849E-02	6.3857450E-02

PRODUCTS OF INERTIA ABOUT THE CENTER OF MASS

I (XY)	I (XZ)	I (YZ)
-6.8459127E-14	-1.2698176E-14	-8.7117813E-15

M E M O R Y E S T I M A T E

PROCESS	FLOATING PT OPERATIONS PER ITERATION	MINIMUM MEMORY REQUIRED (MBYTES)	MEMORY TO MINIMIZE I/O (MBYTES)
1	1.02E+12	472	5023

NOTE:

(1) SINCE ABAQUS DOES NOT PRE-ALLOCATE MEMORY AND ONLY ALLOCATES MEMORY AS NEEDED DURING THE ANALYSIS,

THE MEMORY REQUIREMENT PRINTED HERE CAN ONLY BE VIEWED AS A GENERAL GUIDELINE BASED ON THE BEST

KNOWLEDGE AVAILABLE AT THE BEGINNING OF A STEP BEFORE THE SOLUTION PROCESS HAS BEGUN.

(2) THE ESTIMATE IS NORMALLY UPDATED AT THE BEGINNING OF EVERY STEP. IT IS THE MAXIMUM VALUE OF THE

ESTIMATE FROM THE CURRENT STEP TO THE LAST STEP OF THE ANALYSIS, WITH UNSYMMETRIC SOLUTION TAKEN

INTO ACCOUNT IF APPLICABLE.

(3) SINCE THE ESTIMATE IS BASED ON THE ACTIVE DEGREES OF FREEDOM IN THE FIRST ITERATION OF THE

CURRENT STEP, THE MEMORY ESTIMATE MIGHT BE SIGNIFICANTLY DIFFERENT THAN ACTUAL USAGE FOR

PROBLEMS WITH SUBSTANTIAL CHANGES IN ACTIVE DEGREES OF FREEDOM BETWEEN STEPS (OR EVEN WITHIN THE SAME STEP). EXAMPLES ARE: PROBLEMS WITH SIGNIFICANT CONTACT CHANGES, PROBLEMS WITH MODEL CHANGE, PROBLEMS WITH BOTH STATIC STEP AND STEADY STATE DYNAMIC PROCEDURES WHERE ACOUSTIC ELEMENTS WILL ONLY BE ACTIVATED IN THE STEADY STATE DYNAMIC STEPS.

(4) FOR MULTI-PROCESS EXECUTION, THE ESTIMATED VALUE OF FLOATING POINT OPERATIONS FOR EACH PROCESS IS BASED ON AN INITIAL SCHEDULING OF OPERATIONS AND MIGHT NOT REFLECT THE ACTUAL FLOATING POINT OPERATIONS COMPLETED ON EACH PROCESS. OPERATIONS ARE DYNAMICALLY BALANCED DURING EXECUTION, SO THE ACTUAL BALANCE OF OPERATIONS BETWEEN PROCESSES IS EXPECTED TO BE BETTER THAN THE ESTIMATE PRINTED HERE.

(5) THE UPPER LIMIT OF MEMORY THAT CAN BE ALLOCATED BY ABAQUS WILL IN GENERAL DEPEND ON THE VALUE OF THE "MEMORY" PARAMETER AND THE AMOUNT OF PHYSICAL MEMORY AVAILABLE ON THE MACHINE. PLEASE SEE THE "ABAQUS ANALYSIS USER'S MANUAL" FOR MORE DETAILS. THE ACTUAL USAGE OF MEMORY AND OF DISK SPACE FOR SCRATCH DATA WILL DEPEND ON THIS UPPER LIMIT AS WELL AS THE MEMORY REQUIRED TO MINIMIZE I/O. IF THE MEMORY UPPER LIMIT IS GREATER THAN THE MEMORY REQUIRED TO MINIMIZE I/O, THEN THE ACTUAL MEMORY USAGE WILL BE CLOSE TO THE ESTIMATED "MEMORY TO MINIMIZE I/O" VALUE, AND THE SCRATCH DISK USAGE WILL BE CLOSE-TO-ZERO; OTHERWISE, THE ACTUAL MEMORY USED WILL BE CLOSE TO THE PREVIOUSLY MENTIONED MEMORY LIMIT, AND THE SCRATCH DISK USAGE WILL BE ROUGHLY PROPORTIONAL TO THE DIFFERENCE BETWEEN THE ESTIMATED "MEMORY TO MINIMIZE I/O" AND THE MEMORY UPPER LIMIT. HOWEVER ACCURATE ESTIMATE OF THE SCRATCH DISK SPACE IS NOT POSSIBLE.

(6) USING "*RESTART, WRITE" CAN GENERATE A LARGE AMOUNT OF DATA WRITTEN IN THE WORK DIRECTORY.

E I G E N V A L U E O U T P U T

MODE NO	EIGENVALUE	FREQUENCY		GENERALIZED MASS
COMPOSITE MODAL DAMPING		(RAD/TIME)	(CYCLES/TIME)	
1	-3.61542E-04	0.0000	0.0000	3.27951E-05
0.0000				
2	-2.49531E-04	0.0000	0.0000	1.83741E-05
0.0000				
3	-6.08313E-05	0.0000	0.0000	2.81028E-05
0.0000				
4	5.69160E-03	7.54427E-02	1.20071E-02	6.99135E-06
0.0000				
5	5.84183E-03	7.64318E-02	1.21645E-02	7.73675E-06
0.0000				
6	6.43295E-03	8.02057E-02	1.27651E-02	1.00066E-05
0.0000				
7	2.00657E+07	4479.5	712.93	6.43959E-06
0.0000				
8	2.53583E+07	5035.7	801.46	1.04538E-05
0.0000				
9	1.06152E+08	10303.	1639.8	5.33448E-06
0.0000				
10	1.39877E+08	11827.	1882.3	8.92942E-06
0.0000				
11	1.69198E+08	13008.	2070.2	6.16326E-06
0.0000				
12	2.45013E+08	15653.	2491.2	3.59336E-06
0.0000				

P A R T I C I P A T I O N F A C T O R S

MODE NO	X-COMPONENT	Y-COMPONENT	Z-COMPONENT	X-ROTATION	Y-
ROTATION	Z-ROTATION				

1	1.1611	2.80118E-03	2.77164E-03	8.48551E-02	
3.2195	-31.127				
2	0.35145	0.35626	-3.51209E-03	-0.96797	
1.0785	-49.460				
3	-6.82481E-02	1.2553	-3.80752E-03	-3.9121	-
0.10220	79.743				
4	-7.24261E-03	6.17761E-04	1.3824	21.720	-
127.03	-1.86852E-02				
5	4.99586E-03	1.15889E-02	1.4277	33.084	-
20.515	-1.45443E-03				
6	-5.69688E-03	1.74413E-03	1.3218	81.789	-
78.048	0.63259				
7	3.78762E-13	-4.81652E-12	-9.07194E-12	7.34193E-10	
2.51013E-10	-3.58668E-10				
8	4.26953E-13	-7.70635E-13	-2.31121E-11	-1.63057E-09	
7.68037E-10	-1.64698E-10				
9	-1.72319E-13	9.94216E-14	1.21692E-11	5.25167E-10	-
2.28301E-10	-3.41678E-11				
10	-1.87165E-13	6.89291E-14	2.69856E-12	1.50217E-10	
6.92072E-11	1.32546E-11				
11	2.18224E-13	-1.22344E-13	6.38952E-12	3.12955E-10	-
1.98334E-10	-1.36686E-11				
12	3.64454E-13	3.23242E-13	2.86583E-12	-7.20118E-11	-
6.29783E-11	6.53629E-12				

E F F E C T I V E M A S S

MODE NO	X-COMPONENT	Y-COMPONENT	Z-COMPONENT	X-ROTATION	Y-ROTATION
1	4.42137E-05	2.57331E-10	2.51931E-10	2.36137E-07	
3.39933E-04	3.17739E-02				
2	2.26951E-06	2.33206E-06	2.26639E-10	1.72159E-05	
2.13726E-05	4.49483E-02				
3	1.30897E-07	4.42816E-05	4.07411E-10	4.30091E-04	
2.93555E-07	0.17870				
4	3.66734E-10	2.66810E-12	1.33611E-05	3.29828E-03	
0.11282	2.44094E-09				
5	1.93099E-10	1.03906E-09	1.57711E-05	8.46807E-03	
3.25625E-03	1.63662E-11				

6	3.24759E-10	3.04401E-11	1.74819E-05	6.69393E-02
6.09559E-02	4.00437E-06			
7	9.23829E-31	1.49391E-28	5.29978E-28	3.47119E-24
4.05743E-25	8.28404E-25			
8	1.90561E-30	6.20829E-30	5.58411E-27	2.77943E-23
6.16650E-24	2.83564E-25			
9	1.58401E-31	5.27295E-32	7.89976E-28	1.47125E-24
2.78040E-25	6.22766E-27			
10	3.12805E-31	4.24257E-32	6.50261E-29	2.01493E-25
4.27687E-26	1.56875E-27			
11	2.93506E-31	9.22514E-32	2.51621E-28	6.03636E-25
2.42440E-25	1.15148E-27			
12	4.77296E-31	3.75455E-31	2.95121E-29	1.86341E-26
1.42522E-26	1.53520E-28			
TOTAL	4.66150E-05	4.66150E-05	4.66150E-05	7.91532E-02
0.17740	0.25543			

THE ANALYSIS HAS BEEN COMPLETED

ANALYSIS COMPLETE

JOB TIME SUMMARY

USER TIME (SEC)	=	1111.9
SYSTEM TIME (SEC)	=	33.760
TOTAL CPU TIME (SEC)	=	1145.7
WALLCLOCK TIME (SEC)	=	1151

APPENDIX C

EIGENVALUE OUTPUTS OF SAMPLE 3 in ABAQUS

Abaqus 6.9-2

Date 13-Feb-2012 Time 19:16:34

For use at Wayne State University under license from Dassault Systemes or its subsidiary.

The Abaqus Software is a product of:

Dassault Systemes Simulia Corp.
Rising Sun Mills
166 Valley Street
Providence, RI 02909-2499, USA

Available for internal use at Wayne State University.
The Abaqus Online Support System is accessible
through the "My Support" section of the SIMULIA
Home Page at <http://www.simulia.com>.

Support policies for academic licenses are described
on the SIMULIA web site at
http://www.simulia.com/academics/academic_support.html.

On machine lan1.grid.wayne.edu
you are authorized to run
Abaqus/Standard until 04-Oct-2012

Your site id is: 08WAYNEUA

For assistance or any other information you may
obtain contact information for your local office
from the world wide web at:

<http://www.simulia.com/about/locations.html>

* * * * *


```

*FREQUENCY, EIGENSOLVER = LANCZOS, NORMALIZATION = DISPLACEMENT
*STEP, INC =          1000, PERTURBATION
*STEP, INC =          1000, PERTURBATION
*FREQUENCY, EIGENSOLVER = LANCZOS, NORMALIZATION = DISPLACEMENT
*FREQUENCY, EIGENSOLVER = LANCZOS, NORMALIZATION = DISPLACEMENT
*EL FILE, POSITION = AVERAGED AT NODES
*END STEP
*STEP, INC =          1000, PERTURBATION
*FREQUENCY, EIGENSOLVER = LANCZOS, NORMALIZATION = DISPLACEMENT
*FREQUENCY, EIGENSOLVER = LANCZOS, NORMALIZATION = DISPLACEMENT
*NODE FILE
*END STEP

```

P R O B L E M S I Z E

```

NUMBER OF ELEMENTS IS          19440
NUMBER OF NODES IS             86493
NUMBER OF NODES DEFINED BY THE USER      86493
TOTAL NUMBER OF VARIABLES IN THE MODEL    259479
(DEGREES OF FREEDOM PLUS ANY LAGRANGE MULTIPLIER VARIABLES)

```

END OF USER INPUT PROCESSING

JOB TIME SUMMARY

```

USER TIME (SEC)      =    5.6800
SYSTEM TIME (SEC)    =    0.89000
TOTAL CPU TIME (SEC) =    6.5700
WALLCLOCK TIME (SEC) =   101

```

```

Abaqus 6.9-2                      Date 13-Feb-2012   Time
19:16:47

```

For use at Wayne State University under license from Dassault Systemes or its subsidiary.

```

STEP      1  INCREMENT      1
TIME COMPLETED IN THIS STEP  0.00

```


MOMENTS OF INERTIA ABOUT THE CENTER OF MASS

I (XX)	I (YY)	I (ZZ)
5.1860013E-03	1.1579316E-02	1.6622618E-02

PRODUCTS OF INERTIA ABOUT THE CENTER OF MASS

I (XY)	I (XZ)	I (YZ)
5.0306981E-15	-2.3171569E-15	-1.1236671E-15

M E M O R Y E S T I M A T E

PROCESS	FLOATING PT OPERATIONS PER ITERATION	MINIMUM MEMORY REQUIRED (MBYTES)	MEMORY TO MINIMIZE I/O (MBYTES)
1	1.04E+12	475	5118

NOTE:

- (1) SINCE ABAQUS DOES NOT PRE-ALLOCATE MEMORY AND ONLY ALLOCATES MEMORY AS NEEDED DURING THE ANALYSIS, THE MEMORY REQUIREMENT PRINTED HERE CAN ONLY BE VIEWED AS A GENERAL GUIDELINE BASED ON THE BEST KNOWLEDGE AVAILABLE AT THE BEGINNING OF A STEP BEFORE THE SOLUTION PROCESS HAS BEGUN.
- (2) THE ESTIMATE IS NORMALLY UPDATED AT THE BEGINNING OF EVERY STEP. IT IS THE MAXIMUM VALUE OF THE ESTIMATE FROM THE CURRENT STEP TO THE LAST STEP OF THE ANALYSIS, WITH UNSYMMETRIC SOLUTION TAKEN INTO ACCOUNT IF APPLICABLE.
- (3) SINCE THE ESTIMATE IS BASED ON THE ACTIVE DEGREES OF FREEDOM IN THE FIRST ITERATION OF THE CURRENT STEP, THE MEMORY ESTIMATE MIGHT BE SIGNIFICANTLY DIFFERENT THAN ACTUAL USAGE FOR PROBLEMS WITH SUBSTANTIAL CHANGES IN ACTIVE DEGREES OF FREEDOM BETWEEN STEPS (OR EVEN WITHIN THE SAME STEP). EXAMPLES ARE: PROBLEMS WITH SIGNIFICANT CONTACT CHANGES, PROBLEMS WITH MODEL CHANGE, PROBLEMS WITH BOTH STATIC STEP AND STEADY STATE DYNAMIC PROCEDURES WHERE ACOUSTIC

ELEMENTS WILL ONLY BE ACTIVATED IN THE STEADY STATE DYNAMIC STEPS.

(4) FOR MULTI-PROCESS EXECUTION, THE ESTIMATED VALUE OF FLOATING POINT OPERATIONS FOR EACH PROCESS

IS BASED ON AN INITIAL SCHEDULING OF OPERATIONS AND MIGHT NOT REFLECT THE ACTUAL FLOATING

POINT OPERATIONS COMPLETED ON EACH PROCESS. OPERATIONS ARE DYNAMICALLY BALANCED DURING EXECUTION,

SO THE ACTUAL BALANCE OF OPERATIONS BETWEEN PROCESSES IS EXPECTED TO BE BETTER THAN THE ESTIMATE

PRINTED HERE.

(5) THE UPPER LIMIT OF MEMORY THAT CAN BE ALLOCATED BY ABAQUS WILL IN GENERAL DEPEND ON THE VALUE OF

THE "MEMORY" PARAMETER AND THE AMOUNT OF PHYSICAL MEMORY AVAILABLE ON THE MACHINE. PLEASE SEE

THE "ABAQUS ANALYSIS USER'S MANUAL" FOR MORE DETAILS. THE ACTUAL USAGE OF MEMORY AND OF DISK

SPACE FOR SCRATCH DATA WILL DEPEND ON THIS UPPER LIMIT AS WELL AS THE MEMORY REQUIRED TO MINIMIZE

I/O. IF THE MEMORY UPPER LIMIT IS GREATER THAN THE MEMORY REQUIRED TO MINIMIZE I/O, THEN THE ACTUAL

MEMORY USAGE WILL BE CLOSE TO THE ESTIMATED "MEMORY TO MINIMIZE I/O" VALUE, AND THE SCRATCH DISK

USAGE WILL BE CLOSE-TO-ZERO; OTHERWISE, THE ACTUAL MEMORY USED WILL BE CLOSE TO THE PREVIOUSLY

MENTIONED MEMORY LIMIT, AND THE SCRATCH DISK USAGE WILL BE ROUGHLY PROPORTIONAL TO THE DIFFERENCE

BETWEEN THE ESTIMATED "MEMORY TO MINIMIZE I/O" AND THE MEMORY UPPER LIMIT. HOWEVER ACCURATE

ESTIMATE OF THE SCRATCH DISK SPACE IS NOT POSSIBLE.

(6) USING "*RESTART, WRITE" CAN GENERATE A LARGE AMOUNT OF DATA WRITTEN IN THE WORK DIRECTORY.

E I G E N V A L U E O U T P U T

MODE NO	EIGENVALUE	FREQUENCY	GENERALIZED MASS
COMPOSITE MODAL DAMPING	(RAD/TIME)	(CYCLES/TIME)	
1	1.38202E-03	3.71755E-02	1.34714E-05
0.0000			
2	1.45764E-03	3.81791E-02	1.99187E-05
0.0000			
3	1.50466E-03	3.87900E-02	1.03773E-05
0.0000			
4	2.90581E-03	5.39056E-02	4.21582E-06
0.0000			
5	3.71025E-03	6.09118E-02	4.67978E-06
0.0000			
6	4.58821E-03	6.77363E-02	5.23703E-06
0.0000			
7	7.40874E+07	8607.4	3.31095E-06
0.0000			
8	9.52390E+07	9759.0	5.42667E-06
0.0000			
9	3.83506E+08	19583.	2.76997E-06
0.0000			
10	5.11879E+08	22625.	4.65017E-06
0.0000			
11	6.09957E+08	24697.	3.23294E-06
0.0000			
12	8.78634E+08	29642.	1.89337E-06
0.0000			

P A R T I C I P A T I O N F A C T O R S

MODE NO	X-COMPONENT	Y-COMPONENT	Z-COMPONENT	X-ROTATION	Y-
ROTATION	Z-ROTATION				
1	0.95371	-0.37978	-6.44996E-03	1.0943	
3.3273	-60.993				

2	0.53035	0.93882	-1.28857E-03	-2.8432	
1.7338	26.978				
3	-0.75555	0.64246	1.82017E-02	-1.3735	-
2.9255	13.435				
4	2.02348E-02	-8.36290E-03	1.7213	63.662	-
85.968	-0.42614				
5	1.96469E-02	-5.52846E-03	1.2354	4.1529	-
55.615	-0.89382				
6	-4.55517E-03	-8.06971E-03	0.88982	25.407	
8.6058	0.23925				
7	6.21022E-13	-5.27354E-13	8.51435E-12	2.87655E-10	-
2.33245E-10	-3.28042E-11				
8	4.89916E-14	-6.18284E-13	2.00332E-11	6.82347E-10	-
1.80723E-10	-4.84656E-12				
9	-3.37615E-14	7.26246E-14	3.57663E-12	1.62604E-10	-
7.25975E-11	6.31117E-13				
10	-8.39684E-14	3.33876E-14	7.18570E-13	7.84051E-13	-
6.11942E-11	2.27057E-12				
11	3.16418E-14	-1.40095E-13	3.82781E-12	1.02853E-10	-
5.24337E-11	-3.85976E-12				
12	5.01154E-14	-8.43225E-14	9.80503E-13	4.26016E-11	
1.30021E-11	-5.94614E-12				

E F F E C T I V E M A S S

MODE NO	X-COMPONENT	Y-COMPONENT	Z-COMPONENT	X-ROTATION	Y-ROTATION
1	1.22530E-05	1.94297E-06	5.60437E-10	1.61332E-05	
1.49143E-04	5.01154E-02				
2	5.60250E-06	1.75561E-05	3.30735E-11	1.61018E-04	
5.98736E-05	1.44972E-02				
3	5.92399E-06	4.28328E-06	3.43800E-09	1.95755E-05	
8.88169E-05	1.87304E-03				
4	1.72616E-09	2.94847E-10	1.24906E-05	1.70860E-02	
3.11571E-02	7.65587E-07				
5	1.80640E-09	1.43032E-10	7.14193E-06	8.07109E-05	
1.44744E-02	3.73878E-06				
6	1.08666E-10	3.41037E-10	4.14662E-06	3.38060E-03	
3.87856E-04	2.99766E-07				

7	1.27693E-30	9.20781E-31	2.40024E-28	2.73966E-25
1.80126E-25	3.56297E-27			
8	1.30249E-32	2.07448E-30	2.17787E-27	2.52664E-24
1.77240E-25	1.27468E-28			
9	3.15731E-33	1.46097E-32	3.54343E-29	7.32380E-26
1.45988E-26	1.10330E-30			
10	3.27869E-32	5.18370E-33	2.40108E-30	2.85863E-30
1.74137E-26	2.39740E-29			
11	3.23684E-33	6.34513E-32	4.73696E-29	3.42007E-26
8.88829E-27	4.81635E-29			
12	4.75529E-33	1.34624E-32	1.82026E-30	3.43627E-27
3.20082E-28	6.69431E-29			
TOTAL	2.37832E-05	2.37832E-05	2.37832E-05	2.07440E-02
4.63173E-02	6.64905E-02			

THE ANALYSIS HAS BEEN COMPLETED

ANALYSIS COMPLETE

JOB TIME SUMMARY

USER TIME (SEC)	=	1217.1
SYSTEM TIME (SEC)	=	37.430
TOTAL CPU TIME (SEC)	=	1254.5
WALLCLOCK TIME (SEC)	=	1263

REFERENCES

1. Abaqus Example Problems Manual, 'Eigenvalue Analysis of a Structure Using the Parallel Lanczos Eigensolver' Version 6.3, 2.2.4
2. Abaqus Theory Manual, 'Continuum Elements with Incompatible Modes' Version 5.7, 3.2.5
3. Abaqus Theory Manual, 'Eigenvalue Extraction' Version 5.7, 2.5.1-1
4. Abdul- Razzak.A.A., and Haido.J.H. 'Free Vibration Analysis of Rectangular Plates Using Higher Order Finite Layer Method' Al-Rafidain Engineering Vol.15, No.3, pp. 19-32, 2007.
5. ABS Material Euro pipe (http://xahax.com/subory/Spec_ABS.pdf)
6. Avitabile.P., 'Experimental Modal Analysis-A Simple Non-Mathematical Presentation' Sound and Vibration Magazine, JANUARY 2001
7. Bruel and Kjaer, 'Primers Handbooks' Measuring Vibration, 1982.
8. Bruel and Kjaer, 'Primers Handbooks' Vibration Testing, 1983.
9. Chakraverty.S., 'Vibration of Plates' Vol.10
10. Ding.Z., 'Natural Frequencies of Rectangular Plates Using a Set of Static Beam Functions in Rayleigh-Ritz Method' Journal of Sound and Vibration 189(1), pp. 81-87, 1996.
11. Gorman.D.J., 'Free In-Plane Vibration Analysis of Rectangular Plates by the Method of Superposition' Journal of Sound and Vibration 272(2004), pp. 831-851, 2004.
12. Gorman.D.J., 'Free Vibration Analysis of the Completely Free Rectangular Plate by the Method of Superposition,' Journal of Sound and Vibration 57(3), pp. 437-447, 1978.
13. Inman.D.J., 'Engineering Vibration' Finite Element Method, Prentice Hall, Englewood Cliffs, New Jersey 07632, Chapter 8, 1994.
14. K-Mac Plastics, Typical Property Data to Compare Types of Plastics.
15. Lassoued. R., and Guenfoud.M, 'Accurate Calculation of Free Frequencies of Beams and Rectangular Plates', World Academy of Science, Engineering and Technology ,October 2005.
16. Leissa. A.W., 'The Free Vibrations of Rectangular Plates', Journal of Sound and Vibration (1973) 31(3), pp. 257-293

17. Liew, K.M., Wang, C.M., Xiang, Y., and Kitipornchai, S., 'Vibration of Mindlin Plates,' Elsevier Science pp. 1-3, 1998.
18. Szilard.R., 'Theory and Analysis of Plates: Classical and Numerical Methods,' Prentice Hall, Upper Saddle River, New Jersey, 1974.
19. The Fundamentals of Modal Testing: Modal Parameter Estimation', Application Note 243-3, Chapter 4, pp.35-40
20. Waller.M.D., 'Vibrations of Free Rectangular Plates', The Proceedings of the Physical Society, Vol.62, Part 5, no. 353B, 1 May 1949.
21. Weaver.W., Timoshenko.S.P, and, Young.D.H., 'Vibration Problems in Engineering: Transverse Vibrations of Plates' Fifth Edition, Chapter5, pp. 495-497
22. Wu.J.H., Liu.A.Q., and Chen. H.L., 'Exact Solutions for Free-vibration Analysis of Rectangular Plates Using Bessel Functions' Journal of Applied Mechanics Vol.74, pp. 1247-1251, 2007
23. Vargas, L.R., and Walsh, M.S., 'Innovative Materials and Design for the Improvement of Warfighter Head Protection' U.S Army Research Library, MD 21005-5069

ABSTRACT

FREE VIBRATION ANALYSES OF ABS (ACRYLONITRILE-BUTADIENE-STYRENE) RECTANGULAR PLATES WITH COMPLETELY FREE BOUNDARY CONDITIONS

by

MEHMET AKIF DUNDAR

May 2012

Advisor: Dr. E.O. Ayorinde**Major:** Mechanical Engineering**Degree:** Masters of Science

Acrylonitrile-Butadiene-Styrene (ABS) represents a family of engineering thermoplastics with a wide field of performance characteristics. ABS materials have been receiving a great deal of attention because of their unique properties, such as outstanding formability, high tensile strength and stiffness, very high impact strength, excellent ductility, excellent high and low temperature performance, and resistant to many chemicals and plasticizers. Particularly, ABS exhibits really high impact strength; therefore, it is used in industry products which require high impact strength materials, such as military helmets and construction safety helmets. The vibration analyses of ABS rectangular plates are incredibly significant for design in military applications. The modal parameters of three various ABS rectangular samples, such as deflection mode shapes, resonance frequencies and damping ratios, were obtained in the frequency range of 0 Hz to 6400 Hz by the PULSE 15.1 software which is produced by the Bruel&Kjaer company. The Lancsoz Eigensolver method in ABAQUS/STANDARD 3D software, which is a powerful tool for extraction of the extreme Eigenvalues, was used to determine the natural frequencies and mode shapes of the ABS rectangular samples. The modal

densities of the samples were experimentally determined in the frequency range of 0 Hz to 12800Hz to find out which sample requires a more effort and money in design process. The experimental and finite element results were compared very favorably with one another.

AUTOBIOGRAPHICAL STATEMENT

Mehmet Akif Dundar earned his Bachelor's degree from the Mechanical Engineering Department of Kirikkale University in Turkey. He worked in some private companies for almost three years, after his graduation. He obtained very competitive scholarship from the Turkish government and he was sent to Ohio University to learn English by his government on April, 2008. He joined Wayne State University to earn his master's degree in fall 2010.